Applications of Hydroxymethylphosphines

A thesis

submitted in partial fulfilment

of the requirements for the degree

of

Master of Science in Chemistry

at

The University of Waikato

by

Megan Jane Wyllie

THE UNIVERSITY OF
WAIKATO
Te Whare Wānanga o Waikato

2015

Abstract

Hydroxymethylphosphines are compounds containing P-CH_2-OH functional groups. They have numerous applications, of which three types were explored in this project.

The cross-linking ability of tris(hydroxymethyl)phosphine (THP) was investigated for use as a fixative for biological samples for visualisation by scanning electron microscopy (SEM). THP has similar cross-linking ability to glutaraldehyde, the most commonly used fixative for SEM samples. Samples fixed with THP were compared with samples fixed with glutaraldehyde and an unfixed sample, under the SEM. THP appears to have a similar effect on the preservation of the samples, and seems to be successful as a fixative.

The bonding between $Ph_2P(S)CH_2OH$ and diiodine was investigated. The resulting adduct was unable to be crystallised. It was partially characterised by ^{31}P NMR and IR spectroscopy. The related compound, $Ph_3PS.I_2$ was synthesised successfully and characterised by ^{31}P NMR and IR spectroscopy.

The ability of THP to immobilise compounds to solid supports, in the interest of immobilising fluorescent compounds was investigated. THP was used to immobilise *N*-(2-aminoethyl)-1,8-naphthalimide onto aminopropyl silica, and analysed under UV light. The resulting solid however, fluoresced only slightly. The reaction between $Ph_2P(CH_2OH)_2Cl$ and *N*-(2-aminoethyl)-1,8-naphthalimide was also investigated, but the product was unable to be crystallised.

Acknowledgements

Firstly I would like to thank my supervisor Bill Henderson for all his help and guidance through this project. I am very grateful for his help in answering my many questions and problems over the last two years.

A big thanks goes to Helen Turner for her expertise and assistance when preparing and running my samples in the SEM, and for her advice each step of the way. I would also like to thank Pat Gread and Wendy Jackson for helping me numerous times in finding equipment and reagents, and for other miscellaneous problems that arose; additional thanks goes to Pat for helping me obtain my mass spectra. To Michael Mucalo, thank you for reading over a draft of my thesis when Bill was away.

Thanks to my friends and family, for supporting me over my years at university. A special thanks goes to my friend and flatmate Alicia for working hard on your own thesis with me, I would not have been able to get this done without you. I am also grateful to my family for funding from the Maud Malcomson Whanau Trust for help with printing and binding.

Lastly, thank you to my high school chemistry teacher Mrs Pemberton, without whom as a teacher I do not think I would have the love of chemistry and science that I do today, and to my fourth form typing teacher Mrs Carr, for teaching me to type with all my fingers, one of the most useful skills I have ever needed at university.

Table of Contents

List of Figures

List of Tables

List of Abbreviations

cm^{-1}	Wavenumbers (IR)
CPD	Critical Point Drying
ESI-MS	Electrospray Ionisation Mass Spectrometry
eV	Electron volts
IR	Infra-red
m/z	Mass to charge ratio (ESI-MS)
NMR	Nuclear Magnetic Resonance
Ph	Phenyl
ppm	Parts per million
SEM	Scanning Electron Microscopy
TEM	Transmission Electron Microscopy
THP	Tris(hydroxymethyl)phosphine
THPC	Tetrakis(hydroxymethyl)phosphonium chloride
UV-Vis	Ultraviolet-Visible spectroscopy
δ	Chemical shift (NMR) in ppm
υ	Stretching vibration (IR) in cm^{-1}

Chapter One: Introduction to Hydroxymethylphosphines

1.1 Structure and Properties:

Hydroxymethylphosphines are trivalent phosphorus compounds that contain at least one >P-CH_2-OH group. P(V) compounds are also known. The best example of a hydroxymethylphosphine is tris(hydroxymethyl)phosphine, $P(CH_2OH)_3$ (THP). It can be prepared from the phosphonium salt, tetrakis(hydroxymethyl)phosphonium chloride, $[P(CH_2OH)_4]^+Cl^-$ (THPC). Another hydroxymethylphosphine that was used in this project was $Ph_2P(CH_2OH)$, which can be made from the precursor $Ph_2P(CH_2OH)_2Cl$. The structures for these compounds appear in Figure 1.1.

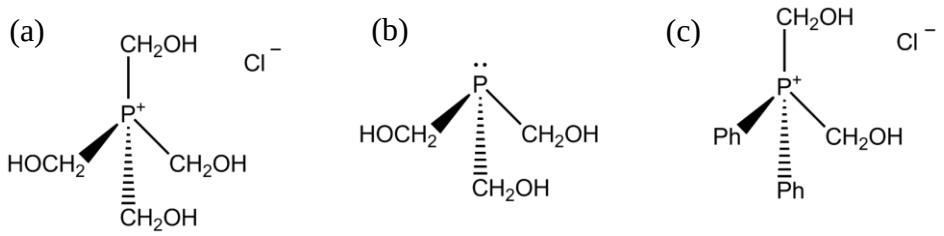

Figure 1.1: The structures of the compounds used in this project: (a) THPC, (b) THP and (c) $Ph_2P(CH_2OH)_2Cl$

THP is a water soluble compound that has been known for about 50 years[1]. It is also soluble in methanol, ethanol, pyridine, and dimethylformamide[2]. Because THP is water soluble it is of interest, for example, as a ligand in the formation of water soluble catalysts[1]. THP is 'moderately air-stable' in the solid state and in aqueous solution. Studies show that there is no oxidation at room temperature over 7 days[3] at pH 7. At alkaline pH (pH 10) it undergoes base promoted oxidation to the oxide. At acidic pH (pH <7) THP decomposes with the loss of

CH_2O to give the secondary phosphine, bis(hydroxymethyl)phosphine[1] and the tetrakis(hydroxymethyl)phosphonium cation $(HOCH_2)_4P^+)$[3].

1.2 Preparation of Hydroxymethylphosphines:

1.2.1 Preparation of Tetrakis(hydroxymethyl)phosphonium Chloride (THPC):

THPC is a precursor to THP. THPC can be prepared from formaldehyde and phosphine[4], shown below in equation (1).

$$PH_3 + 4CH_2O + HCl \xrightarrow{\text{catalyst}} [(HOCH_2)_4P]Cl \quad (1)$$

PH_3 gas, however, is very hazardous as it is spontaneously inflammable at room temperature. An alternative, but no less hazardous, preparation method is the reaction of yellow phosphorus with formaldehyde[5], shown in equation (2). An electropositive metal such as Zn can also be used.

$$P_4 + 16CH_2O + 6Zn + 16HCl \longrightarrow 4[P(CH_2OH)_4]Cl + 6ZnCl_2 \quad (2)$$

THPC is usually marketed as an 80% aqueous solution. It is a colourless crystalline compound that is soluble in water and lower aliphatic alcohols and insoluble in most common organic solvents[4].

1.2.2 Preparation of Tris(hydroxymethyl)phosphine (THP):

Hydroxymethylphosphines of the type $P(CH_2OH)_xR_{3-x}$, where R = H, alkyl, aryl and x = 1, 2, 3, can be made through insertion of formaldehyde into the P-H bonds of PH_3, or of secondary and primary phosphines[6]. This is shown in equation (3), showing the preparation of THP from phosphine and formaldehyde[1]. The reaction

can be catalysed[7] by compounds such as $[PtCl_4]^{2-}$ and $NiCl_2$ in the presence of ethylenediamine[1].

$$PH_3 + 3CH_2O \xrightarrow{\text{catalyst}} P(CH_2OH)_3 \underset{\text{base}}{\overset{CH_2O + H^+}{\rightleftharpoons}} [P(CH_2OH)_4]^+ \qquad (3)$$

However this reaction also requires handling of hazardous PH_3. THP is much more conveniently prepared by the addition of base to the air stable phosphonium salts, THPC or the equivalent sulfate, $[P(CH_2OH)_4]_2SO_4$, THPS[1, 7], also shown in equation (3). Bases used can include tertiary amines or stoichiometric OH^-. The phosphine can be oxidised by excess OH^- to the oxide, tris(hydroxymethyl)phosphine oxide (THPO)[1] but a mild base such as NEt_3 can be used in excess.

1.2.3 Preparation of Other Phosphines:

Other hydroxymethylphosphines, of the type R_2PCH_2OH or $RP(CH_2OH)_2$, where R = alkyl or aryl, are often used as ligands for metal ions. The main route of synthesis is in a similar manner to the preparation of THP in equation (3). For example, the diphosphine analogue of THP, bis[bis(hydroxymethyl)phosphino]ethane, $(HOCH_2)_2P(CH_2)_2P(CH_2OH)_2$, bhpe, can be prepared by the reaction of CH_2O with $H_2P(CH_2)_2PH_2$, a similar reaction[1] as for PH_3 in equation (3) above.

1.3 Reactions of Hydroxymethylphosphines and Their Applications:

The chemistry of hydroxymethylphosphines is of interest because they have the physical properties of common organophosphine donor ligands as well as the properties of hydrophilic alcohols[6]. This makes them useful precursors for

synthesis of a variety of water soluble organic and organometallic phosphorus compounds[6]. Hydroxymethylphosphines can undergo a number of reactions which are typical of PH_3 or organophosphines, including oxidation reactions, nucleophilic substitution and addition reactions to activated multiple bonds, or formation of phosphonium salts via nucleophilic addition to alkylhalides[6]. A summary of some important reactions is shown in Figure 1.2.

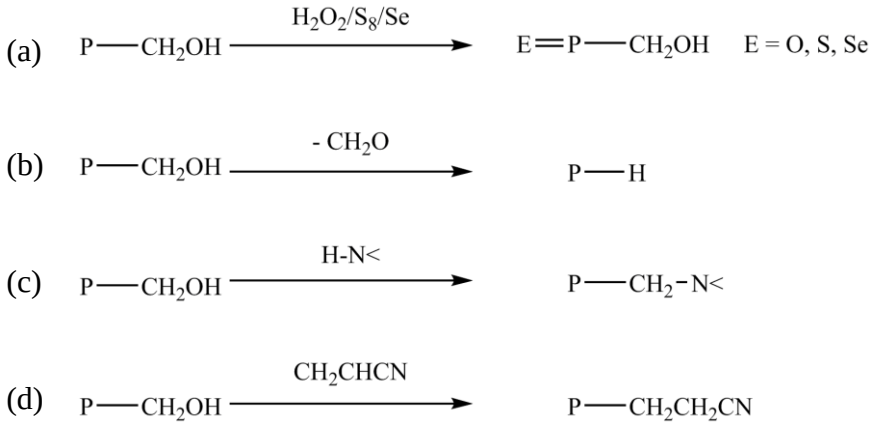

Figure 1.2: Selected reactions of hydroxymethylphosphines.

Hydroxymethylphosphines can form chalcogenide compounds through reaction with elemental sulfur or selenium[8], as shown in Figure 1.2 (a), and they can also be oxidised by H_2O_2 to form the oxide compound. These reactions are discussed further in section 1.3.2. At pH <7, hydroxymethylphosphines such as THP decompose with the loss of CH_2O[1]. This is illustrated in (b) as well as in equation (3). This allows reformation of the P-H bond. Another important reaction of hydroxymethylphosphines is the Mannich-type condensation with amine groups, as shown in (c). This is discussed in more detail in section 1.3.1. Addition of the phosphine across a compound containing a double bond, for example CH_2=CHCN with loss of formaldehyde, is shown in (d). This allows the formation of alkyl phosphines[2].

There are various applications of hydroxymethylphosphines. For example, tetrakis(hydroxymethyl)phosphonium salts, such as THPC, are inexpensive and readily available because of their industrial use in a flame retardant, multiple wash-resistant, treatment for cotton textiles[4, 9], and as biocides for oil and waste-water industries[1].

Metal complexes of hydroxymethylphosphines have attracted interest for some years[10]. THP has been used as a ligand in the development of water soluble catalysts[11]. Water soluble gold complexes containing a nucleoside ligand have been synthesised[12]. This has been extended to THP-bound gold nanoparticles which have been used to create nanowires as narrow as 30-40 nm, by using THP to bind the nanoparticles to DNA[13]. Hydroxymethylphosphines have been used in ferrocene complexes, such as $FcCH_2P(CH_2OH)_2$ and its derivatives[14]. Water soluble iridium and rhodium complexes with THP have been used to catalyse the selective hydrogenation of the C=O bond in cinnamaldehyde as well as the hydroformylation of pent-1-ene[15].

1.3.1 The Mannich-type Condensation Reaction and its use in Enzyme Immobilisation:

Hydroxymethylphosphines can undergo Mannich-type condensation reactions with amino-functionalised compounds such as amines, amino acids, or enzymes and proteins[6]. This forms aminomethylphosphines containing a $P\text{-}CH_2\text{-}N$ moiety[16] with the loss of water, shown below in Figure 1.3[17]. The reaction of THP with N-H groups occurs spontaneously at room temperature[18].

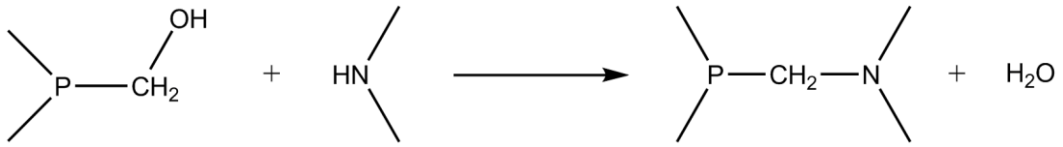

Figure 1.3: The Mannich-type condensation reaction between hydroxymethylphosphine P-CH_2-OH groups and amines.

This Mannich-type condensation has been used in the past in the immobilisation of enzymes onto amino-functionalised supports using THP as a coupling agent[16]. Immobilised enzymes have applications in the development of new classes of catalysts, such as supported catalysts, water soluble catalysts or metal-based drugs[6]. Advantages of immobilised enzymes include reuse of the enzyme, ease of separation of the catalyst and reaction mixture, and it often leads to improved thermal, pH[16] and storage stability[18]. However, issues with coupling enzymes include the creation of undesirable cross-links within the protein[19] and compromised enzyme activity upon immobilisation[18]. Ideally the coupling reaction uses non-essential NH_2 groups to minimise enzyme inactivation[16].

Types of supports used for enzyme immobilisation come in three categories: organic, polysaccharide and inorganic[17]. Supports that belong to all three respective categories are magnetite-derived polyacrylamide (PAM), chitosan, and aminopropyl-functionalised silica (APS)[17]. Chitosan is especially suitable as support, as it is inexpensive, biocompatible and it has a hydrophilic nature, which minimises non-specific adsorption of the enzyme to the support[16].

Other coupling reagents that are used to attach enzymes onto solid surfaces include glutaraldehyde, carbodiimides and benzoquinone[16], with glutaraldehyde the most commonly used. Crosslinking occurs via the formation of a Schiff's base[20], as shown in Figure 1.4.

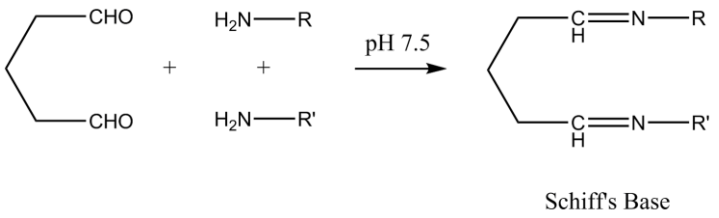

Figure 1.4: The reaction between glutaraldehyde and amines showing the formation of the Schiff's base.

Glutaraldehyde, however, is toxic, and is prone to polymerisation upon storage, varying the composition. Another problem is the Schiff's base that is formed is susceptible to hydrolysis[18]. The P-CH_2-N linkages formed by the reaction of THP with amines are, however, robust towards hydrolysis[18]. THP also has an increased number of immobilising groups. Use of THP as a coupling reagent represents a superior method for immobilising enzymes onto supports.

1.3.2 Phosphine Chalcogenides:

Phosphine chalcogenide compounds can be prepared via the reaction of the phosphine with elemental sulfur or selenium, or through oxidation with H_2O_2, as shown previously in Figure 1.2. Phosphine chalcogenides are good hydrogen bond acceptors[8]. They can be used as co-crystallising agents, for example, hydrogen bonding through the P=O group of triphenylphosphine oxide is used to crystallise alcohols[21] and other compounds[22]. For this reason these compounds may have some usefulness for the purposes of crystal engineering[8].

A number of phosphine chalcogenides involving O-H groups as hydrogen bond donors have been crystallised[8]. There are fewer examples of heavier chalcogenide P-S or P-Se examples than P=O compounds. Studies have been done on a series of chalcogens compounds of the type $Ph_2P(E)CH_2OH$ (E = O, S, Se), which have the donor and acceptor molecules within the same molecule[8]. The phosphine

oxide has a dimer motif, the sulfide and selenide form infinite chains. These structures arise from hydrogen bonding between the OH group and the chalcogens[8].

1.4 Aims of This Work:

1.4.1 Application of THP as a Fixative in Scanning Electron Microscopy:

Both glutaraldehyde and THP are used as coupling reagents in the immobilisation of enzymes, and THP has advantages over glutaraldehyde as mentioned previously.

Aldehydes are often used as a fixative for biological samples in scanning electron microscopy (SEM), most commonly, glutaraldehyde and formaldehyde[20]. The fixation occurs by cross-linking the amine groups that make up the proteins in the sample, forming the Schiff's base[20] as shown earlier in Figure 1.4. It is proposed that THP could be used as an alternative to glutaraldehyde in the fixing process, because it has been shown previously to immobilise enzymes onto amine-functionalised supports through a Mannich-type condensation reaction[16].

The main advantage THP has as a fixative is the lowered toxicity. Glutaraldehyde and formaldehyde are toxic[18] and when used as a fixative in SEM, glutaraldehyde is buffered with cacodylic acid to prevent polymerisation. Cacodylic acid, shown in Figure 1.5, is a toxic arsenic compound that is used in pesticides[23].

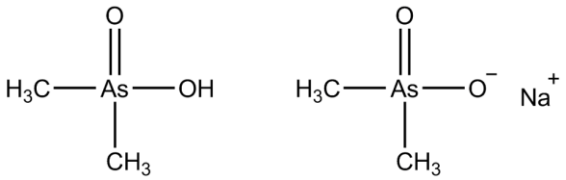

Figure 1.5: Cacodylic acid (left) and its salt, sodium cacodylate (right)

Replacement of these compounds with THP would reduce exposure to toxic compounds. There are also issues with the composition of glutaraldehyde solutions, as it is known to polymerise upon storage[18]. THP can be prepared easily and inexpensively from the phosphonium salt, THPC, which is available commercially at low cost[9]. In this project, samples prepared with the traditional glutaraldehyde-fixative method were compared with samples prepared using THP as a fixative and examined using scanning electron microscopy.

1.4.2 An Investigation of New Diiodine Adducts of the Hydroxymethylphophine Sulfide $Ph_2P(S)CH_2OH$:

A second aim of this project was to explore hydroxymethylphosphine sulfide adducts of diiodine. As shown in Figure 1.2, hydroxymethylphosphines can react with elemental sulfur or selenium to form chalcogenides. Other tertiary phosphines, such as triphenylphosphine (Ph_3P), can also undergo this reaction. The resulting phosphine chalcogenides can react with halogen compounds to form charge-transfer halogen adducts[24]. Synthesis is by combination of equimolar quantities of halogen and phosphine chalcogenide. The most common structures formed are 1:1 adducts between the phosphine chalcogenide and the di- or inter-halogen such as those shown in Figure 1.6.

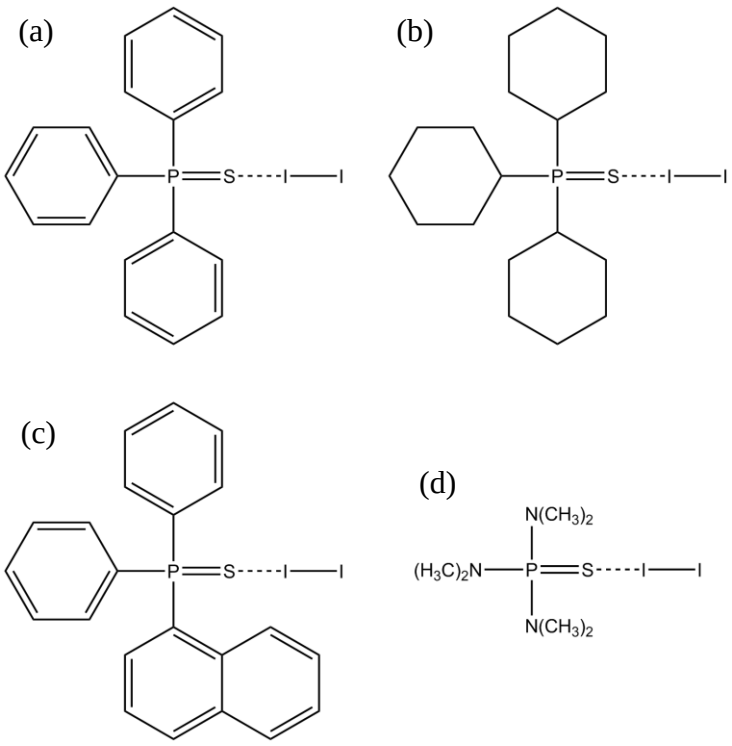

*Figure 1.6: Diiodine adducts of (a) triphenylphosphine sulfide, (b) tris(cyclohexyl)phosphine sulfide, (c) diphenyl-1-naphthylphosphine sulfide and (d) tris(*N,N-*dimethylamino)phosphine sulfide.*

Diiodine adducts of phosphine sulfides have a wide range of possible substituents on the phosphorus atom. Many contain aromatic substituents. They can be of the type $R_3PS.I_2$ such as compound (a) in Figure 1.6, or $R_2R'PS.I_2$ compounds such as (c). Non-aromatic substituents such as (b) and (d) and others not pictured such as trimethylphosphine sulfide diiodine have also been prepared[24]. The phosphine sulfide compound used in this project was of the type $R_2R'PS$, and the structure is shown in Figure 1.7 as compound **1**. It contains two aromatic phenyl rings as well as the hydroxymethyl group. The theoretical structure of the charge-transfer adduct with diiodine, **2**, is also shown in Figure 1.7.

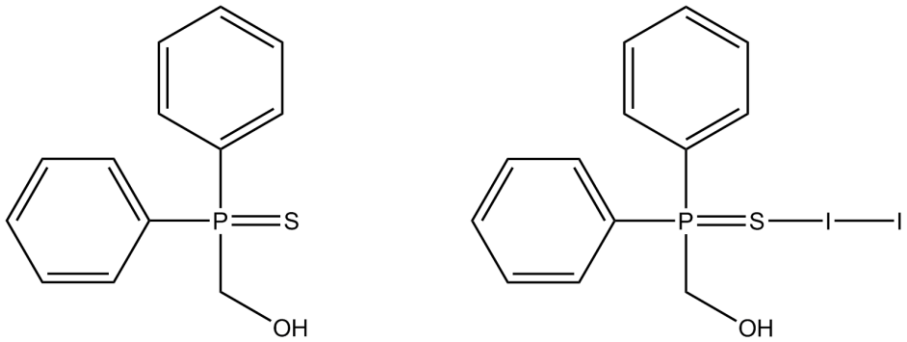

1 **2**

*Figure 1.7: The structures of compounds **1**, $Ph_2P(S)CH_2OH$, and the diiodine adduct **2**, $Ph_2P(S)CH_2OH.I_2$.*

As discussed previously, phosphine chalcogenides are good hydrogen bond acceptors[8]. The hydroxymethylphosphine compounds, $Ph_2P(E)CH_2OH$ (E = O, S, Se), contain both hydrogen bond donor and acceptor groups in the same compound, and the –OH groups have been shown to become involved in hydrogen bonding to the chalcogen atom[8]. In the theoretical compound in Figure 1.8 (a), hydrogen bonding between –OH groups and the chalcogen atom, S, could lead to an increase in stability. The halogens, in the charge-transfer compounds, bind through the chalcogen atom. The oxygen atom in the hydroxymethyl group in **1** may also interact with diiodine, shown in (b). This could also potentially increase stability, as halogen adducts with phosphine oxides are known[24].

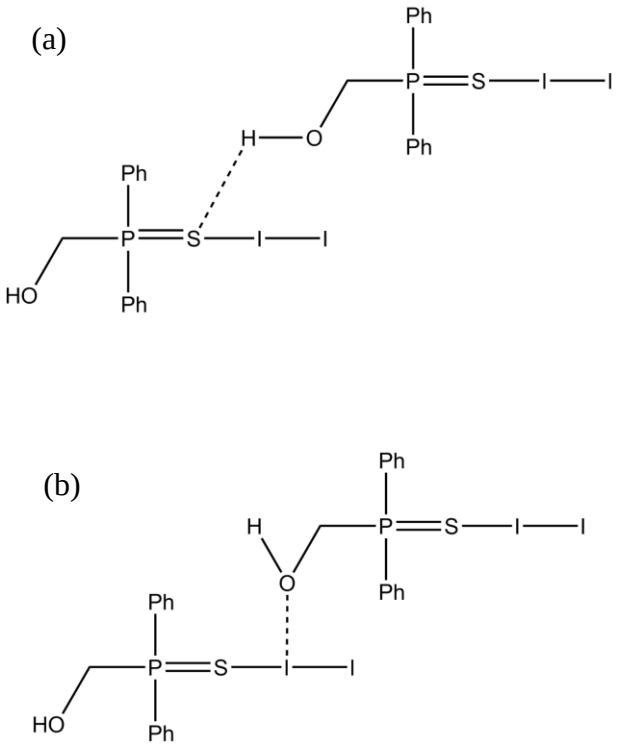

Figure 1.8: Possible structures of the charge-transfer compound $Ph_2P(S)CH_2OH.I_2$.

1.4.3 Application of Hydroxymethylphosphines as Coupling Agents for Fluorescent Labels:

A third aim of this project was to use THP as a coupling agent to immobilise fluorescent labels onto a support material. THP is known to couple compounds containing N-H groups (for example amines and proteins) to solid supports that also contain N-H groups[16]. This could be applied to the coupling between a fluorescent label and a biological support material. This has applications in viewing biological samples with fluorescence microscopy[25]. The fluorescent label, *N*-(2-aminoethyl)-1,8-naphthalimide, **4**, shown in Figure 1.9, contains the necessary N-H group for a Mannich-type condensation reaction with THP, and is conveniently synthesised from inexpensive precursors, naphthalic anhydride and ethylenediamine[26].

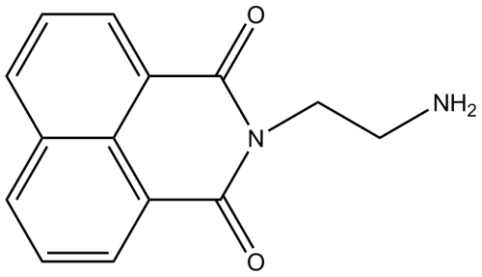

4

Figure 1.9: The fluorescent label N-*(2-aminoethyl)-1,8-naphthalimide.*

This project used THP to couple the above fluorescent label to amine-functionalised silica, and aimed to extend this to materials such as bone containing residual collagen. THP has previously been used to immobilise enzymes on bone samples through residual collagen in the bone[27].

Another reaction that was investigated in this project was the combination of *N*-(2-aminoethyl)-1,8-naphthalimide with a related hydroxymethyl phosphonium compound, $Ph_2P(CH_2OH)_2Cl$, which is used to generate the phosphine Ph_2PCH_2OH. The expected product is shown below in Figure 1.10. This reaction is also a Mannich-type condensation.

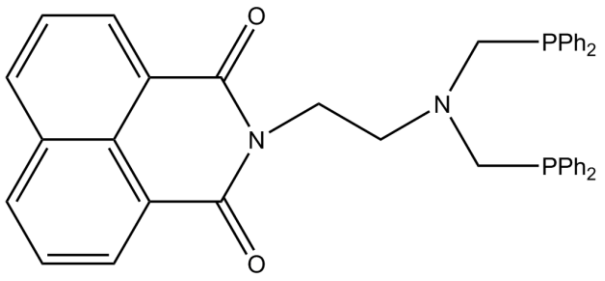

5

Figure 1.10: The expected product, ***5****, of the reaction between N-(2-aminoethyl)-1,8-naphthalimide and* $Ph_2P(CH_2OH)_2Cl$.

This compound is a molecular (rather than an immobilised) derivative of the naphthalimide label. As a bis(phosphine) is could be expected to form six-membered chelate ring complexes with metal ions, thereby attaching a distal fluorescent label onto the metal. Such compounds might find use in development

of metal-based drugs, which as mentioned earlier are often examined using fluorescence microscopy[28], or catalysts.

Chapter Two: An Investigation into the use of Tris(Hydroxymethyl)Phosphine (THP) as a Potential Fixative in Scanning Electron Microscopy (SEM)

2.1 Introduction:

2.1.1 An Overview of Electron Microscopy:

Electron microscopy is a practical technique used to examine samples that are too small to be observed by light microscopy. Instead of light, electron microscopes use a beam of electrons to visualise either the surface or interior of the sample[29]. The resolution of electron microscopy is much greater than light microscopy because resolution is inversely proportional to wavelength[29] and electrons have a much shorter wavelength than light[30]. Unlike light, electrons do not penetrate very well and cannot even penetrate a single cell[30]. There are two types of electron microscopes: scanning and transmission. Transmission electron microscopy (TEM) is used to study the interior of samples, for example the interior of a cell. The beam of electrons needs to travel through the sample, therefore special sample preparations are required that involve very thinly slicing samples and staining with heavy metals such as osmic acid, permanganate or lead salts, which scatter electrons well and improve contrast[30]. In scanning electron microscopy (SEM) the beam of electrons is scanned across the surface of the sample, providing a detailed analysis of the surface as the electrons cannot penetrate the interior of the sample[30]. The surface of the sample is usually coated in a thin layer

of a conductive metal such as gold or platinum. SEM is a versatile technique that can be used to examine many different samples, from cheese microstructure[31] to hair and skin cells from an Egyptian mummy[32].

The energy of the electron beam in SEM is measured in electron volts (eV) and can be between a few hundred eV to tens of thousands of keV. The samples in this research used a relatively low energy (3keV) because they were not flat samples, and high electron energies can lead to charging. Charging occurs when the electron current is unable to leak away to the earth via the stub the sample is mounted on[33]. This can result in a flickering image that is unable to be focused. Electrons that are scattered from the surface of the metal-coated sample are collected by a secondary electron collector[33]. A photomultiplier is then used to amplify the signal which is processed and displayed[33]. In SEM the magnification of images is a ratio between the dimensions of the images displayed on screen and the area scanned on the sample. For example, if an area of 1 mm^2 is scanned on the sample, and displayed on screen at 100mm^2 then the magnification is x100. The magnification can be changed by altering the area scanned on the sample and keeping the area on screen constant[33]. The specimen chamber contains a movable stage on which the specimen is mounted[33]. By moving the sample, this allows the area scanned by the electron beam to change, allowing the image on screen to change to different parts of the surface.

This specimen chamber is evacuated to a high vacuum of below $1x10^{-4}$ mbar. This presents problems when examining moist samples like biological specimens. Environmental scanning electron microscopy (ESEM) is an alternative SEM technique which uses a variable pressure chamber unit that replaces the high pressure chamber used in conventional SEM. This enables imaging of samples

that would normally require extensive preparation to preserve the structure[34]. Another modified SEM method is cryo-SEM, which uses rapid freezing (cryofixation) to view the samples on a special cold-stage[35].

When viewing moist samples using conventional SEM, the samples need to be prepared in a manner that most closely preserves the native state of the sample[36]. Moist samples present a number of problems when the moisture provides much of the volume of the sample, or has to be extracted from fine cells or capillaries, because simple air drying irreversibly modifies the internal structure[33]. The general procedure for sample preparation is chemical fixation using a cross-linking agent, dehydration in ethanol or acetone, critical point drying, before mounting the sample on aluminium stubs and sputter-coating it with a metal such as gold or platinum[33].

The most commonly used drying method, critical point drying (CPD), ensures no phase transitions affect the specimen (i.e. no freezing or evaporation), which is a major disruptive force in drying[33]. At the critical point of a liquid, which is at a certain temperature and pressure, there is an instantaneous transition from liquid to vapour. The critical point of water is impractically high, therefore other liquids such as carbon dioxide are used (the critical point of CO_2 occurs at 31.0ºC and 1080 psi)[33]. Before the sample is placed in the critical point drier, it has to be dehydrated, and the water replaced with a solvent that is miscible in liquid CO_2[33]. The most common method is through a graded series of ethanol or acetone solutions (for example from 30-100%)[20]. The sample is then placed into the critical point drier immersed in the ethanol or acetone solution, and the liquid is replaced with liquid CO_2[33].

An alternative drying technique is lyophilising or freeze-drying[35]. It involves freezing the sample, followed by sublimation of the water in a vacuum[37]. Hexamethyldisilazane (HMDS) can also be used to chemically dry moist samples. The initial procedure is similar to CPD in that once the sample has been treated with 100% ethanol, it must be transferred to 100% HMDS through a graded series of ethanol-HMDS mixtures. The sample in the 100% HMDS solution is then air-dried[38].

The removal of water can affect the structure of biological samples, therefore standard SEM procedures involve chemical fixation of the sample, before dehydration and drying[35]. Aldehydes such as glutaraldehyde and formaldehyde in a buffered solution are the most common fixing agents. Glutaraldehyde buffered with cacodylic acid is frequently used as a fixative. Additional staining with heavy metals such as osmium tetroxide can enhance contrast of the sample[39]. Osmium tetroxide is also useful for stabilising lipids, and therefore membrane structure[20]. Glutaraldehyde reacts with the proteins in the sample, cross-linking them through the formation of Schiff's base linkages, as mentioned earlier in section 1.4.1 on page 8. However, the Schiff's base formed is susceptible to hydrolysis[18] and glutaraldehyde solutions are prone to polymerisation, altering the composition[18]. Glutaraldehyde and formaldehyde are also toxic[20], as is cacodylic acid[23], an arsenic compound (shown in Figure 1.5 on page 9). Many buffer species can have an impact on the biological systems, enzyme activities, substrates or cofactors. Cacodylic acid is often used as a buffer for glutaraldehyde as it does not react with aldehyde fixatives, unlike some other buffers such as Tris, (tris(hydroxymethyl)aminomethane)[20].

Cacodylic acid has been shown to be toxic; it causes DNA damage in the lungs and it promotes certain cancers as well as being a carcinogen itself[40]. It is currently used in pesticides[41], and was used as Agent Blue in the Vietnam War[23]. Agent blue or Phytar 560-G contained 26.4 % sodium cacodylate and 4.7 % cacodylic acid[23].

Sample preparation can cause changes in the cell structure, such as shrinkage, cell membrane discontinuities and distortion of membrane-associated components[39]. Glutaraldehyde fixation is known to have an effect on the size of bacterial cells when observed by atomic force microscopy (AFM)[42].

Glutaraldehyde has also been known to occasionally discolour some samples. Alkaline glutaraldehyde solutions can react with various proteins from the sample, turning both the solution and the sample yellow[43]. To prevent this, glutaraldehyde solutions that are used for fixing biological samples are buffered, for example with cacodylate buffer, usually to around neutral pH. Silk yarns treated with glutaraldehyde have been found to discolour, but not when treated with a glutaraldehyde-$NaHSO_3$ adduct[44]. A liver sample fixed with glutaraldehyde displayed a pale yellow zone around the outside of the sample, corresponding to the extent of the glutaraldehyde penetration (and therefore fixation). The yellow colour was confirmed as being due to the reaction between glutaraldehyde and protein amino acids or primary amines in an alkaline solution[45]. The yellow colour that arises from solutions with proteins increases over time, and with some proteins, the solution can also form a gel[46].

A potential alternative to glutaraldehyde fixation is tris(hydroxymethyl)phosphine (THP). THP can bind to proteins through Mannich-type condensations with amines (see page 6)[16]. Glutaraldehyde is used as a coupling reagent for

immobilisation of enzymes onto supports, and THP has been shown to do this more effectively[16]. The resulting –P-CH_2-N- linkages are stable towards hydrolysis, unlike the Schiff's base formed by glutaraldehyde. THP is also inexpensive, water soluble and reasonably air-stable[47].

2.1.2 The Structure of Skeletal Muscle:

In this project, the ability of THP to fix skeletal muscle (specifically raw chicken) was investigated. Organisation of the skeletal muscle is shown in Figure 2.1.

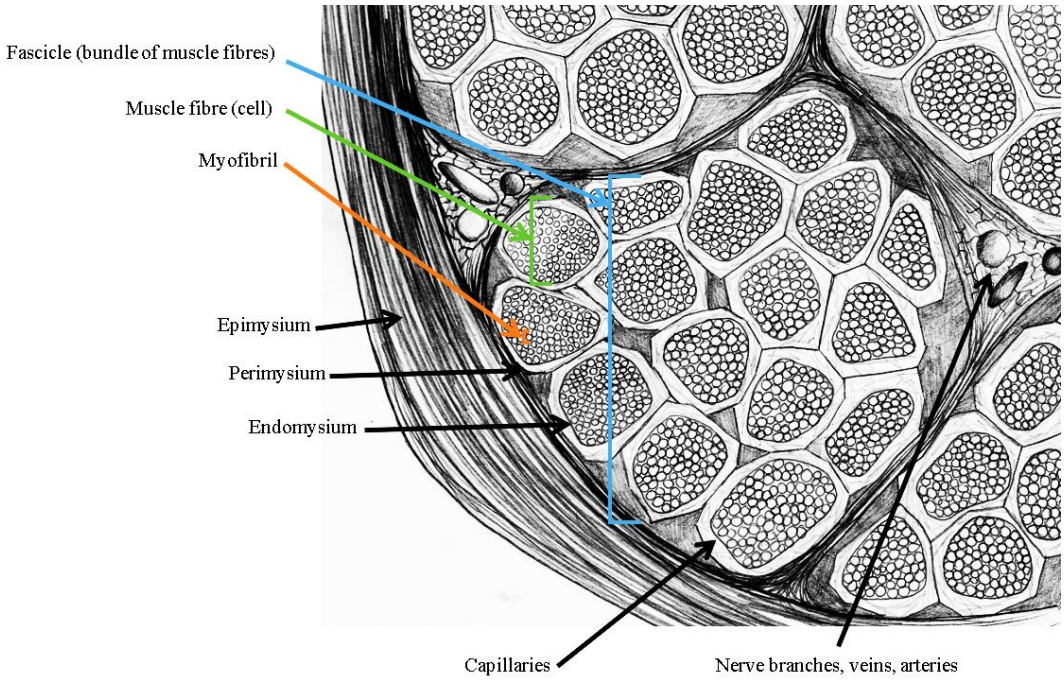

Figure 2.1: A schematic diagram of a cross-section of skeletal muscle, showing the organisation of muscle fibres, myofibrils and connective tissue.

Vertebrate skeletal muscle is attached to bone by tendons and is encased in a thick layer of connective tissue called the epimysium[48]. The muscle belly is made up of bundles of muscle fibre cells (fascicles), which are bound together with the perimysium[48]. Nerve branches, veins and arteries are located between the bundles. Each muscle fibre runs the length of the muscle belly and is actually a single cell with multiple nuclei, as it was formed from the fusion of many embryonic cells[29].

The muscle fibres are in turn made up of smaller myofibrils which are bound with the endomysium[48]. The endomysium contains the capillaries. The myofibrils are made up of thin filaments (two strands of actin and two strands of a regulatory protein) and thick filaments (staggered arrays of myosin)[29]. The arrangement of these proteins creates light and dark bands (visible under a light microscope), which gives muscle its striated pattern. Under a scanning electron microscope the striated pattern appears as "bumpy" bands[49], shown in Figure 2.2. Each repeating unit (of light and dark bands) is called a sarcomere[29].

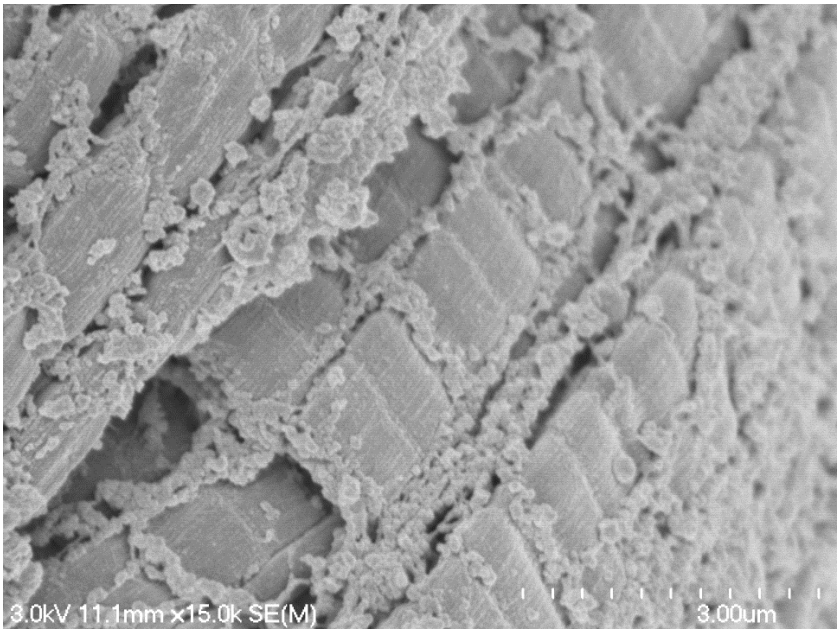

Figure 2.2: An SEM image of the striated pattern of myofibrils in skeletal muscle.

SEM can be used to visualise the surface of the sample, so the muscle belly was cross-sectioned, allowing the ends of the muscle fibres, and the myofibrils that make up the fibres, to be examined. Myofibrils, such as those in Figure 2.2, have been exposed and can be viewed using the SEM.

2.1.3 Aims of this Project:

THP was tested as a potential alternative fixative to glutaraldehyde, for the examination of samples by SEM. Comparison of glutaraldehyde-treated samples to THP-treated samples, and an untreated sample was done. The fixing procedure used was the one used by this university, where the samples are treated for a certain time in the fixative, dehydrated in an ethanol series, dried using CPD before mounting and sputter-coating with platinum. The amount of time the sample was treated in the fixative was varied, as different times are often used for different sample types.

2.2 Experimental:

2.2.1 General Procedures:

The chemicals used in this project were sourced as follows: glutaraldehyde was obtained from Electron Microscopy Services; THPC was used as an 80% w/w aqueous solution from Albright & Wilson, UK Ltd.; sodium cacodylate from BDH Chemicals Ltd.; HCl from Univar. The water used was high grade MilliQ water which had been deionised using the Barnstead E-pure system (18.0MΩcm).

The samples were dried in a Polaron Critical Point Dryer (CPD) using liquid CO_2. Sputter coating with platinum was done using a Hitachi E-1030 Ion Sputter Coater. The SEM images were taken using a Hitachi S-4700 Field Emission - Scanning Electron Microscope. The accelerating voltage used to view the samples was 3.0 keV.

2.2.2 Preparation of Tris(hydroxymethyl)phosphine:

Tris(hydroxymethyl)phosphine (THP, $P(CH_2OH)_3$) solution was prepared fresh before use. When prepared fresh, no precautions to exclude air are needed, because THP oxidises relatively easily in air. A solution of $P(CH_2OH)_4Cl$ (3.00 g) was made up to 25 mL with distilled water. To this, with stirring, a freshly prepared solution of KOH (0.707 g made up to 10 mL in water, 1.26 mol L^{-1}) was added dropwise. This generates a solution of THP (0.45 mol L^{-1}, 35 mL).

2.2.3 Preparation of 2.5% Glutaraldehyde Solution:

Cacodylate buffer (0.1 mol L^{-1}, 50 mL) was prepared by dissolving sodium cacodylate trihydrate (1.07 g) in distilled water (45 mL). HCl (1 mol L^{-1}, 0.3 mL)

was added and the solution was made up to 50 mL with distilled water. The buffer was prepared fresh each time. 9 mL of the buffer was added to 1 mL of glutaraldehyde (25%, vial stored in a fridge). The 2.5% glutaraldehyde solution was prepared fresh for each SEM experiment.

2.2.4 Treatment of Biological Samples:

Raw chicken was used as a protein sample for the fixative experiments. Small pieces, approximately 1 mm thick, were cut with a scalpel, cross-sectioning the muscle fibres. It was decided that chicken breast was the best cut to use as it gave the largest amount of muscle fibres running in the same direction. The chicken samples were bought from the local supermarket or butchers and stored in a fridge (except expt. 1 which was stored in the freezer) until ready for fixing.

To determine the best procedure for fixing using THP, four different experiments were performed. The variations between the experiments are summarised in Table 2.1.

Table 2.1: Fixing times and tissue types for each SEM experiment.

Expt. #:	Chicken Tissue Type:	Treatment Times Used:	Sub-sampled:
1	Breast (Frozen)	5 min, 1 hr, 4 changes over 30 min, 6 hrs	No
2	Thigh (Fresh)	5 min, 1 hr, 4 changes over 30 min	Yes
3	Leg (Fresh)	1 hr, 4 changes over 30 min, 1 month (at 4 °C), untreated	No
4	Breast (Fresh)	1 hr, 4 changes over 30 min, untreated	Yes

The chicken pieces were fixed by soaking in either THP or glutaraldehyde solution (using enough solution to cover the sample) at room temperature for a varying amount of time (see Table 2.1 for details) and then rinsed thoroughly with

distilled water. After the fixative, the samples were dehydrated using an ethanol series of 50%, 75%, 95% and 100%, soaking for an hour in each one. The samples were then stored in 100% ethanol at room temperature until they were dried using CPD. In order for some of the samples to fit into the CPD, they had to be cut into smaller sub-samples (details appear in Table 2.1). After drying the samples were mounted on aluminium stubs with double-sided carbon tape and sputter coated with platinum. The samples were then ready for viewing with the SEM.

2.3 Results and Discussion:

2.3.1 First Trial: Determining Whether THP is Viable as a Fixative

Standard SEM fixing procedures for moist samples require some kind of chemical fixation to prevent shrinking during drying and preserve internal cell structures[35]. The most common method is soaking a sample in a buffered solution of glutaraldehyde for a varying amount of time[36]. The time required depends on the sample type (for example, longer treatment times for plant tissues[35] and comparatively shorter times for bacterial biofilms[34]) and sample size[36]. Diffusion limits how large these samples can be to approximately 1 mm^3.

The aim of this initial trial was to determine whether THP acts as a fixative for biological samples in a similar manner to glutaraldehyde. Glutaraldehyde can be used to immobilise enzymes on surfaces, and it has been shown that THP can be used in the same way[47], as discussed in section 1.3.1 on page 5. As well as determining whether THP worked as a fixative, a suitable treatment time needed to be established. Treatment times for samples in glutaraldehyde can vary greatly: for example from 1 hour[39] to 20 hours[50], both for bacterial biofilms. This led to three initial soaking times being chosen which give a large range to work with: five minutes, 1 hour and 6 hours. Soaking the samples for 30 minutes but changing the solution four times is how the standard method used by this university for fixing with glutaraldehyde is achieved, so this fixing time was also included.

This experiment used frozen chicken breast, which was also refrozen after treatment with the fixative solutions before going through the ethanol series. As

this was only the initial trial experiment, preserving the fine structure of the tissue samples was not as important as getting a general overview as to whether THP would work as a fixative. Slow freezing, for example by placing a sample in a freezer, damages the morphology of the tissue cells. It leads to the formation of ice crystals, and the more slowly the sample is frozen, the larger the ice crystals[51]. Freezing can also denature proteins in the cell due to dehydration with a slow freezing withdrawing up to or more than 90% of the water content of the cell[51]. THP and glutaraldehyde work as fixatives by cross-linking the amino acids in the cell proteins[47]. As a result the appearance of the samples in the SEM may not be the same as the native state of the tissue samples[36]. It was decided that subsequent trials would use fresh chicken which would give better results.

During treatment of the samples with the fixative solutions, the glutaraldehyde solution would give the chicken a yellow tint, while the THP would bleach the chicken samples. Alkaline glutaraldehyde solutions containing amine functional groups can sometimes become yellow and discolour the sample being treated. This was discussed in section 2.1.1 on page 19. Over time the glutaraldehyde solution would become more strongly coloured. The samples with longer treatment times in glutaraldehyde would also become a darker yellow. The four changes samples showed the most yellowing. The extent of fixation can be inferred from the area of discolouration of the sample[45]. This may show that the four changes fixing time was the most effective at having the most fixative diffuse into the tissue sample.

The THP solutions did not change colour, but the chicken samples appeared to bleach of colour. THP has been used as a bleaching agent in some pulps, as a ligand in metal catalysts, or on its own[1]. The bleaching works by hydrogenation of

aromatic residues or conjugated C=C-C=O moieties in the lignin that makes up the pulp, removing the yellow colour[52]. Similar reactions could be happening in the chicken samples.

2.3.1.1 A comparison of the two fixing solutions:

Glutaraldehyde-treated: THP-treated:

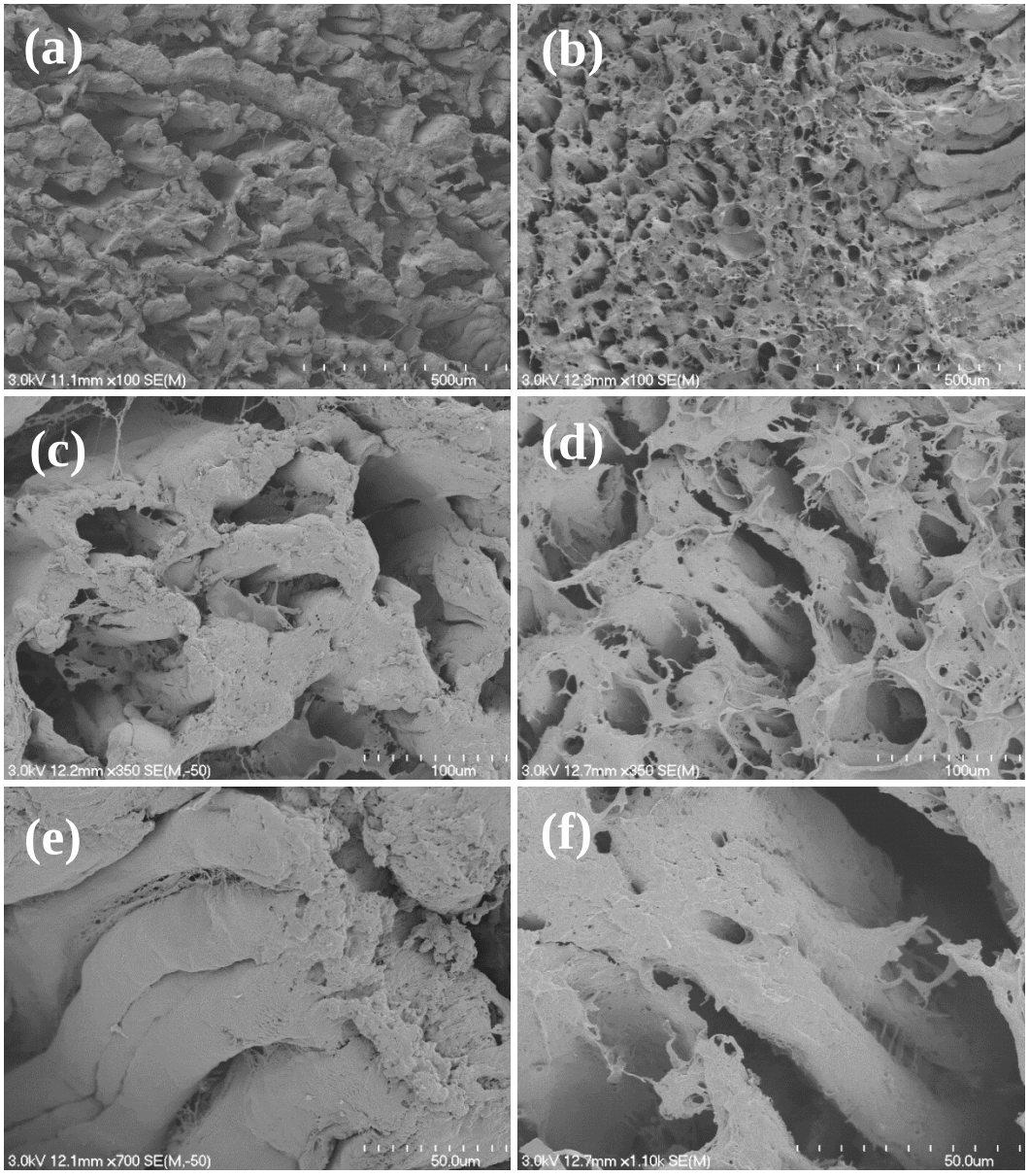

Figure 2.3: SEM micrographs of chicken breast samples treated with either glutaraldehyde or THP for 6 hours. Magnifications for: (a) and (b) are x100, for (c) and (d) are x350, (e) is x700 and (f) x1.10k.

The initial impressions from looking at the samples under the SEM were that the THP had been successful in fixing the samples as they looked very similar to the

glutaraldehyde samples. The bundles of muscle fibres do not appear as expected, most likely due to the freezing of the samples.

The greatest difference between the glutaraldehyde and the THP-fixed samples is between the ones that were treated for 6 hours, shown in Figure 2.3. The muscle fibres in the glutaraldehyde samples appear more solid-looking, with larger gaps between the fibres than the THP samples. The muscle fibres in the THP treated samples, however, are less distinct and the gaps between the fibres are filled with the connective tissue that binds the muscle fibres, perimysium[48]. Under an SEM, collagen looks "cob-web" like[53], similar to the images in Figure 2.3. THP appears to be fixing and therefore preserving the structure of the connective tissue more effectively than glutaraldehyde. THP has been known to react with collagen[27] and would therefore fix the connective tissue. There is still a large amount of space between the fibres, despite the differences in how well the connective tissue was preserved. This may be due to dehydration of the fibres on freezing[51], because when compared with samples from the later experiments that were not frozen, there is much less space between the fibres (see section 2.3.2 onwards).

The higher magnification images in Figure 2.3 (c) and (d), show there is connective tissue visible in the glutaraldehyde-treated sample. The muscle fibres appear thicker than the THP-treated muscle fibres in images (c) and (d), which may be because glutaraldehyde was more successful at fixing the muscle proteins, while THP fixed the collagen fibres of the connective tissue. The cobweb-like connective tissue that appears all over the image (d) could be the perimysium, which is composed of collagen fibrils that run in all directions and connect to the endomysium[48].

Some of the fine structure of the muscle fibres is visible in image (e). Because the chicken samples were cut against the grain of the fibres, the ends of the fibres are seen in the SEM. This is useful for visualising the whole muscle and how the fibres and connective tissue are organised and how well the fixatives preserve this, but it does not show much of the fine structure of the muscle fibres, especially the myofibrils and their striated pattern[48]. This is looked at in the fourth experiment (section 2.3.4) when the way the samples had been cut allowed a look at the sides of some of the fibres and hence their striated pattern. In Figure 2.3 (e), the way the fibres were cut destroyed some of the myofibrils[48] which make up the muscle fibres. The ends of the muscle fibres are damaged and end in a mass of broken fibres, rather than the fine edges of the fibres in section 2.3.4. The images (e) and (f) show some more examples of the endomysium, appearing between the large fibres in (e) and like rungs on a ladder between two fibres in (f).

Similar differences in the glutaraldehyde- and THP-treated samples are visible in the samples that used different fixing times, as seen in Figure 2.4. The glutaraldehyde-treated samples show less connective tissue and thicker muscle fibres than the THP-treated samples. This is illustrated in Figure 2.4 (e) and (f). Both methods for fixing show a relatively large amount of space between the fibres. As mentioned earlier, this is likely due to the freezing of the samples. In Figure 2.4, the image (a) shows an example of the perimysium in the bottom right as does (d) also in the bottom right (as indicated by the arrows). Samples treated for four changes over 30 minutes are discussed later as they appear quite different from the other samples.

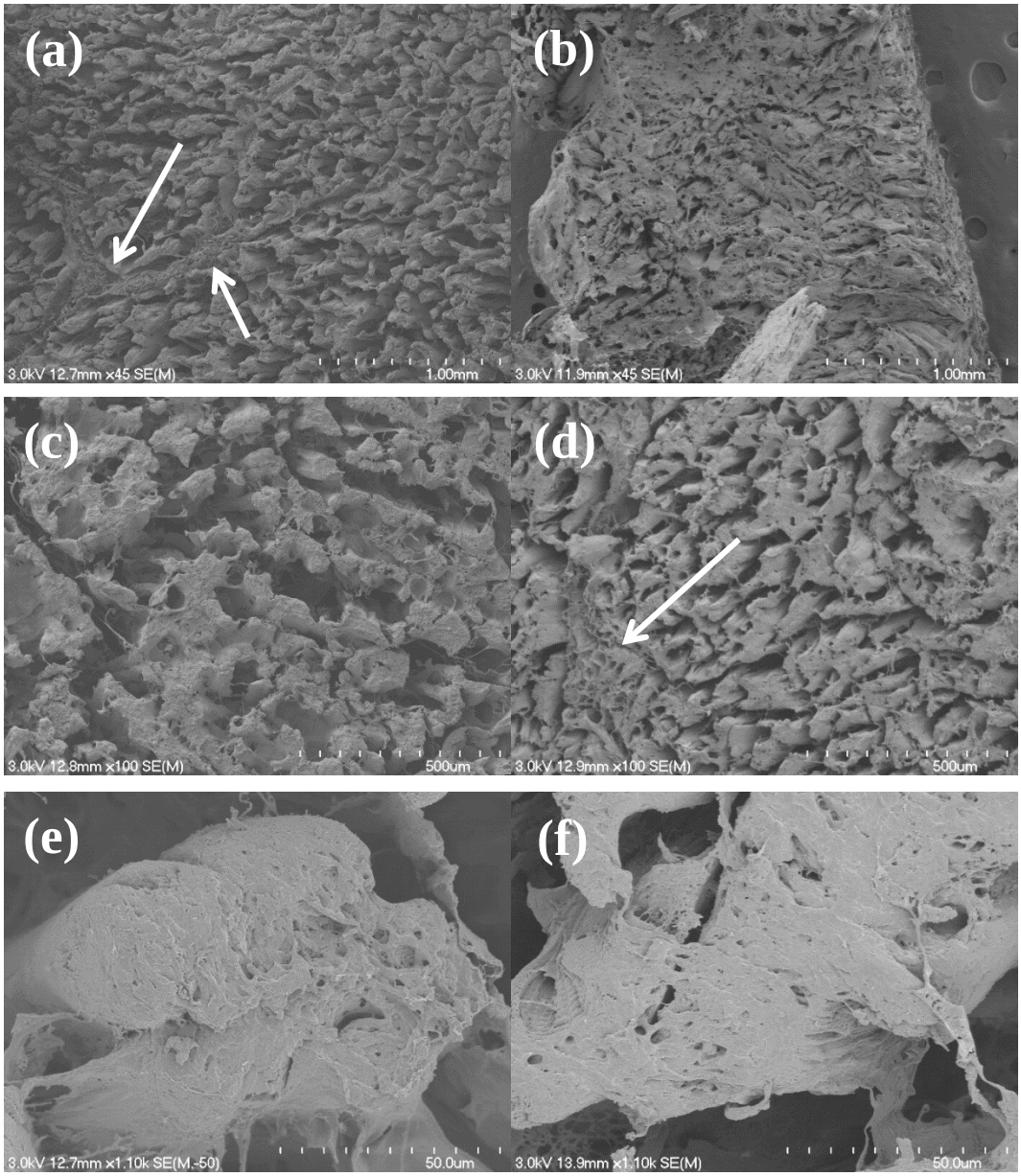

Figure 2.4: SEM images comparing glutaraldehyde with THP over a range of different fixing times: (a) fixed with glutaraldehyde for 1 hour, (b) fixed with THP for 1 hour, (c) and (e) fixed with glutaraldehyde for five minutes, (d) and (f) fixed with THP for five minutes. Magnifications for: (a) and (b) are x45, (c) and (d) are x100, and (e) and (f) are x1.10k.

2.3.1.2 Comparing fixing times:

Figure 2.5 shows different fixing times between glutaraldehyde- and THP-treated samples. The samples that differ the most are the ones that were fixed for 30 minutes, changing the solution four times. The most noticeable difference is that the muscle fibres appear much fuller in the four changes samples, for both glutaraldehyde and THP, when compared with ones from other fixing times. There appears to be slightly less connective tissue visible in the THP-treated samples. The other treatment times show a large amount of space between the muscle fibres, likely due to damage to the tissues during freezing. Therefore the four changes treatment time appears to have more successfully prevented the damage and held the muscle fibres together than the other treatment times.

Glutaraldehyde-fixed: THP-fixed:

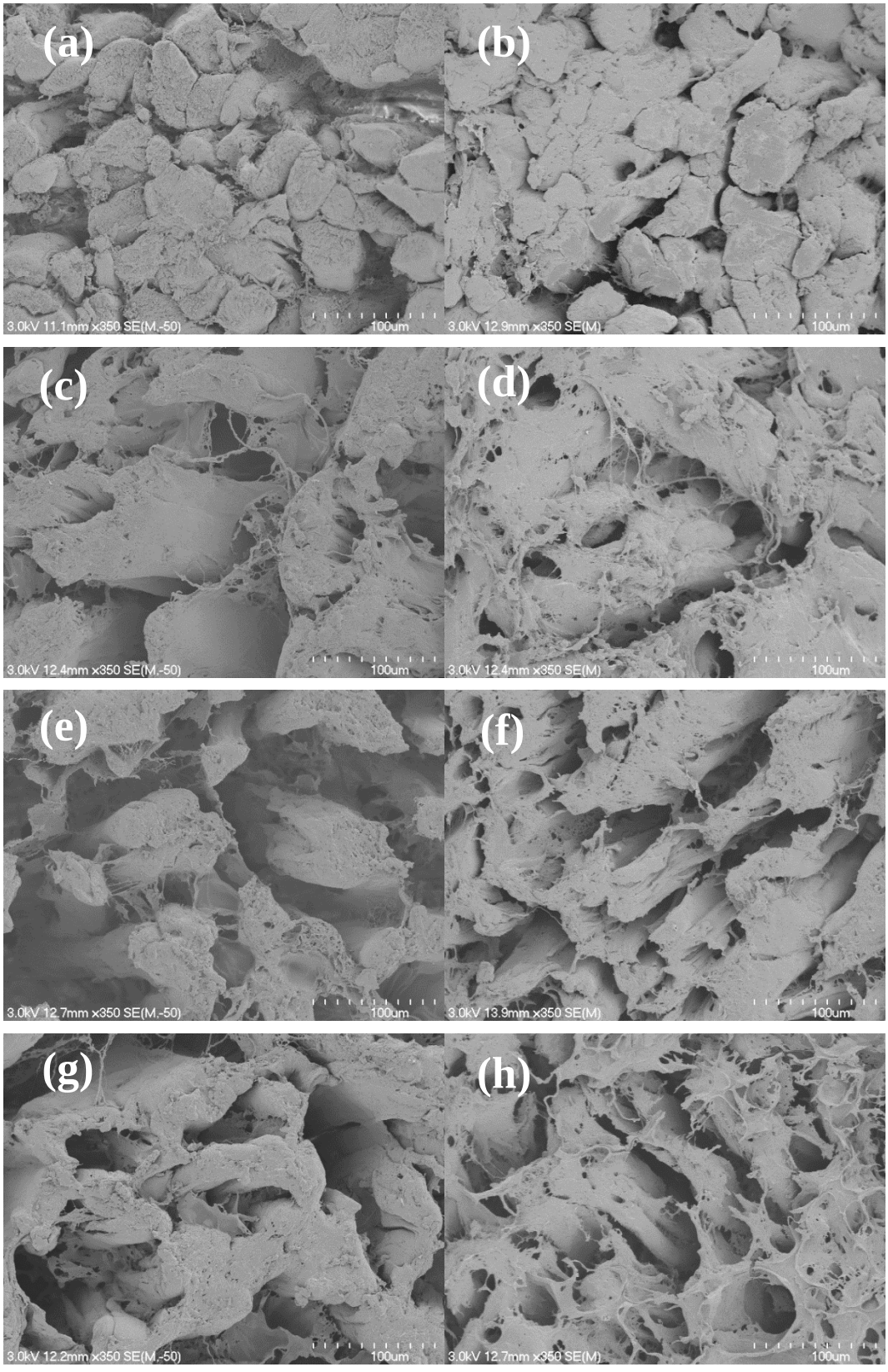

Figure 2.5: SEM images comparing fixing times: (a) and (b) treated for four changes over 30 minutes; (c) and (d) for 1 hour; (e) and (f) for five minutes; (g) and (h) for 6 hrs. Magnifications used are x350 for all images.

When looking under a higher magnification some of the finer endomysium lattice is seen on the muscle fibre, indicated by the arrow in Figure 2.6. The THP-treated sample does not have these same fine collagen fibres between the muscle fibres. The reason for this is unknown, as THP has been shown to bind to collagen[27], and therefore should preserve the connective tissue. The ends of the muscle fibres themselves are also very flat. What appears to be marks from cutting the chicken with the scalpel can be seen on the right of the image (b). Because the muscle fibres in the four changes samples are thicker, and likely were fixed more effectively than the other treatment times, there is less space between the fibres. It is still there, however, which could be due to dehydration when the samples were frozen.

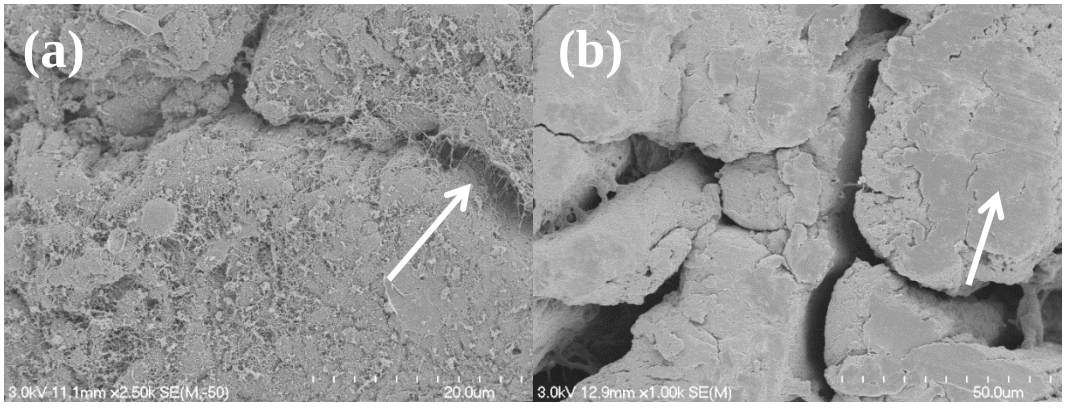

Figure 2.6: SEM images at higher magnification of the four changes fixing time. (a) four changes of glutaraldehyde, x2.50k magnification; and (b) four changes of THP, x1.00k magnification.

2.3.1.3 Conclusion:

Initial tests showed that the THP-treated chicken samples appeared very similar to the glutaraldehyde samples, therefore THP seemed to be fixing the samples to a satisfactory extent. More trials were needed to prove this, but the chicken samples needed to be fresh not frozen to get improved samples for both glutaraldehyde and THP.

A suitable fixing time was not determined during this trial, however, the six hour treatment time did not appear much different from the one hour and four changes over 30 minutes fixing times. Therefore it was not used in the next trial because the next trial aimed to do the fixing process and then dehydration in the ethanol series in the same day. A six hour treatment time is not suitable for this timeframe.

2.3.2 Second Trial: Using Fresh Chicken

The first trial had used frozen chicken because this was the most convenient way to store the samples while they were going through the treatment steps. This second trial used fresh chicken, where the samples were stored in the fridge prior to fixing, instead of the freezer. The muscle fibres in the samples appear to be more successfully fixed than in the first trial and this reinforces the idea that freezing damages the muscle tissue.

As outlined in Table 2.1, this trial used the same fixing times as the first trial only without storing the chicken samples in the freezer. The type of chicken used was thigh meat instead of breast meat like the first trial. Chicken breast is the best type to use because slices of the muscle belly give the best cross-section of the muscle fibres. The chicken thigh used in this experiment gave adequate cross-sections of the muscle fibres but leg meat (as used in the third trial) was not suitable. During treatment the glutaraldehyde solution and the chicken samples became yellow and the THP-treated chicken was bleached of colour, in the same way as the first experiment.

2.3.2.1 A comparison of the two fixing solutions:

As in the first experiment, there is still space between the muscle fibres but the muscle fibres appear much thicker than the previous samples. This time however, some of the fine structure of the muscles was able to be fixed. The end of a single muscle fibre can be seen in Figure 2.7 and Figure 2.8. They show a fine mesh of collagen fibres (the endomysium), labelled (e). More importantly, some of the myofibrils (m) that make up the muscle fibre can be seen alongside the edges of

the muscle fibre. The striated pattern appears in the SEM as "bumpy" patches[49, 54] instead of how it appears as light-dark patterns in TEM[55] or light microscopy[29].

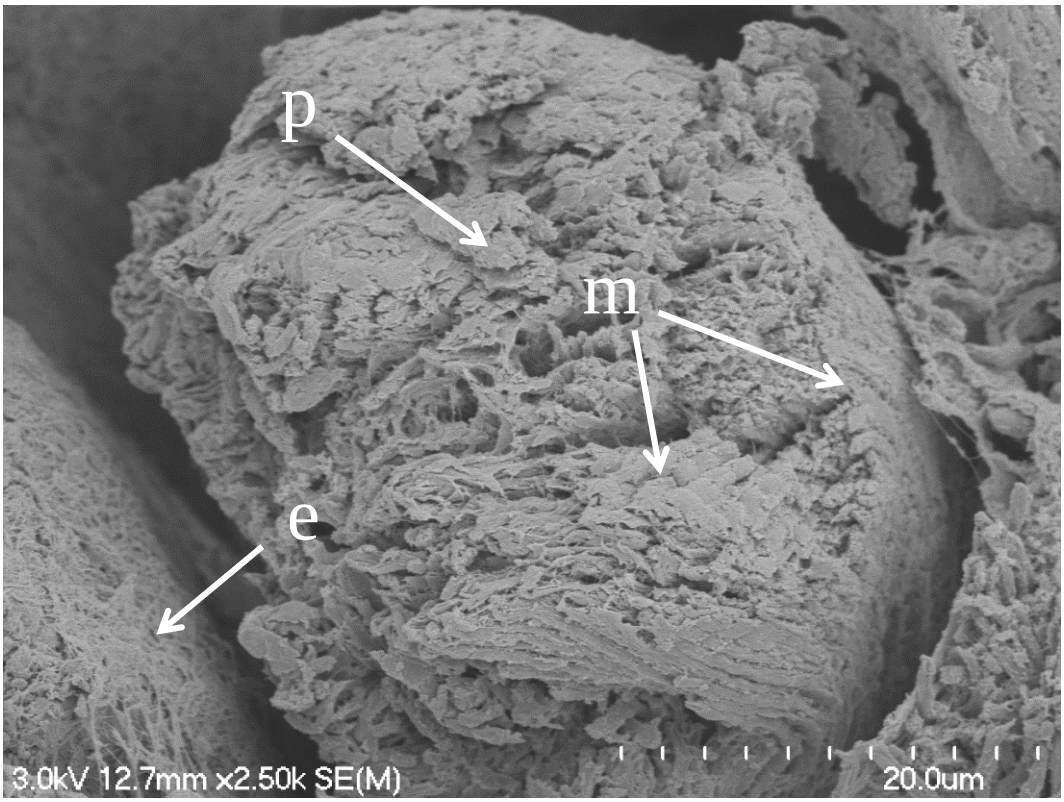

Figure 2.7: The fine structure of a single muscle fibre, showing myofibrils (m) and endomysium (e). "Plate-like" ends of myofibrils are also present (p). Treated with glutaraldehyde for 1 hour, x2.50k magnification.

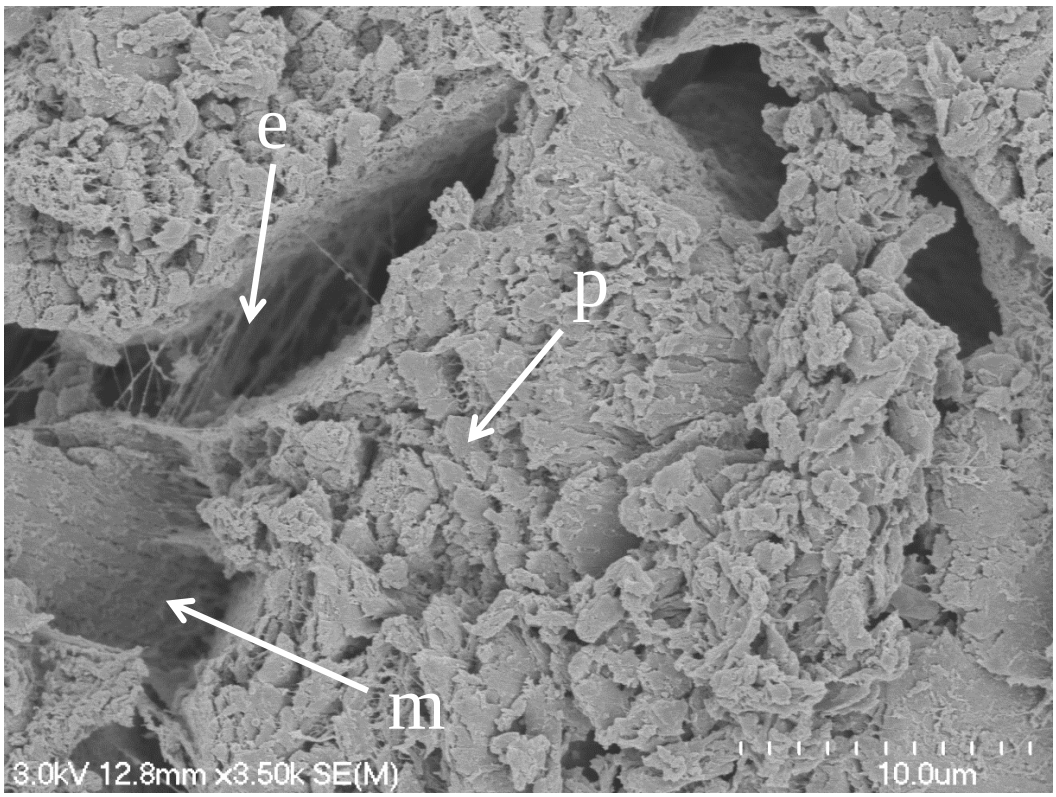

Figure 2.8: Another example of the fine structure of muscle fibres, showing the striated patterned myofibrils (m), endomysium (e) and more "plate-like" ends of myofibrils (p). Treated with THP for 5 minutes, x3.50k magnification.

The sample shown in Figure 2.7 was fixed with glutaraldehyde, showing the type of fine structure expected when fixing skeletal muscle. Figure 2.8 shows the same details in a sample fixed with THP. This shows that THP can be used as a biological fixative for SEM. However, for a complete comparison, samples fixed with glutaraldehyde and THP need to be compared with an untreated sample. This was done in the next set of samples.

At low magnifications, as seen in Figure 2.9 (a) and (b), the glutaraldehyde-treated and THP-treated samples appear very similar. There is less space between the muscle fibres than in the first experiment. This was likely due to the samples being used fresh for this experiment instead of being frozen between stages in the treatment. At higher magnification, the ends of the myofibrils in the muscle fibre in the THP-fixed sample, Figure 2.9 (d), look "plate-like" as mentioned earlier.

The myofibrils in the glutaraldehyde-treated sample, (c), look more like individual fibres. There are some “plate-like” myofibrils also present in the glutaraldehyde-treated sample. The appearance of the ends of these myofibrils may be due to the cutting technique used.

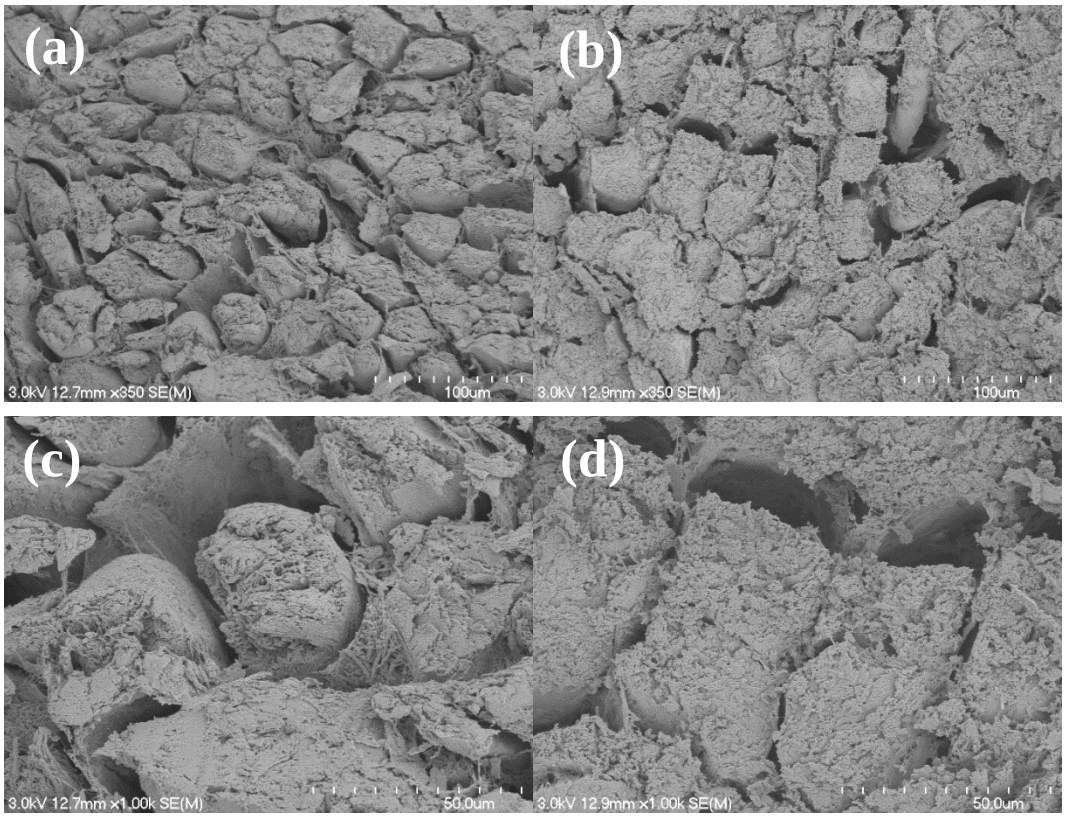

Figure 2.9: A comparison of glutaraldehyde-treated samples (a) and (c), x350 magnification; and THP-treated samples (b) and (d), x1.00k magnification. All samples were treated for 1 hour.

An interesting image was taken of the THP sample treated for 1 hour, shown in Figure 2.10. It shows the collagen fibres that make up the connective tissue. The fibres are possibly part of the perimysium, which collects the muscle fibres into bundles or fascicles. The endomysium is more “cob-web” like and the magnification is too high for it to be part of the epimysium.

Figure 2.10: An image from the sample fixed with THP for 1 hour, showing collagen fibres, x15.0k magnification.

2.3.2.2 Comparing fixing times:

Samples that were fixed for five minutes, as shown in Figure 2.11, look similar to those that were fixed for 1 hour. Both THP and glutaraldehyde have fixed the samples somewhat successfully with soaking for only five minutes. This is why a range of fixing times was trialled in these experiments.

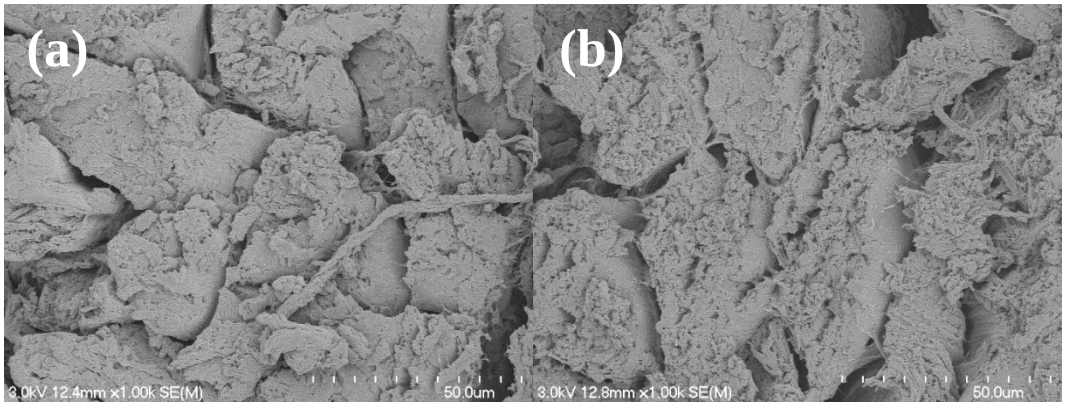

Figure 2.11: A comparison of samples fixed for five minutes, (a) fixed with glutaraldehyde and (b) fixed with THP; x1.00k magnification.

The sample that was fixed with THP for four changes over 30 minutes was equally successful; Figure 2.12 shows the THP treated sample. Another example of the "plate-like" myofibrils can be seen in the image (b). There is also some connective tissue filling in the gaps between the muscle fibres visible in (a). The gaps between these muscle fibres are smaller than those of the other samples (1 hour and five minutes) for both glutaraldehyde- and THP-treated samples. These gaps between the muscle fibres are due to the sample shrinking as it is dried, which is what fixing aims to prevent. It therefore appears that fixing for four changes over 30 minutes is the most successful fixing regime.

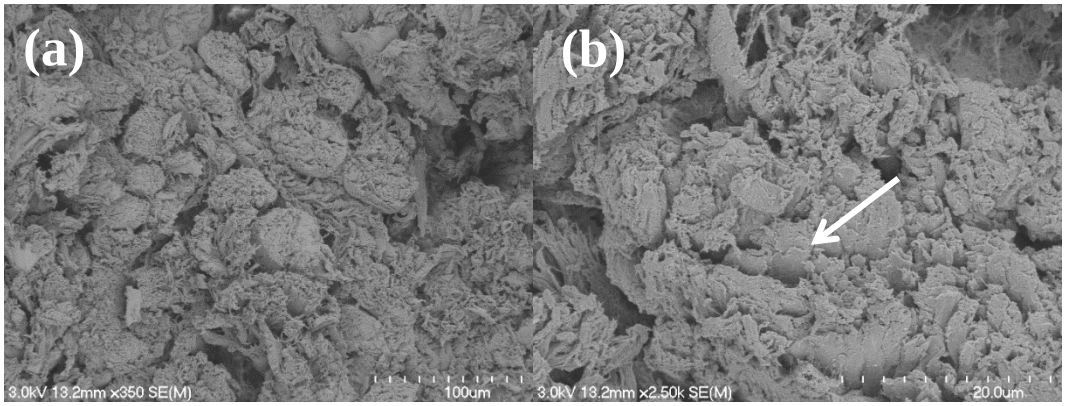

Figure 2.12: The sample treated with THP for four changes over 30 minutes: (a) is x350 magnification showing muscle fibres and (b) is x2.50k magnification showing the myofibrils that make up the muscle fibres.

However, the four changes sample fixed with glutaraldehyde appeared completely different from all of the other samples. Figure 2.13 shows the visible appearance of the chicken pieces during sub-sampling. After dehydration with ethanol the glutaraldehyde-treated samples had darkened around the edges (both the five minutes and 1 hour samples) while the four changes sample appeared nearly completely black. All the THP samples appeared pink, as shown in the image (c) in Figure 2.13. The way the samples are orientated in the pictures is so that the muscle fibres are facing up, cross-sectioning them in the way that all samples were prepared.

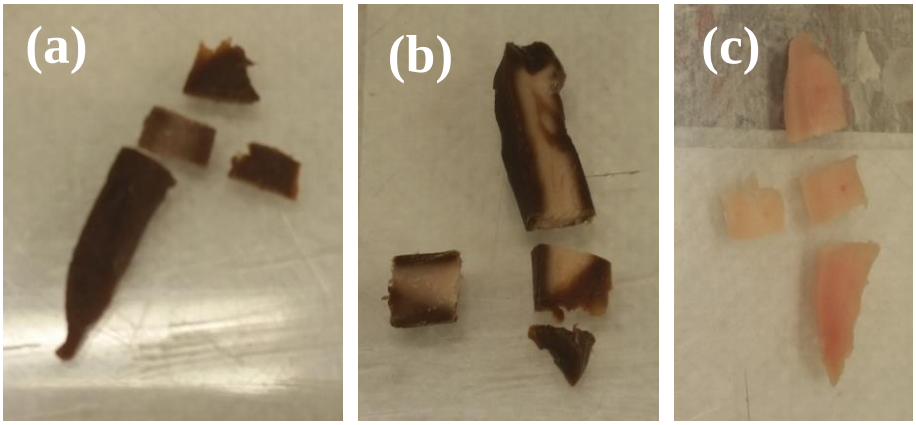

Figure 2.13: Images of selected glutaraldehyde- and THP-treated samples after dehydration with ethanol, before CPD. They also show the way the chicken pieces were sub-sampled before CPD. (a) is glutaraldehyde four changes, (b) is glutaraldehyde 1 hour and (c) is THP four changes. Each sample is approximately 1.5 cm long.

During the fixing process, the glutaraldehyde solution and samples appeared yellow, while the THP solution remained colourless and the samples bleached of colour slightly. The other trials, however, showed this same discolouration, yet the samples looked normal under the SEM. The differences in the fixing solutions are shown in Figure 2.14.

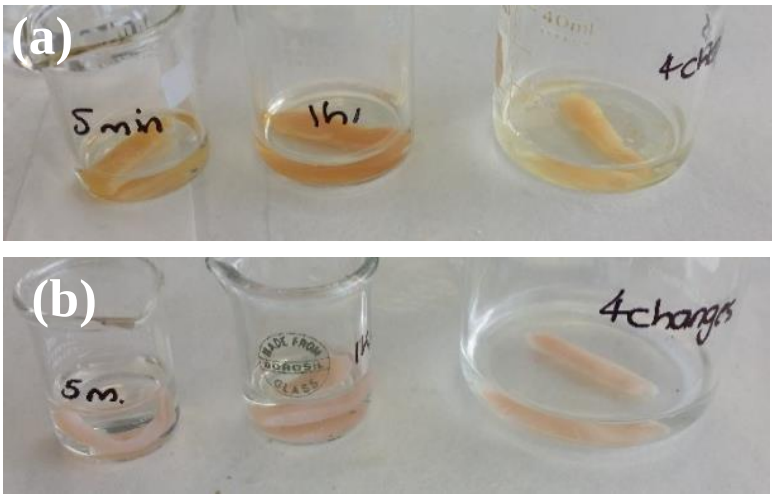

Figure 2.14: Differences in solution and sample colour for (a) glutaraldehyde-fixed samples and (b) THP-fixed samples taken five minutes into the experiment. The beakers are labelled left to right, five minutes, 1 hour, four changes.

Under the SEM, Figure 2.15 (a) and (b), the four changes sample appeared smooth, without the distinct bundles of fibres that the other samples showed. Even at higher magnifications, image (b), it appears as if a layer of broken fibres has coated the surface of the sample.

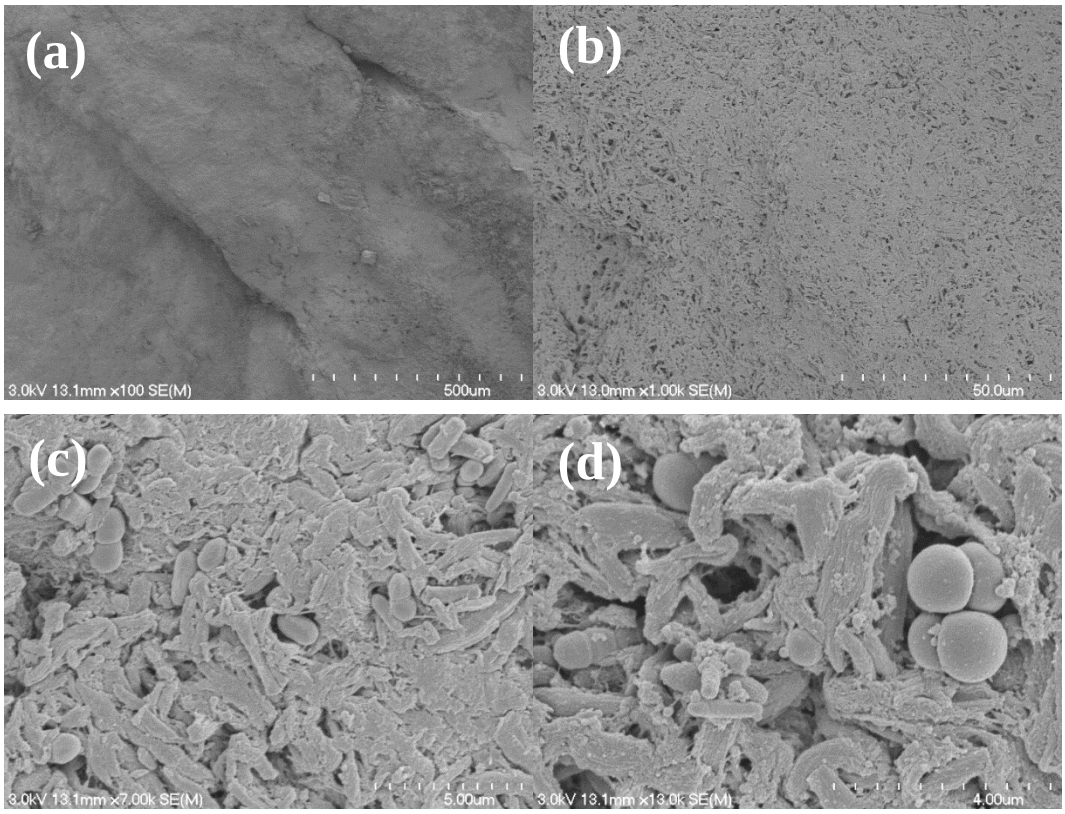

Figure 2.15: SEM images from the sample treated with glutaraldehyde for four changes over 30 minutes. Magnification is: (a) x100, (b) x1.00k, (c) x7.00k and (d) x13.0k

At even higher magnifications bacteria can be seen on the surface of the sample, as shown in Figure 2.15 (c) and (d). There are both rod-shaped (bacilli) and oval-shaped (cocci) bacteria, in groups or filaments, or on their own. After finding these bacteria, the other samples were re-examined using higher magnifications, but no other sample had this many. On the glutaraldehyde sample treated for 1 hour, four cells were found but they were much smaller than the ones on the four changes sample. None were found on the THP samples. The bacteria most likely originated from a chicken sample that was contaminated after cutting, because they only appear on one sample. Glutaraldehyde is used to fix bacteria for

examination under the SEM so if the sample became contaminated then the bacteria would be preserved along with the sample.

The reason for the darkened sample (and as to why the edges of the other glutaraldehyde samples also darkened) is unknown. While the literature mentions discolouration of samples by glutaraldehyde, it did not seem to have any cases of glutaraldehyde altering a sample to this extent. The appearance of the discoloured four changes sample under the SEM is also unusual, as the other glutaraldehyde samples in the other trials showed discolouration, but appeared normal under the SEM. While artefacts can be introduced to samples when they are fixed for SEM[37], it is usually something caused by dehydration[34]. It was thought that maybe the cacodylate buffer used when preparing the 2.5% glutaraldehyde solution may have caused it, because it was not made up fresh when these samples were prepared. The next experiment included samples prepared with a glutaraldehyde solution made from the old buffer and one made up with a freshly prepared buffer. The glutaraldehyde itself may also have been the cause since it undergoes polymerisation when in storage[47] and is known to discolour protein samples[45]. The opened vial of glutaraldehyde was kept in an air-tight container and refrigerated for the duration of this research. Long-term storage in fixative solutions can introduce artefacts[38] which may be similar to the darkened four changes sample. With this in mind, the next set of samples would include fixing times of approximately one month for glutaraldehyde and THP.

It should also be noted that while the outsides of the other glutaraldehyde samples (five minutes and 1 hour) had darkened, under the SEM the edges of the sub-sampled pieces did not have the same smoothness to them that the four changes sample did, seen in Figure 2.16. If the reason for the darkened four changes

sample was a mistake in, e.g. preparing the glutaraldehyde fixing solution then all of the glutaraldehyde samples should have been affected the same way, with the same kind of smoothness under the SEM.

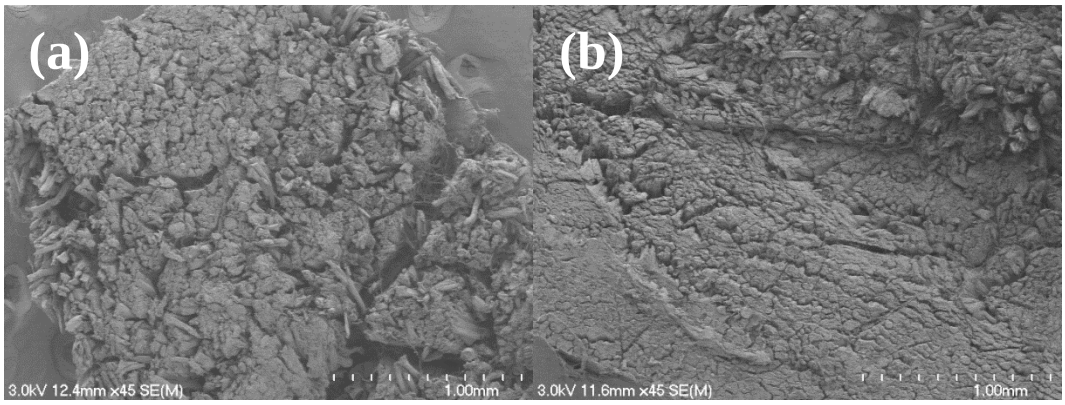

Figure 2.16: Low magnification images (x45) of two glutaraldehyde samples: (a) fixed for five minutes and (b) fixed for 1 hour.

2.3.2.3 Conclusion:

Overall, the trial appears to have been successful in fixing the chicken samples (except for the four changes glutaraldehyde-treated sample). The THP-treated samples appear similar to the glutaraldehyde-treated samples. The muscle fibres in both samples appear to be fuller than in the first trial, and some of the myofibrils that make up the muscle fibres are visible in samples from both fixative solutions. The trial was not, however, successful in fixing the glutaraldehyde-treated sample, treated for four changes over 30 minutes. Because of this abnormal sample, the experiment was repeated.

When comparing glutaraldehyde fixing times in the literature the average appears to be approximately an hour (when fixed at room temperature). The five minute fixing time was not included in the next trial because it seemed insufficient.

2.3.3 Third Trial: Determining the Reason for the Discoloured Chicken Sample

One of the aims of this trial was to see whether the age of the cacodylate buffer was the reason for the darkened four changes over 30 minutes sample in the previous experiment. A fresh cacodylate buffer solution was used to make up a glutaraldehyde solution as well as a glutaraldehyde solution made up with the old buffer (approximately three months old) and separate samples were treated with these. In order to compare glutaraldehyde and THP as fixative solutions, untreated chicken (no fixative solution but dehydration and drying still done the same) was required as a control, so it was included in this trial. The effect of long-term fixation was looked at also, by placing chicken samples in either glutaraldehyde or THP and storing them in the fixative solutions in the fridge for approximately one month. The samples were examined under the SEM with the samples from the fourth trial. The other two fixing times that were used in this experiment were one hour and four changes over 30 minutes, because these appeared to be the most effective fixing times in previous trials.

As mentioned in Table 2.1, the chicken type used for this experiment was leg meat, and it is because of this the sample quality is poorer. The size of the muscle belly on the leg samples was smaller and therefore slices of the chicken piece do not show suitable cross-sectioning of the muscle fibres. The fibres in these samples are not aligned in one direction like with chicken breast. They need to be end-on like the previous samples, which is what is required to view the inside of the muscle fibres. The poor quality of the samples when viewed under the SEM were because of this and cannot be compared with the previous two trial experiments.

The surface of all of the samples (including the THP ones) appeared under the SEM as very smooth with no distinct bundles of fibres, as shown in Figure 2.17, unlike samples in the two previous trials. Some of the samples, especially the THP four changes sample (f), show muscle fibres running length-ways instead of being end on. Because of this the experiment was repeated (see section 2.3.4).

Treatment times:

One hour: Four changes over 30 minutes:

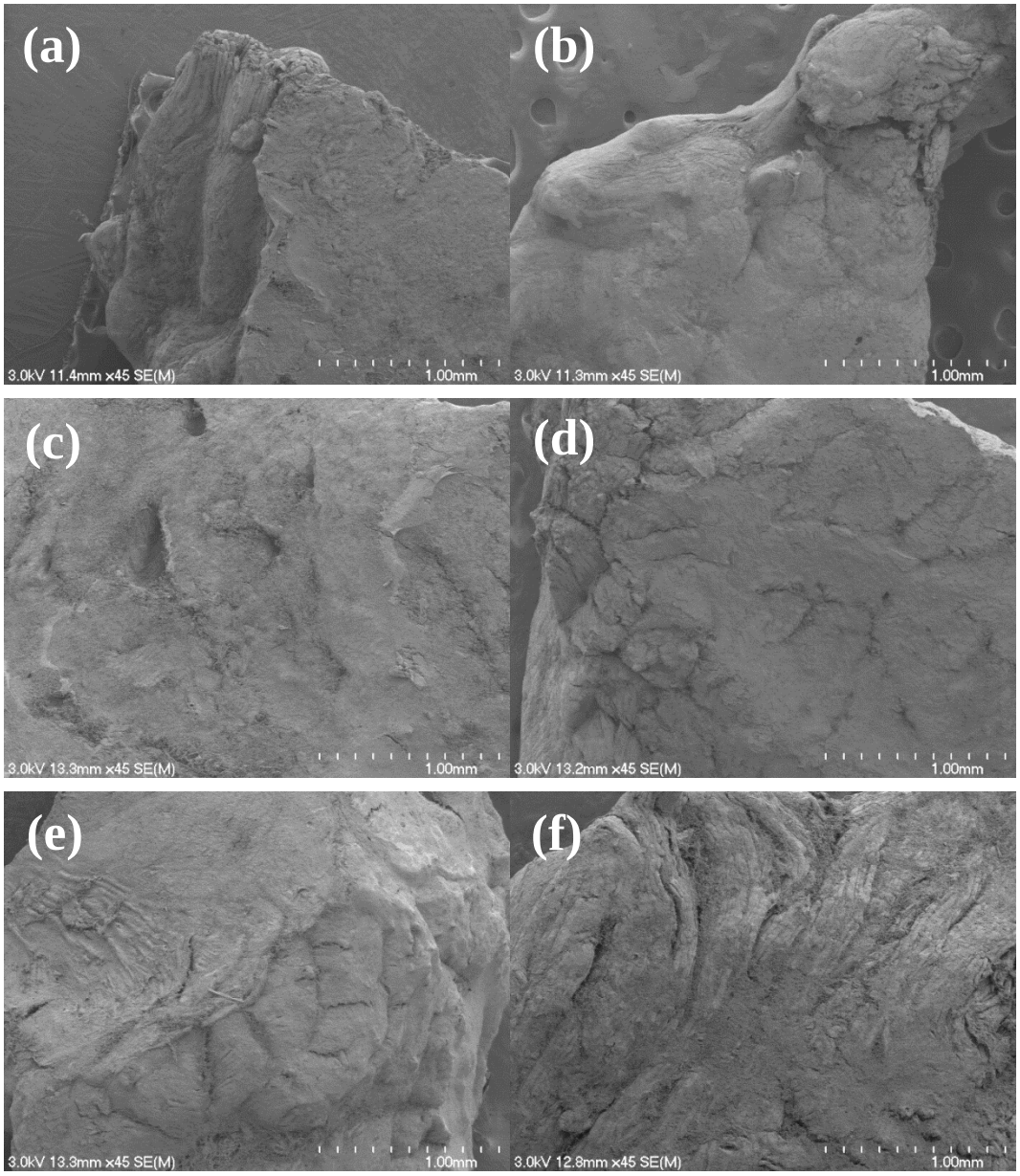

Figure 2.17: Low magnification (x45) images showing the smooth surface of the samples: (a) and (b) fixed with glutaraldehyde and the new buffer; (c) and (d) fixed with glutaraldehyde and the old buffer; (e) and (f) fixed with THP.

In the previous experiment, the glutaraldehyde-treated, four changes over 30 minutes sample appeared smooth because the surface was covered with what appeared to be broken myofibrils from the muscle fibres. The surface of all of this set of samples also looked like this, except there were no bacteria present. Figure 2.18 shows a higher magnification of the surface of the samples and shows that the surfaces of these samples are also covered with broken myofibrils. Muscle

fibres running length-ways are visible beneath some of the broken myofibrils, which can be seen in image (d). The image (a) shows some broken muscle fibres as well as broken myofibrils, which make up the muscle fibre.

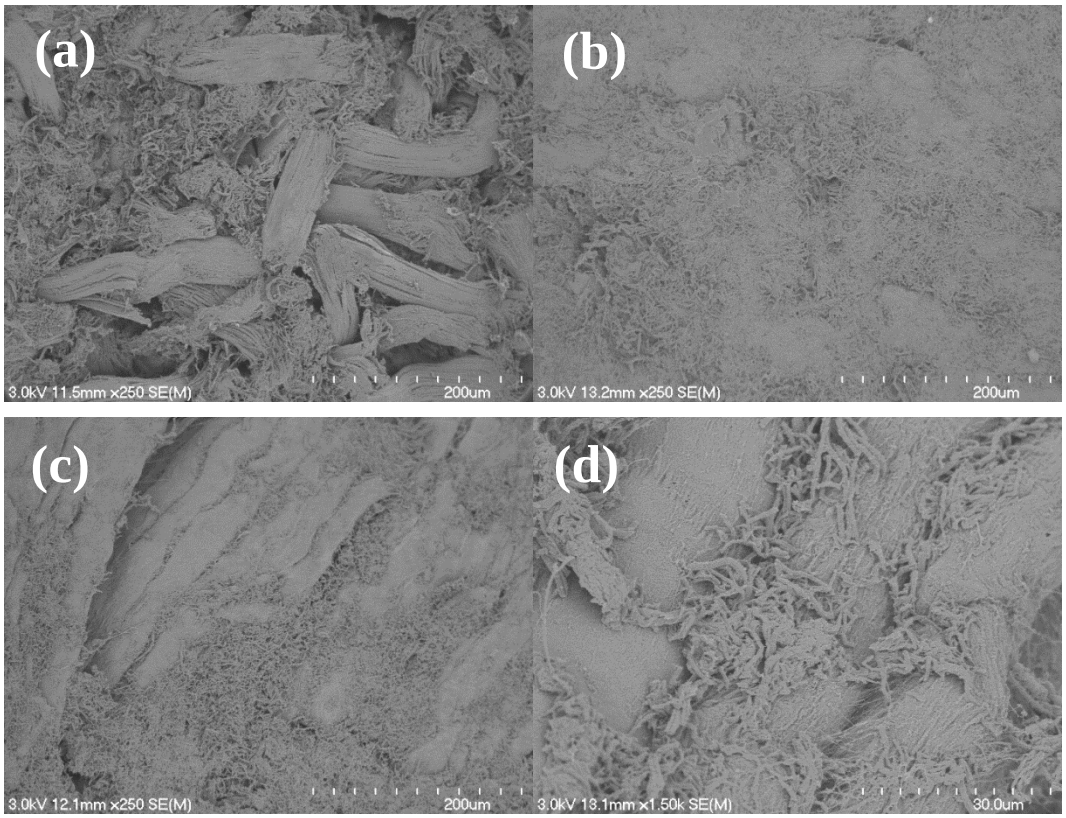

Figure 2.18: Close ups of the broken myofibrils: (a) glutaraldehyde, new buffer, 1 hour; (b) glutaraldehyde, old buffer, 1 hour; (c) and (d) THP four changes. Magnification is x250 for (a) – (c) and x1.50k for (d).

2.3.3.1 A comparison of fixing solutions and times:

The images in Figure 2.19 compare samples treated with the two different buffers (the "old" buffer had been prepared for the first set of samples in the first trial and the "fresh" buffer was made up the same day as these samples were treated). They were taken where the muscle fibres appeared most distinct, as the rest of the chicken sample looked quite smooth. Most of the fibres visible in these images were not cut end-on but run long-ways along the surface of the sample.

Old Buffer: Fresh Buffer:

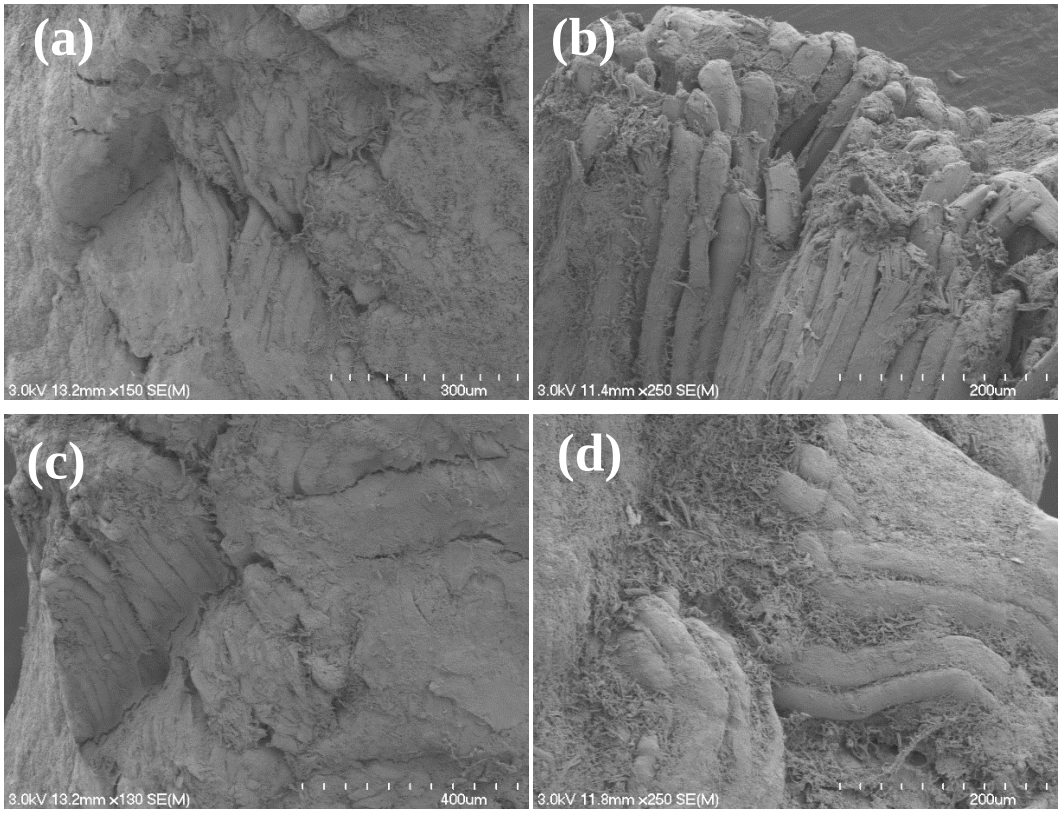

Figure 2.19: Glutaraldehyde-treated samples comparing the old buffer with the fresh buffer: (a) and (b) were treated for one hour, (c) and (d) were treated for four changes over 30 minutes. Magnification is (a) x150, (b) and (d) x250, and (c) x130.

Higher magnification images, shown earlier in Figure 2.18 (a) and (b) show the surface of these glutaraldehyde-treated samples (both buffers) covered with broken myofibrils. The samples fixed using the two different buffers have the same appearance and it appears that the buffer has no effect on the quality of the sample. The discolouring of the samples from the previous experiment may therefore, have been a more severe reaction of the proteins to glutaraldehyde, which can cause yellowing of the sample[45].

The samples that were stored in each fixative solution for one month in the fridge (which were looked at under the SEM with the next set of samples) had to be sub-sampled before CPD unlike the other chicken samples in this trial. The glutaraldehyde-treated sample had discoloured and the THP-treated sample had

bleached, both like the other samples in this trial. The surface of both these samples appears smooth like the samples from the other treatment times. This smoothness, like the other samples in this trial, also appears to come from broken myofibrils coating the surface, as can be seen in Figure 2.20 (c). The THP-treated sample in (d) shows where some of the myofibrils are breaking off the end of a muscle fibre (indicated by the arrow). It was taken from the area where the sample was cut during sub-sampling. Image (c) shows the un-subsampled surface. The discolouration of the samples can be an indication of the penetration of the fixative[45]. Because the entire sample appeared blackened (which could be seen during subsampling), the area of the sample where the images were taken should not affect the results in terms of the effectiveness of the fixative.

Glutaraldehyde-treated THP-treated

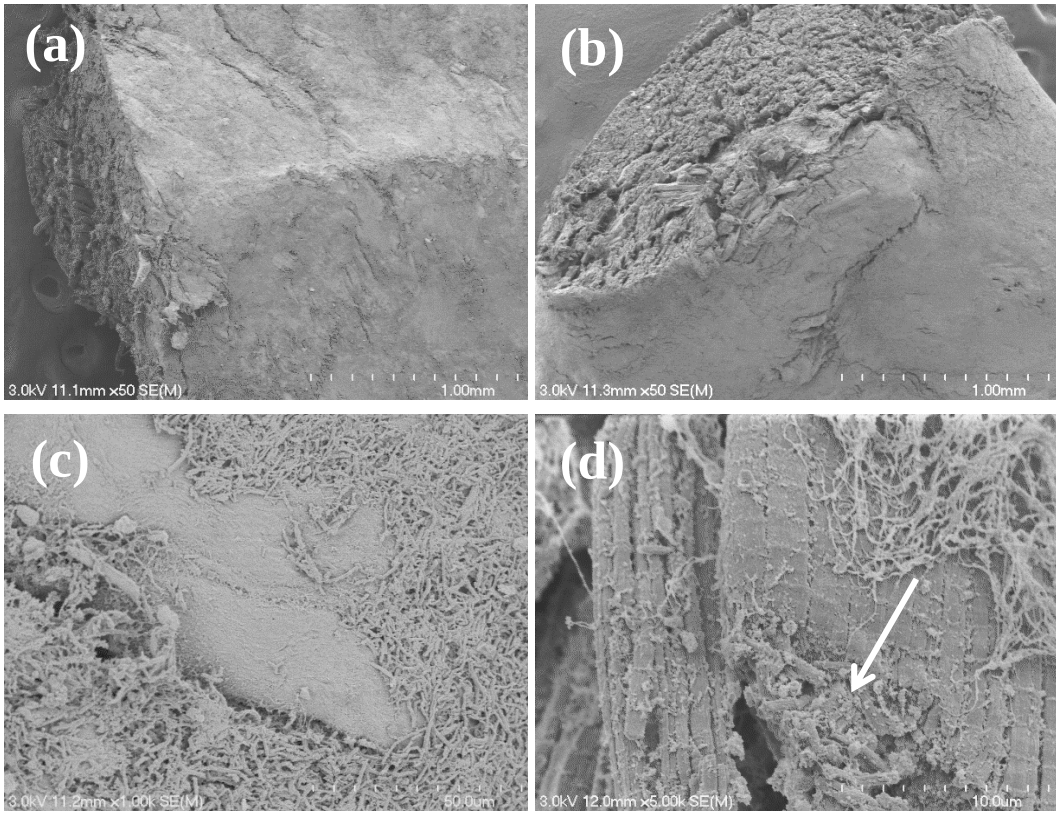

Figure 2.20: Samples treated for one month in the fridge: left treated with glutaraldehyde, right treated with THP; (a) and (b) are x50 magnification, (c) is x1.00k and (d) is x5.00k magnification.

This trial aimed to use untreated chicken as a control when comparing glutaraldehyde and THP as fixatives from this experiment and the previous experiments. However, because the samples did not appear as expected due to the chicken type, the untreated sample cannot be compared to the other samples. When this experiment was repeated in the final trial, an untreated sample was included.

Some bundles of muscle fibres are visible in this sample, as can be seen in Figure 2.21 (a). The gaps between the bundles of muscle fibres (indicated by the arrows) are larger in this sample than the other treated samples in this trial. This is likely due to shrinking when the sample was dehydrated and dried. At a higher

magnification (image (b)) the surface of the sample appears to also be covered in broken myofibrils like the other samples.

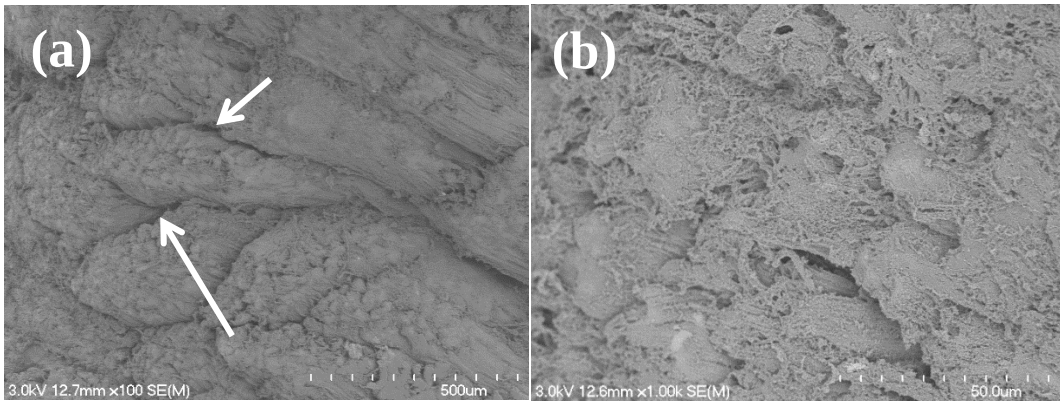

Figure 2.21: The untreated chicken sample. Magnification is (a) x100 and (b) x1.00k

2.3.3.2 Conclusion:

The age of the buffer solution does not appear to have any effect on the glutaraldehyde-treated samples. Long-term treatment of a sample for one month also appears to not affect the appearance of the samples. The type of chicken meat used in the experiment does appear to have an effect on the sample appearance. Because of this the experiment was repeated.

2.3.4 Final Experiment:

The preceding experiments acted as trials to determine whether THP would work as a fixative and what procedures were needed for suitable comparison between glutaraldehyde and THP as fixative solutions. It was concluded that, to obtain suitable SEM images of muscle fibres to compare glutaraldehyde and THP as fixing solutions a number of things needed to be taken into account:

- The chicken type that gave the best cross-sectioned muscle fibres was chicken breast, due to the large size of the muscle belly.
- The chicken had to also be used fresh and not frozen as the freezing process damages the tissue.
- The best treatment times for the chicken samples appear to be one hour and four changes over 30 minutes.
- A control, in the form of an untreated chicken sample, also needed to be included when comparing glutaraldehyde with a new fixative solution to see whether the new solution works as a fixative.

This experiment took into account these points and the samples produced were able to be compared on their effectiveness at fixing the muscle tissue sample towards the native state of the sample[36].

2.3.4.1 A comparison of glutaraldehyde and THP as fixative solutions:

An initial comparison of the images in Figure 2.22 shows that the THP-treated samples appear more similar to the glutaraldehyde-treated samples than the untreated sample. This demonstrates that THP appears to be successful in fixing samples for SEM analysis.

Glutaraldehyde-treated for four changes over 30 minutes.

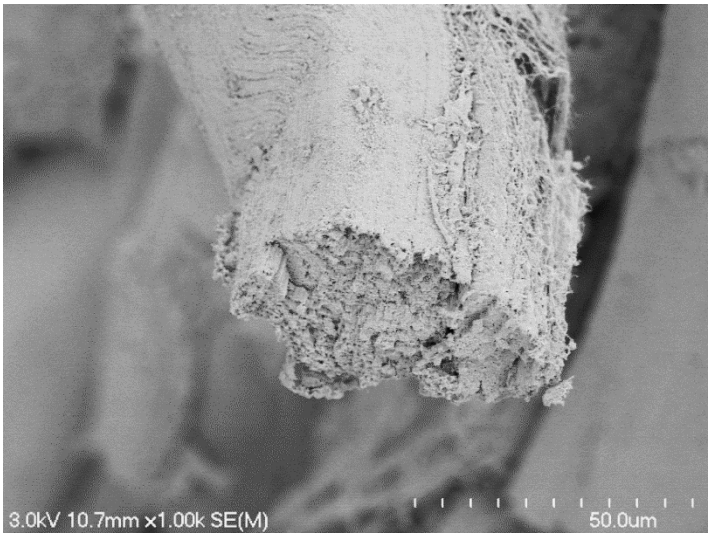

THP-treated for one hour.

The untreated sample.

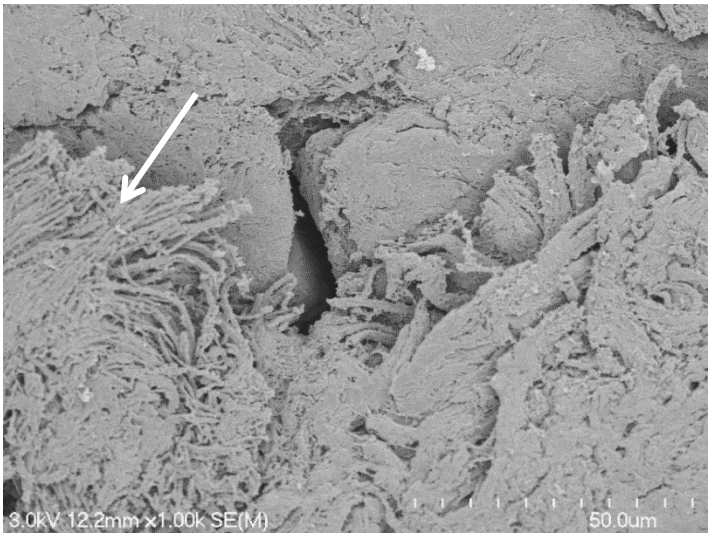

Figure 2.22: A comparison of the three treatments used in this experiment: glutaraldehyde-treated (top), THP-treated (middle) and untreated (bottom). Magnification used x1.00k.

The striated myofibrils that make up the muscle fibre are visible in each of the three images in Figure 2.22. However, the myofibrils in the untreated sample

(indicated by the arrow) do not appear striated and have separated from the muscle fibres, making it hard to distinguish the muscle fibre that the myofibrils make up.

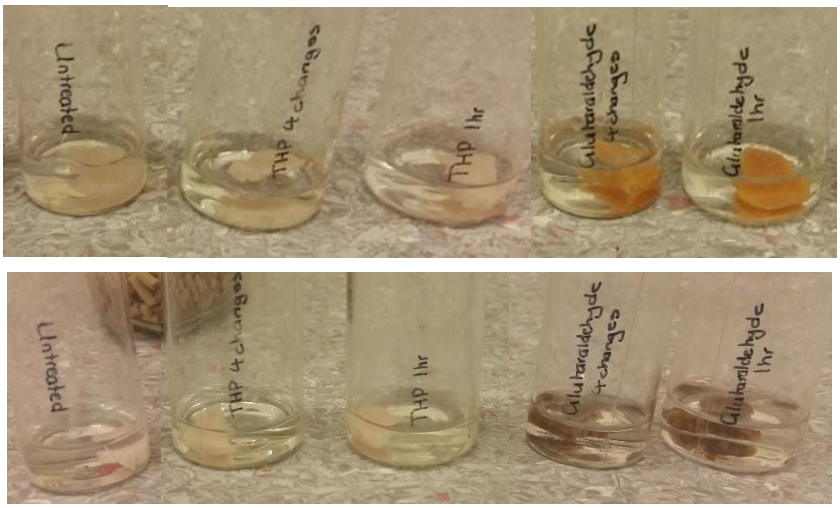

Figure 2.23: Top: Samples after treatment in the fixative solution, bottom: samples after dehydration in the ethanol series. From left to right: untreated, THP four changes, THP 1 hr, glutaraldehyde four changes, and glutaraldehyde 1 hr.

Like the previous trials, the chicken samples changed appearance after treatment in the fixative solution, this can be seen in Figure 2.23. The glutaraldehyde-treated samples gained a yellow tint, as did the solution they were soaked in and became brown in colour after dehydration using an ethanol series. It has been shown that glutaraldehyde appears yellow when reacted with proteins[45]. The THP-treated samples were bleached of colour but did not change after dehydration. THP has been used to bleach lignin[1] as mentioned earlier on page 27. The samples in this experiment had to be sub-sampled before CPD, after dehydration. Most of the SEM images were taken where the sample had been cut during sub-sampling. The extent of the yellowing or bleaching of the samples is an indication of how deep the fixative had penetrated[45]. The samples, shown in Figure 2.23, were discoloured through the entire sample, unlike some samples from the second trial

(see Figure 2.13 on page 43), it can be assumed that the entire sample was fixed with the respective fixative solution.

Low magnification (x50) images of the four treated samples show a few differences between the THP- and glutaraldehyde-treated samples, as seen in Figure 2.24.

Glutaraldehyde-treated THP-treated

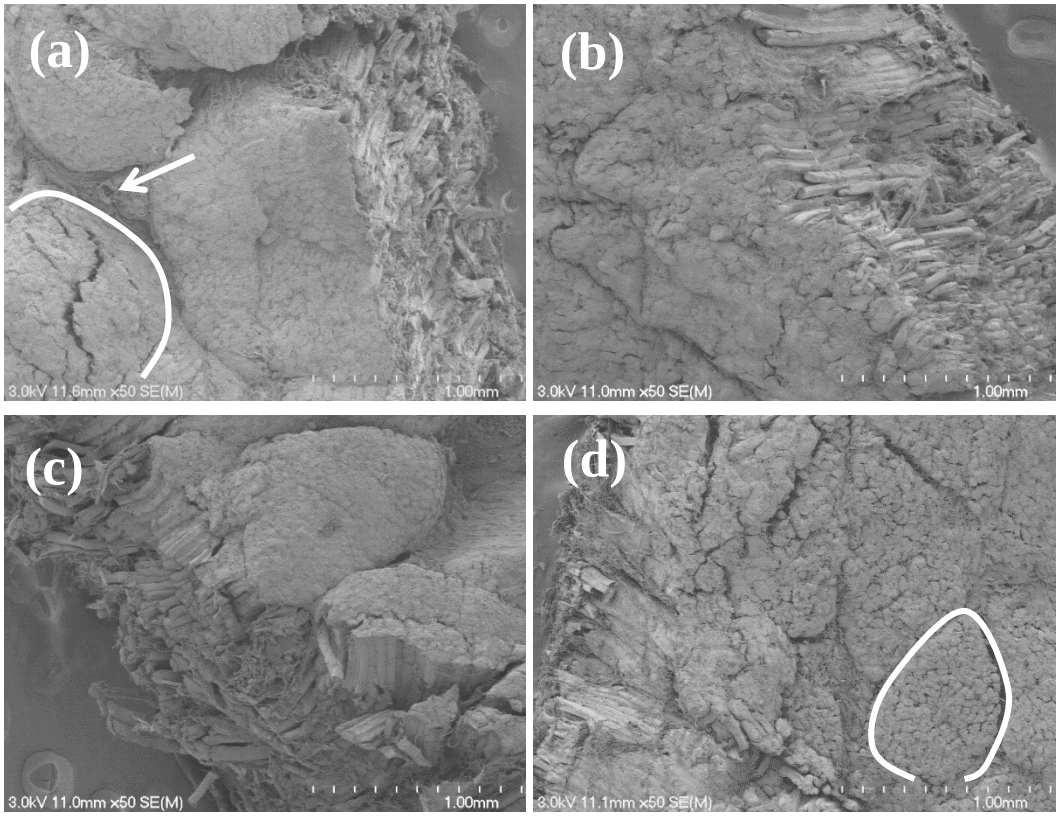

Figure 2.24: Samples from the final experiment: (a) – (b) were treated for one hour, and (c) – (d) were treated for four changes over 30 minutes. Magnification is x50 for all images.

The glutaraldehyde-treated samples appear smoother than the THP-treated samples because the individual muscle fibres are not as visible. The bundles that the muscle fibres are organised into can be seen in all the samples, the lines indicate examples of a muscle fibre bundle in images (a) and (d). Image (a) shows an area of vessels in the perimysium[48] (which also encloses the muscle fibre bundles), indicated by the arrow. The THP-treated samples look closer to the

skeletal muscle diagram, Figure 2.1 on page 20, than the glutaraldehyde-treated samples. The more-visible muscle fibres in the THP-treated samples could be due to dehydration causing them to shrink creating space between them, or it could be due to the glutaraldehyde-treated samples becoming damaged when the samples were discoloured, coating the surface of the sample with broken myofibrils, which occurred in the glutaraldehyde-treated samples in the previous trials. Therefore at low magnification, the effectiveness of the fixative solutions cannot be judged fully.

The samples fixed for one hour, at higher magnification, are shown in Figure 2.25. The muscle fibres in images (a) and (b) between the two fixative solutions look quite dissimilar. The ends of the muscle fibres in the THP-treated sample, image (b), show the myofibrils that make up the sample, broken off where the sample was cut. The glutaraldehyde-treated sample alternatively does not show clearly any myofibrils, despite the images (a) and (b) occurring at the same magnification (x250).

Glutaraldehyde-treated THP-treated

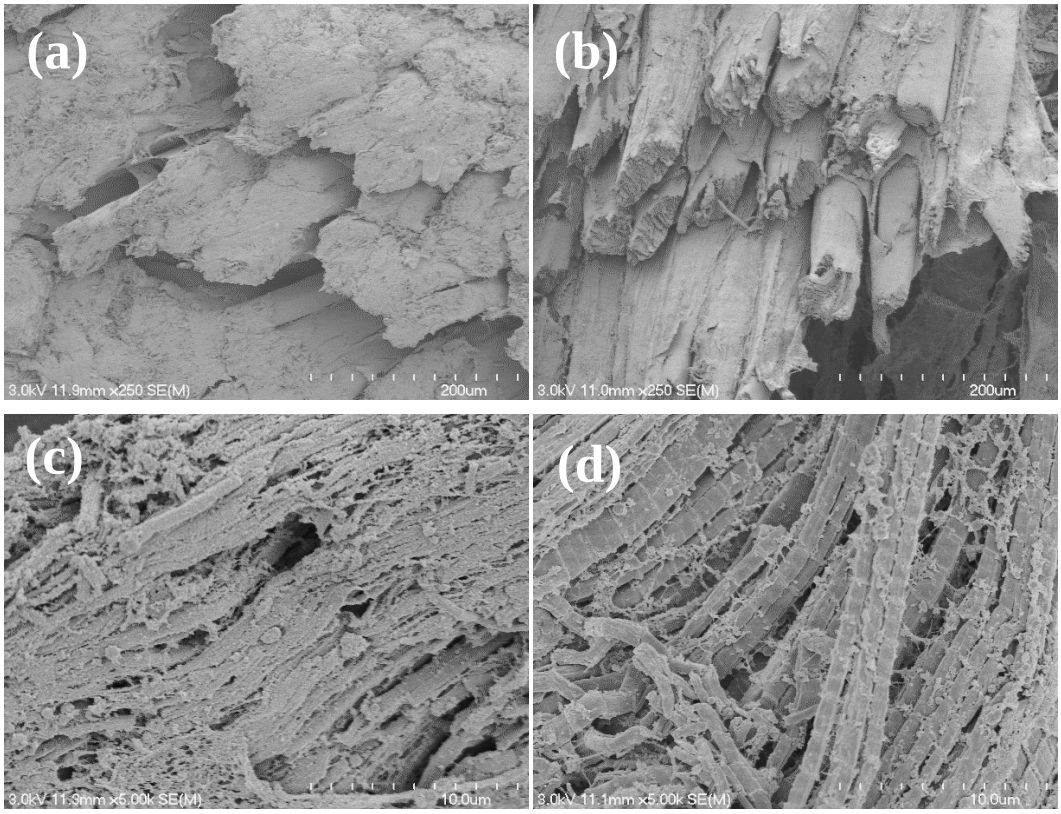

Figure 2.25: A comparison of samples treated for one hour: left treated with glutaraldehyde, right treated with THP, (a) and (b) x250 magnification, (c) and (d) x5.00k magnification.

When viewing the myofibrils themselves, at x5.00k magnification, the THP-treated sample shows a very clear striated pattern along each myofibril. The glutaraldehyde-treated sample however does not. This striated pattern is expected in muscle samples that have been fixed successfully. This shows that the THP is effectively fixing the sample, and may be more effective than glutaraldehyde.

The muscle fibres in the samples treated for four changes over 30 minutes are not as clear as the samples treated for one hour. Shown in Figure 2.26, a large amount of connective tissue is visible around the fibres, indicated by the arrows in images (a) and (b). The fibres themselves appear to have been preserved successfully. At a higher magnification in images (c) and (d), the myofibrils that make up the muscle fibres do not show clear striated patterns, unlike the samples treated for

one hour. Image (d) shows where the myofibrils are breaking off the ends of the muscle fibre. It appears that this fixing time was not as successful at preserving the samples as fixing for one hour.

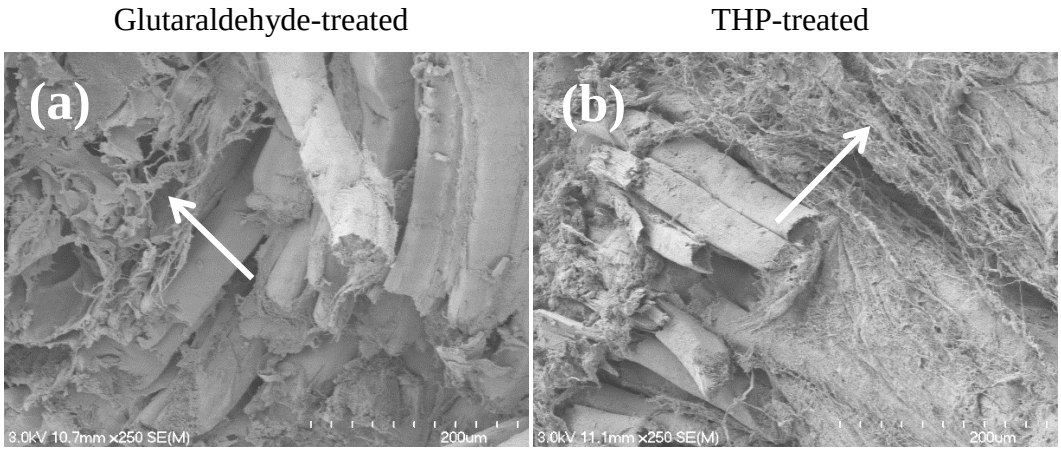

Figure 2.26: A comparison of the samples treated for four changes over 30 minutes: (a) – (b) x250 magnification, (c) – (d) x2.50 magnification.

2.3.4.2 Comparing fixed samples with the untreated sample:

Comparison with an untreated chicken sample was needed to properly test the effectiveness of THP as a fixative. The process of preparing a moist sample for SEM analysis is: chemical fixation (with glutaraldehyde or THP), dehydration (with an ethanol series) and drying (using CPD). A sample of raw chicken breast went through this process, omitting the chemical fixation step. If THP does not work as a fixative for SEM, then the THP-treated samples should look the same as the untreated sample.

As initially shown in Figure 2.22, the THP-treated samples appear more similar to the glutaraldehyde-treated samples than the untreated sample. This shows that THP is working as a fixative for the chicken samples.

During treatment (for all samples except those from the third trial) the chicken pieces kept their flat shape through treatment, dehydration and drying, and only

decreased in size as the water was removed. The untreated sample however, shrunk and curled inwards on itself, which explains the orientation of some of the muscle fibres in Figure 2.27, image (a). While the fixative solutions are meant to preserve the fine structure of the muscle, they also seem to preserve the overall shape of the sample, so it is not warped during treatment.

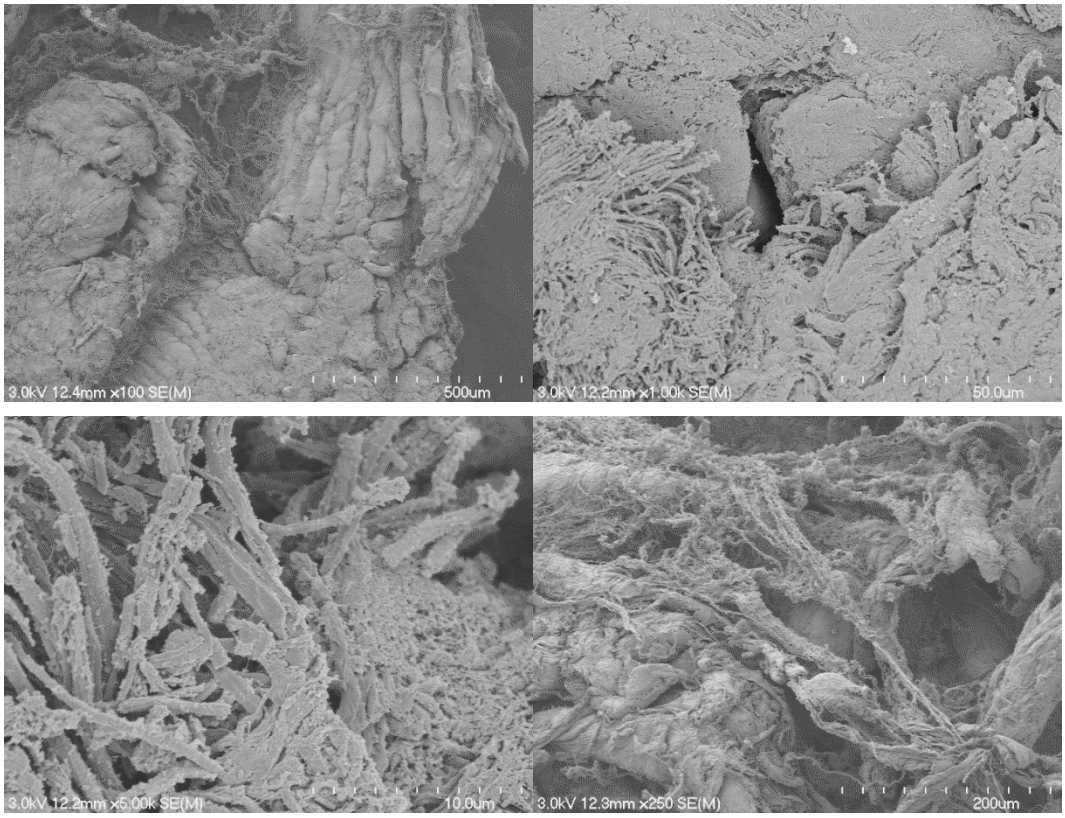

Figure 2.27: The untreated chicken sample. Magnifications: (a) x100, (b) x1.00k, (c) x5.00k, (d) x250.

At low magnifications, in image (a), the surface of the untreated sample looks smooth similar to the glutaraldehyde samples in this experiment in Figure 2.24. When looking closer at the myofibrils they do not appear grouped together in a muscle fibre, they instead are broken apart, as can be seen in images (b) and (c). This may be due to loss of the endomysium connective tissue that holds the muscle fibres together. This may also account for the smoothed out appearance of the surface in image (a). Image (d) shows what appears to be a tangle of connective tissue with no muscle fibres.

2.3.4.3 Conclusion:

From comparison with the untreated sample, the effect of THP as a fixative solution on skeletal muscle tissue can be determined. The THP- and glutaraldehyde-fixed samples appear to hold the sample in its overall shape, keeping the muscle fibres in their correct orientation and position. They also fix the connective tissue (which is made from proteins) which holds the muscle tissue together. THP appears to have been more successful at fixing the chicken samples than glutaraldehyde. The muscle fibres are clearer and the striated pattern of the myofibrils is visible in the THP-treated samples. The glutaraldehyde samples in this experiment appear to have been damaged and are not as successfully fixed as samples from the previous trials. This may be due to polymerisation of the glutaraldehyde[17] rendering it less effective over the course of this research or through reaction of the glutaraldehyde to the proteins in the sample[45]. The one hour fixing time for both fixative solutions also appears to have been more successful than the four changes over 30 minutes fixing time for both THP and glutaraldehyde. These samples that were treated for one hour appear as skeletal muscle is expected to look: muscle fibres are grouped together in bundles and the myofibrils are not breaking off the ends of the fibres, as they are in the samples treated for four changes over 30 minutes.

2.4 Conclusions and Future Work:

This project has demonstrated that THP is suitable as a fixative for biological samples being viewed under the SEM. There were issues with the glutaraldehyde samples. It would be useful to repeat the experiment using an unopened vial of glutaraldehyde when making up the solution. The standard procedure for preparation of the glutaraldehyde solution is to use a whole 10 mL vial with 90 mL of buffer.

The experiment could be extended to different biological samples, for example bacterial biofilms[34, 37] and plant tissues[35], as these are more often studied using SEM. Comparing the THP and glutaraldehyde samples with untreated samples using an ESEM or using cryo-SEM could also be used to compare THP as a fixative to SEM techniques that are closer to the native state of the sample.

There are a wide range of hydroxymethylphosphines known in the literature, and many are more hydrophobic than THP. Use of these may aid in the drying process.

Chapter Three: Attempted Synthesis of the Diiodine Adducts of Hydroxymethylphosphine Sulfides

3.1 Introduction:

3.1.1 Phosphine Chalcogenides:

There is a great affinity between the chalcogens, O, S and Se, and phosphorus. Research into chalcogen-phosphorus chemistry has been occurring for over 200 years[56]. Phosphine chalcogenides range from simple compounds containing just chalcogen and phosphorus, to large biomolecules and metal clusters[56]. Some of the main chalcogen-phosphorus compounds include tertiary phosphine chalcogenides, $R_3P{=}E$, and diphosphine dichalcogenides, $R_2P(E)R'P(E)R_2$, where R = alkyl or aryl and E = O, S or Se[56]. The simplest way to synthesise tertiary phosphine sulfides and selenides is direct combination of the tertiary phosphine with elemental sulfur[56]. The resulting compounds are quite stable in air[57]. Triphenylphosphine sulfide in particular, has high stability[58].

Bonding between phosphorus and the chalcogen atom, in the molecule R_3PE (E = Se, S or O), occurs by an sp hybrid σ-bond and by partial overlap of a pπ-bond with an empty dπ orbital of the phosphorus atom[59]. There is a weakening of the P-E down group 16, as well as increasing thermal and hydrolytic instability. This makes synthesis and handling of heavier chalcogenides more difficult[56].

3.1.2 Tertiary Phosphine Adducts with Halogens:

The chalcogenide atom, E in R_3PE, has two lone pairs, hence tertiary phosphine chalcogenides can act as a Lewis base towards a wide range of electrophiles. In addition to acting as ligands towards metal ions, they can form adducts with halogens by donation of electron density from lone pairs on E to empty orbitals on the halogen. These display a variety of different structural motifs[60], as shown in Figure 3.1.

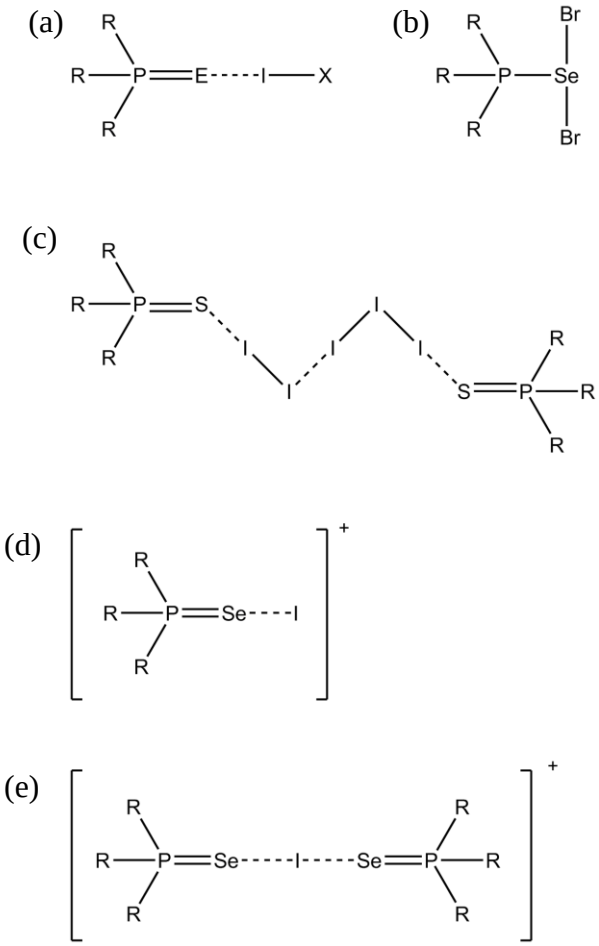

Figure 3.1: Structural motifs formed by halogen adducts of tertiary phosphine chalcogenides.

The two most common structural motifs are the simple 1:1 adducts (a) and (b)[60]. Compounds with the structure (a) are linear E-I-X charge-transfer compounds, where the chalcogen donor molecule interacts with the di- or inter-halogen

acceptor[56]. The second structure type (b) form insertion products with a 'T-shaped' P-E(X_2) structure. This most often occurs with Br_2 compounds[60]. Several more complex structures have also been reported, of the type (d) and (e)[60]. All R_3PE (R = alkyl or aryl) compounds form 1:1 adducts of the type (a) with I_2, IBr and ICl, in solution and the solid state[60-61]. Initially the reaction of Ph_3PS with I_2 produced an adduct of type (c), which had the unusual 2:3 (Ph_3PS:I_2) stoichiometry. The crystal structure showed one I_2 molecule bridging two TPPS.I_2 1:1 adducts by soft I-I interactions[62]. The 1:1 adduct was eventually synthesised and the crystal structure determined[61].

Further work[63] on the ratios of adducts formed showed that different stoichiometries were possible when prepared using a different solvent, even when using equimolar quantities of phosphine and halogen. For example, triphenylphosphine sulfide was shown to form a 2:3 Ph_3PS : I_2 adduct in carbon tetrachloride, a 1:2 adduct in chloroform and a 1:1 adduct in dichloromethane[63-64]. Other phosphines studied were tri-p-tolyl-phosphine sulfide, and the bidentate compounds l,l-methylene- and 1,3-trimethylene- bis(diphenylphosphine) sulfide[63]. For the majority of monodentate phosphine sulfides and selenides, such as those mentioned in Figure 1.6 on page 10, 1:1 adducts typically form. For bidentate compounds 1:2 adducts are the most commonly formed[65].

Bonding between the chalcogenide and halogen atom is through transfer of electron density from the non-bonding orbitals of the donor chalcogen atom into the LUMO of the di- or inter-halogen acceptor (which is a σ_u^* orbital lying along its main axis). This results in a lowering of the di- or inter-halogen bond order and a consequent increase of the halogen-halogen bond length[56, 66]. Studies have shown that the organic substituents on the phosphorus atom, such as phenyl rings,

play no role in influencing the bonding between the chalcogen atom and the halogen[59, 62]. The stability of the compounds, Se > S > O, is related to the ionisation potentials of the chalcogenide. Selenium, which has the lowest potential, has the most loosely bonded pair of electrons, which are more readily available for donation to the acceptor molecule. The same is true for sulfur when compared with oxygen[59].

3.1.3 Aims of This Work:

The aim of this part of the project was to investigate the synthesis of the 1:1 adduct $Ph_2P(S)CH_2OH.I_2$, **2**, from the reaction of equimolar amounts of the phosphine sulfide (**1**) and diiodine, shown in Figure 3.2.

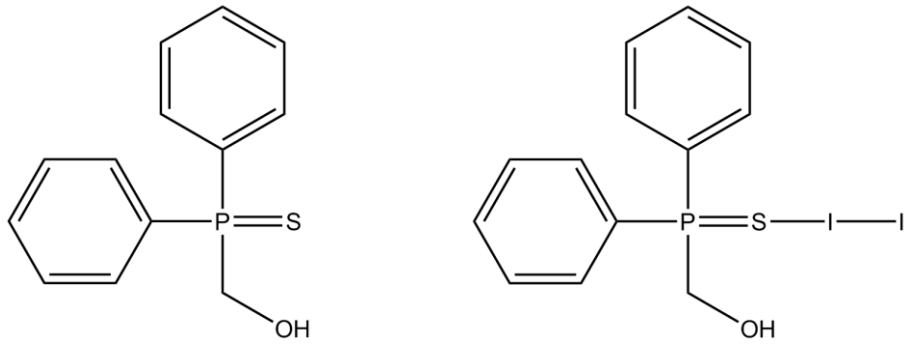

1 **2**

*Figure 3.2: The structures of compounds **1** and **2**.*

Tertiary phosphine sulfides with hydroxyl substituents have not been investigated for their ability to form adducts with halogens. The OH group may become involved in the bonding between the chalcogen atom and diiodine, by means of a secondary interaction. The OH group in $Ph_2P(S)CH_2OH$ (and the equivalent oxide and selenide) has been shown to hydrogen bond to the sulfur atom in the solid state[8], as discussed previously in section 1.4.2 on page 9. These secondary reactions are shown in Figure 1.8 (a) on page 12. Diiodine will also bind to phosphine oxides, but the resulting adducts are sometimes not as stable, which is the case for triphenylphosphine oxide[61]. A combination of binding between

diiodine and sulfur, and a potential interaction to the OH group could also lead to an increase in stability, the structure of which is shown in Figure 1.8 (b).

3.2 Experimental:

3.2.1 General Procedures:

NMR spectroscopic data were obtained on a Bruker DRX400 NMR, with samples dissolved in $CDCl_3$. IR spectroscopic data were obtained on a Perkin-Elmer Spectrum 100FTIR with solid samples made up as KBr discs and liquid samples between KBr windows. UV-Vis spectra were obtained using a CARY 100 Scan UV-Visible Spectrophotometer with samples measured in quartz cells. ESI-mass spectra were obtained on a Bruker MicrOTOF instrument, with solutions made up in methanol, operated under standard conditions. $AgNO_3$ was added to aid ionisation[10].

The chemicals used in this project were sourced as follows: $Ph_2P(CH_2OH)_2Cl$ was provided, made previously by Prof. Bill Henderson[10]; hexane from Unilab; sodium hydroxide from Univar; $MgSO_4$ from May & Baker; isopropanol, dichloromethane and petroleum spirits were all drum grade; diiodine from Univar; and Ph_3PS was provided, made previously by Prof. Bill Henderson[10]. The water used was high grade MilliQ water which had been deionised using the Barnstead E-pure system (18.0MΩcm).

The diiodine adducts and their starting materials were made up in air. Previous work sometimes prepared the phosphine sulfides and halogen adducts under strictly anaerobic and anhydrous conditions, however it was later determined that the products were moisture stable and no precautions were needed in the preparation of these products[67].

3.2.2 Synthesis of $Ph_2P(S)CH_2OH$:

The synthesis of $Ph_2P(S)CH_2OH$ was based on the method from the literature[10]. The phosphonium salt ($Ph_2P(CH_2OH)_2Cl$, 2.00 g) was dissolved in a mixture of water (30 mL) and hexane (30 mL). Powdered sulfur was added (1.2 mol equivalent with the phosphonium salt, 8.490 mmol, 0.28 g) and the mixture was stirred vigorously. A solution of sodium hydroxide (0.99 mol equivalent with the phosphonium salt, 7.004 mmol, 0.31 g) in water (10 mL) was added dropwise, with stirring, over five minutes. The solution was then stoppered and stirred overnight (approximately 9 hours). The layers were separated. The upper (hexane) layer containing the product was dried with $MgSO_4$, and evaporated to dryness. The product was washed with isopropanol, filtered and dried to give 1.15 g (65%) of $Ph_2P(S)CH_2OH$ (**1**) as cream coloured crystals.

The product was characterised by ^{31}P NMR (δ 42.97), ESI-MS (dissolved in MeOH and added $AgNO_3$): (capillary exit voltage = 160 V) *m/z* 354.96 $[M+^{107}Ag]^+$, *m/z* 356.96 $[M+^{109}Ag]^+$; and IR spectroscopy υ(P-S) = 635 cm^{-1} (vs).

3.2.3 Attempted Synthesis of $Ph_2P(S)CH_2OH.I_2$:

The synthesis of $Ph_2P(S)CH_2OH.I_2$ (**2**) was based on the preparation of a related compound, $Ph_3PS.I_2$[61]. $Ph_2P(S)CH_2OH$ (0.20 g, 0.67 mmol) was dissolved in dichloromethane (20 mL). To this, a solution of diiodine (0.17 g, 0.67 mmol), dissolved in the same solvent (20 mL) was added slowly with stirring. The solution was stirred for four hours, after which the solution was allowed to evaporate overnight. A red-brown oil formed.

Attempted precipitation of the product by rapid addition of petroleum spirits to a dichloromethane solution was unsuccessful. The reaction was repeated in

chloroform but the result was unchanged. The product was partially characterised by ^{31}P NMR (δ 41.72 ppm) and IR spectroscopy υ(P–S) = 604 cm^{-1} (vs).

3.2.4 Synthesis of $Ph_3PS.I_2$:

Using the same method[61] to prepare **2** above, Ph_3PS (0.200 g, 0.67 mmol) was dissolved in dichloromethane. A solution of diiodine (0.172 g, 0.67 mmol) in dichloromethane was added slowly and the solution stirred for 4 hours. After evaporating overnight, 0.380 g (102%) of $Ph_3PS.I_2$ (**3**) as red-brown crystals had formed. The product was characterised by ^{31}P NMR (δ 42.53) (literature δ 41.70) and IR spectroscopy υ(P-S) = 592 cm^{-1} (vs) (literature υ(P-S) = 590 cm^{-1}).

3.3 Results and Discussion:

3.3.1 Synthesis of $Ph_2P(S)CH_2OH$, $Ph_2P(S)CH_2OH.I_2$ and $Ph_3PS.I_2$:

The preparation of **1** involved direct combination of elemental sulfur with $Ph_2P(CH_2OH)_2Cl$ in the presence of NaOH, which gave cream coloured crystals. The product was expected to crystallise out of solution, however the solvent had to be evaporated to dryness before crystals formed. This led to impurities in the crystals. The product was washed with isopropanol and examined using ESI-MS, as seen in Figure 3.3. If the compound oxidised during the reaction then the oxide, $Ph_2P(O)CH_2OH$, may have formed instead of the desired sulfide, $Ph_2P(S)CH_2OH$. Mass spectrometry was used to check whether this was the case. Silver nitrate was added to aid ionisation, as it has been used previously to aid ionisation for phosphines and phosphine sulfides[10]. The isotope pattern in the mass spectrum appears the same as the calculated isotope pattern in Figure 3.4. Two peaks, corresponding to $[M+Ag]^+$ for the two silver isotopes (^{107}Ag and ^{109}Ag), appear in the spectrum at *m/z* 354.96 and *m/z* 356.93. Additional peaks at *m/z* 355.96 and *m/z* 357.96 arise from contributions from other isotopes present in the compound (for example, ^{13}C and ^{2}H). There are no peaks at *m/z* 338.97 and *m/z* 340.97 which correspond to the oxide product.

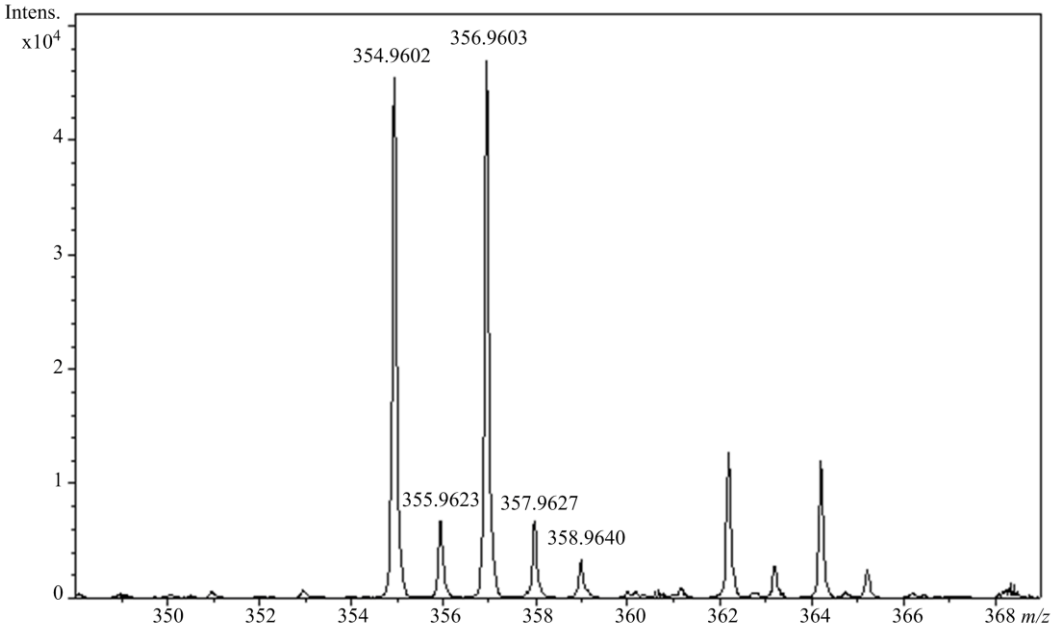

*Figure 3.3: The ESI mass spectrum of **1**.*

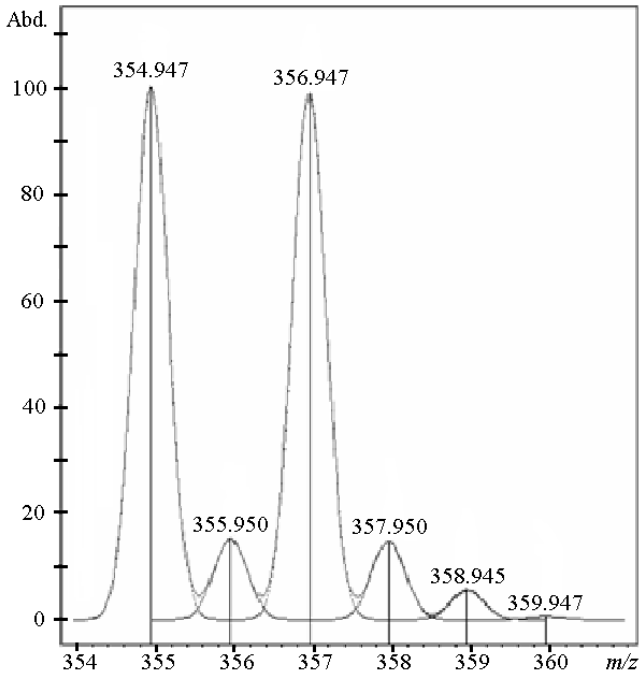

*Figure 3.4: The calculated isotope pattern for **1**.*

There were many other peaks present in the mass spectrum indicating impurities in the product. Therefore the crystals were recrystallized using isopropanol.

The attempted synthesis of the 1:1 adduct **2**, was undertaken by the direct reaction of equimolar quantities of the phosphine sulfide and diiodine in dichloromethane.

UV-Vis spectroscopy can be used to monitor the reaction in solution. Unbound diiodine absorbs at 505 nm in dichloromethane[63] and the spectrum of a solution of I_2 in CH_2Cl_2 is shown in Figure 3.5.

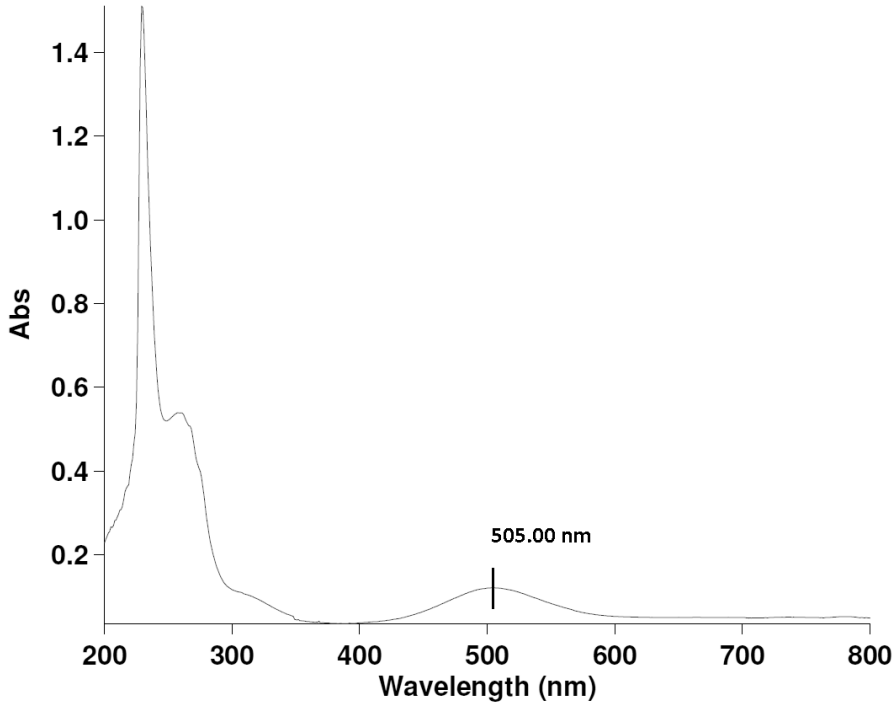

Figure 3.5: The UV-Vis spectrum of a solution of I_2 in CH_2Cl_2.

For complexes with a 1:1 ratio of phosphine sulfide to halogen, when the reaction is completed, two changes in the spectrum occur. A "blue shift" in the diiodine peak occurs and a second, new peak arises in the UV region, corresponding to the charge transfer transition[63, 65]. For compounds such as **2** and **3**, the charge transfer band cannot be detected as the phenyl π-electrons and P-S groups absorb in the same UV region[63].

However, in the reaction solutions of both **2** and **3** after stirring for four hours, seen below in Figure 3.6, the diiodine peak at 503 nm does not undergo a blue shift, but is unchanged from the peak for diiodine in Figure 3.5. The charge transfer peaks cannot be seen under the large absorbance from the other groups in the molecule.

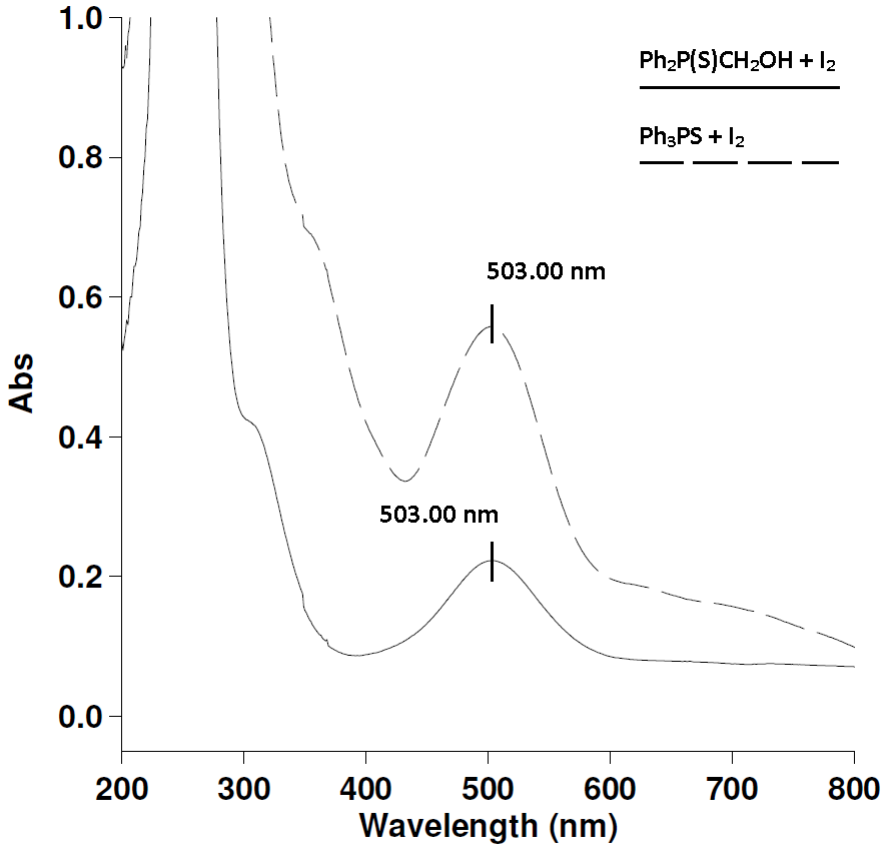

*Figure 3.6: The UV-Vis spectra of the reaction solutions (in CH_2Cl_2) of **2** and **3** after stirring for four hours.*

For the preparation of **3** (Figure 3.6, dashed line) the blue shifted diiodine peak is expected to appear at 436 nm[61] and in a similar region for **2**. Although the preparation of **3** was successful and produced crystals, the UV-Vis spectrum for the completed reaction (in Figure 3.6) does not show a blue shifted peak. Instead, like **2**, the peak appears around 505 nm, which is where the peak appears for unreacted diiodine, as shown in Figure 3.5. The reason there is no blue shift may be due to unreacted diiodine in solution. As the reactants were added in equimolar quantities, this means the products do not have 1:1 stoichiometry.

The literature method used for producing the diiodine adduct compounds[61] produced crystals of **3** that were then able to be used by Apperley and co-workers[61] for x-ray crystallography without any further work up. Unexpectedly,

for the preparation of **2**, when the solvent used in the reaction was evaporated to dryness, no crystals formed. Instead a red-brown oil was left in the flask. As previously mentioned, several attempts were made to get the product to crystallise, or form a powder. These included trying to crystallise the oil in dichloromethane, or precipitating the sample by the rapid addition of petroleum spirits to a dichloromethane solution. However, neither of these methods worked. The product was analysed by NMR and IR spectrometry as an oil.

The method used to prepare the diiodine adducts was based on the method used to make **3** and the equivalent selenium compound $Ph_3Se.I_2$[61]. This reaction was repeated in this work to test the validity of this method. The reaction produced dark red-brown crystals that were analysed by IR and NMR spectroscopy and produced results consistent with previous work[61]. The reaction was also monitored by UV-Vis spectroscopy and the results were indicated previously in Figure 3.6, which was however, unsuccessful.

The stoichiometry of the diiodine adduct is dependent on the solvent used in the reaction[63]. For example, **3** forms as a 1:1 ratio (phosphine : diiodine) in dichloromethane but can also form a 1:2 ratio in chloroform and a 2:3 ratio in carbon tetrachloride[63]. Other phosphine sulfides have different stoichiometry in these solvents[63]. Because of this, the preparation of **2** was repeated in chloroform (the previous reaction had been carried out in dichloromethane). However, the result was the same as the previous attempt, and an oil formed.

3.3.2 NMR Analysis:

The ^{13}C and ^{1}H NMR for all of the phosphine sulfide compounds could not be rationalised. The aromatic region for both contained many overlapping peaks of

varying multiplicity. Therefore the samples were analysed using ^{31}P NMR, as this gave the clearest information. Solution NMR studies of tertiary phosphine sulfides and their adducts with halogens show single peaks as well as solid state NMR studies, showing that the compounds have the same structure in both phases[61].

The chemical shift of the phosphorus atom in the ^{31}P NMR spectrum for the starting material, $Ph_2P(CH_2OH)_2Cl$ appears at 13.39 ppm. Upon reacting $Ph_2P(CH_2OH)_2Cl$ with sulfur and producing **2**, the chemical shift of the phosphorus atom moved upfield to 42.97 ppm (shown in Figure 3.7). This was as expected, since for related compounds such as Ph_3P and $(C_6H_{11})_3P$, the chemical shift increased on conversion of the tertiary phosphine to its sulfide[68].

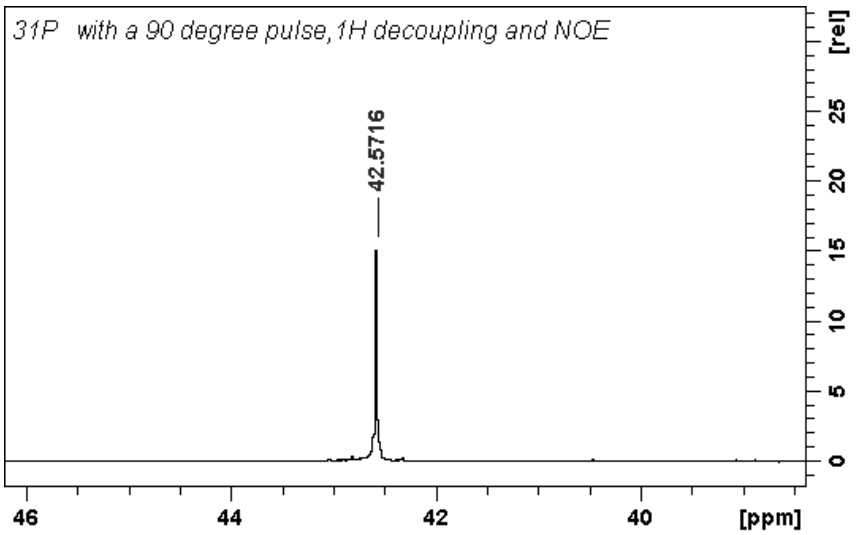

Figure 3.7: The ^{31}P NMR spectrum of $Ph_2P(S)CH_2OH$.

The oil produced in the reaction of $Ph_2P(S)CH_2OH$ with I_2 was analysed by NMR and the ^{31}P spectrum is shown in Figure 3.8.

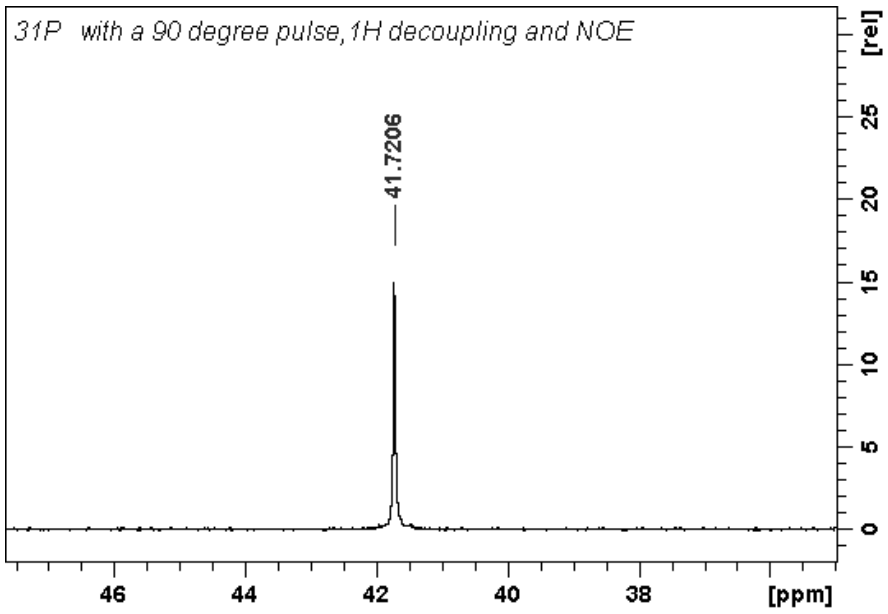

*Figure 3.8: The ^{31}P NMR of **2**, the reaction oil.*

The chemical shift, upon addition of diiodine, moves from 42.97 ppm (Figure 3.7) to 41.72 ppm. A small downfield shift is expected upon the formation of diiodine adducts of phosphine sulfides[61].

Compound **3** was prepared in order to compare with the material obtained in the attempted synthesis of **2**. The ^{31}P NMR spectrum, Figure 3.9, showed a single peak at 42.52 ppm, which is similar to data from previous studies[61]. The chemical shift for the phosphorus atom in the starting material, Ph_3PS appears at 43.36 ppm[68], so the result is consistent with a small downfield shift[61].

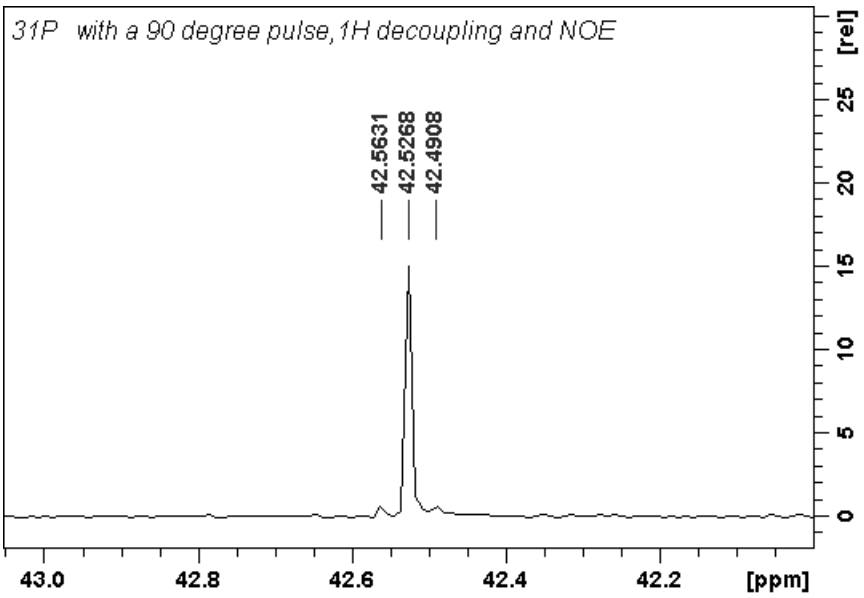

*Figure 3.9: The ^{31}P NMR spectrum of **3**.*

3.3.3 IR Analysis:

IR spectroscopy is commonly used in the analysis of phosphine sulfide compounds[24, 69], in particular the P-S vibration frequency. Generally the P-S vibration (in the uncomplexed phosphine sulfide) appears at 600 ± 20 cm^{-1} [70], although a range of 840-600 cm^{-1} has been suggested[69] based on the highest observed frequency at 860 cm^{-1} for $PS(NH_2)_3$, and the lowest observed frequency at 535 cm^{-1} for triethylphosphine sulfide[69]. Triphenylphosphine sulfide has one of the higher frequencies, while trimethyl- and triethyl-phosphine sulfide have the lowest[70]. The C-P vibration of trimethylphosphine sulfide appears at 663 cm^{-1} and for aromatic substituents on the phosphine it appears at slightly lower frequencies[57].

Upon addition of a halogen or inter-halogen the P-S vibration decreases[69] by about 25-60 cm^{-1}. This is due to a net decrease in $p\pi_s \rightarrow d\pi_p$ back-bonding, which decreases the P-S bond order, which then results in a lowering of the frequency[24].

The fundamental I-I vibrations and overtones, which appear below 300 cm^{-1}, are unable to be viewed due to limits on the instruments used[61].

The υ(P-S) band in the spectrum of compound **1** was assigned by comparison with the starting material, $Ph_2P(CH_2OH)_2Cl$, as shown in Figure 3.10. The peak at 635 cm^{-1} in the spectrum of **1** does not appear in the spectrum of the starting material. Therefore the peak at 635 cm^{-1} was assigned the υ(P-S) vibration.

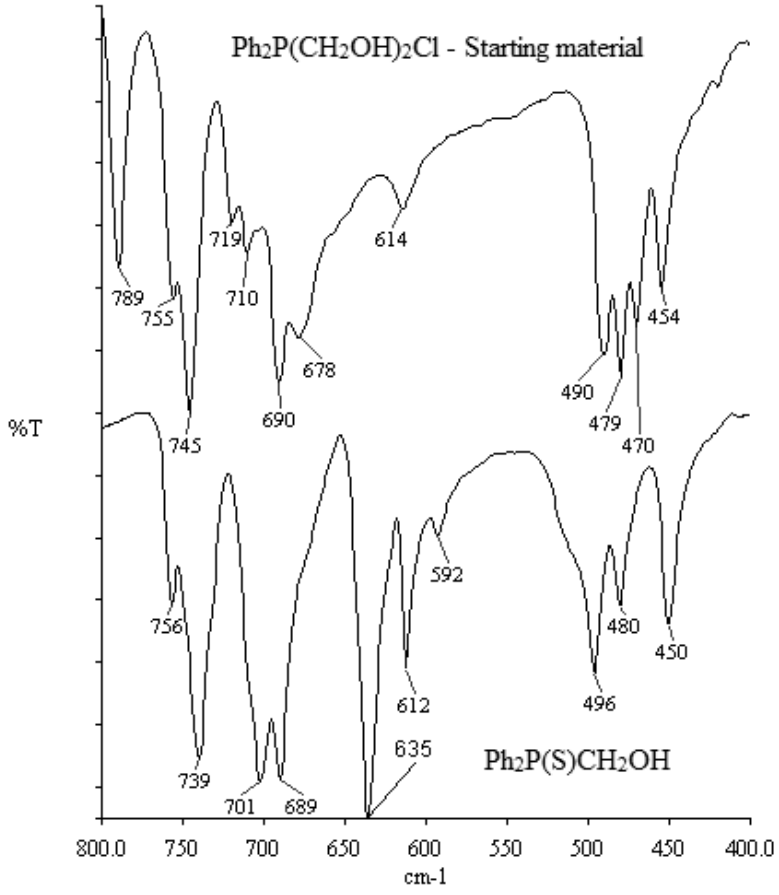

*Figure 3.10: The IR spectra of $Ph_2P(CH_2OH)_2Cl$ (top) compared with compound **1** (bottom)*

The determination of the υ(P-S) band in **1** above agrees with literature values for the related compound $Ph_3PS.I_2$. The literature values of the υ(P-S) band in Ph_3PS appear around 630 cm^{-1} and some examples are shown in Table 3.1.

*Table 3.1: Literature values for the υ(P-S) band in IR spectra of the compounds Ph_3PS and **3**.*

υ(P-S) in Ph_3PS	**υ(P-S) in $Ph_3PS.I_2$ (3)**	**Reference:**
712 cm^{-1}	702 cm^{-1}	Zingaro and Hedges, 1961[24] [i]
	627 cm^{-1}	Zingaro, 1963[69]
637 cm^{-1}	590 cm^{-1}	Apperley et al.,1998[61]
	592, 638 cm^{-1}	Cross et al., 1999[71]

As mentioned previously, upon addition of diiodine, the frequency of the υ(P-S) band decreases. The spectrum of the diiodine compound **2** can also be compared with the spectrum of **1**, in Figure 3.11 below, to assign the υ(P-S) band. The peak at 635 cm^{-1} (in the spectrum of $Ph_2P(S)CH_2OH$) appears to move to a slightly lower wavenumber to 621 cm^{-1}, which does not appear in the spectrum of **1**. The peak at 512 cm^{-1} in the spectrum of **2** is also absent from the previous spectrum, but the magnitude of the change in frequency is much greater than that reported in the literature[69]. This peak does not appear to be due to chloroform[72], the reaction solvent, which has bands in this region at 765 cm^{-1} and between 650-670 cm^{-1}. It could be due to an unexpected by-product. The synthesis was not successful as it produced an oil, so this is possible.

[i] The IR spectra for Zingaro and Hedges, 1961 were recorded as solutions.

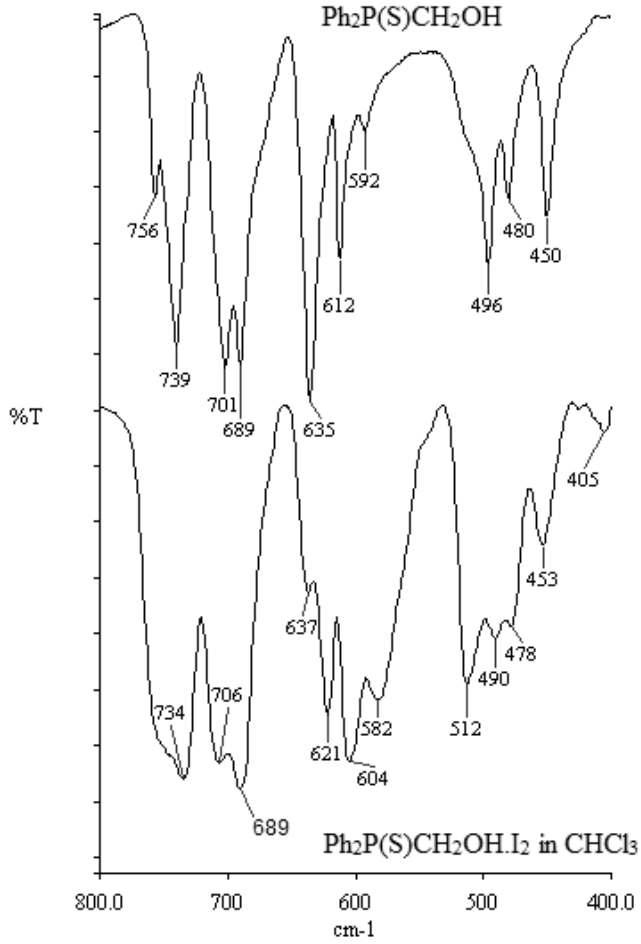

*Figure 3.11: The IR spectra of compounds **1** and **2***

A net decrease in the electron density around the sulfur atom, resulting in a reduction of the P-S bond order, could account for the decrease in the υ(P-S) band[69].

There are numerous IR spectra in the literature for compound **3**, some of which are mentioned previously in Table 3.1. In Figure 3.12, the peak at 638 cm^{-1} in the spectrum of the starting material Ph_3PS was assigned to the υ(P-S) vibration, and it agrees with the literature values.

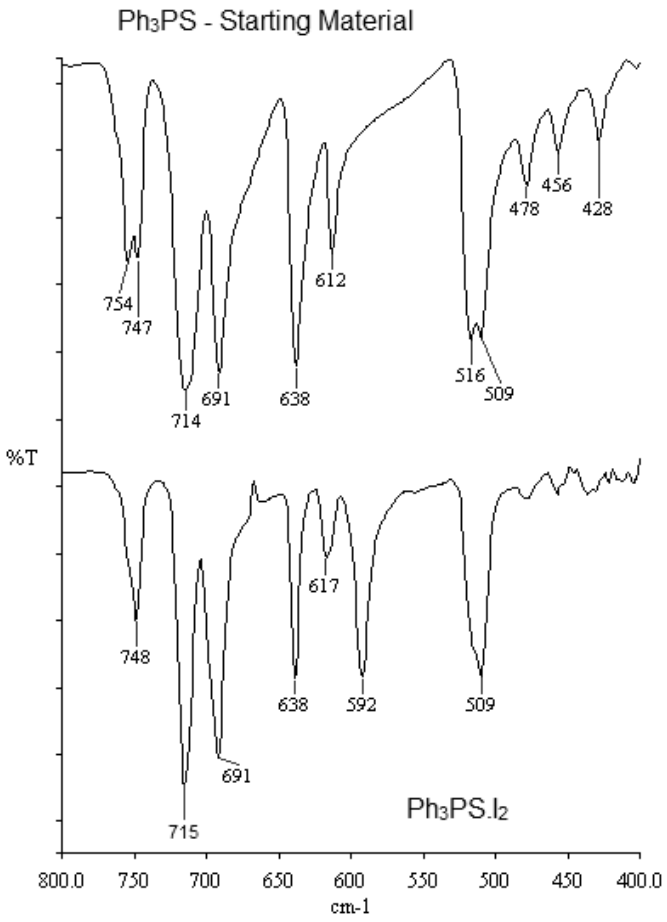

*Figure 3.12: The IR spectra of the compounds Ph_3PS and **3***

However, in the spectrum of **3** the peak at 638 cm^{-1} does not disappear as expected. A new peak at 592 cm^{-1} appears which can be assigned the υ(P-S) band, as it has the expected decrease in frequency[69]. The reason the band at 638 cm^{-1} does not disappear upon addition of diiodine may be due to some unreacted starting material. It may also arise from the υ(C-P) band which could have been overlapping the υ(P-S) band in the phosphine sulfide. The υ(C-P) band is expected to appear at <663 cm^{-1} according to the literature[57].

The other bands in the spectra provide less information, as they do not change between $Ph_2P(CH_2OH)_2Cl$, **1** and **2**. Figure 3.13 below shows the IR spectra of all three compounds.

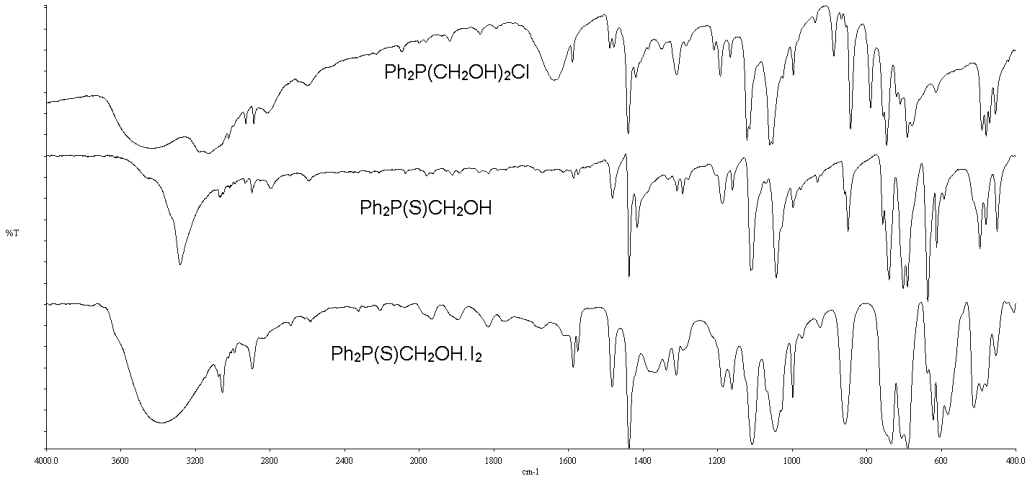

*Figure 3.13: The IR spectra of the compounds: $Ph_2P(CH_2OH)_2Cl$, **1** and **2**.*

3.4 Conclusions and Future Work:

The attempted preparation of $Ph_2P(S)CH_2OH.I_2$ was unsuccessful, though the oil that formed was partially characterised by ^{31}P NMR and IR spectroscopy. The method used was based of the preparation of the related compound, $Ph_3PS.I_2$, which was successfully prepared using the same method. It was thought that the desired product, **2**, would possess increased stability from interactions of the hydroxymethyl substituent, discussed previously in Figure 1.8 on page 12. The hydrogen bonding interaction, however, may not be adding stability as desired, and the interaction between the oxygen in the hydroxymethyl group and diiodine may be interfering with the formation of the 1:1 adduct. Phosphine oxide adducts with diiodine are known, and the hydroxymethyl group could also be coordinating extra diiodine. The starting material was pure according to the ^{31}P NMR and it is unlikely that small levels of impurities would have caused the problems in obtaining crystals of **2**, however there were difficulties in crystallising the starting material, $Ph_2P(S)CH_2OH$.

Future work could look at using different phosphines, such as the sulfide derivative of the bidentate hydroxymethylphosphine, bis[bis(hydroxymethyl)phosphino]ethane, $(HOCH_2)_2P(CH_2)_2P(CH_2OH)_2$. This compound will likely form a 1:2 adduct with diiodine, like other bidentate phosphine sulfides, as mentioned earlier in 3.1.2 on page 66. The reaction of tris(hydroxymethyl)phosphine with sulfur and diiodine could also be attempted. Selenium compounds could also be tested, as the stability of halogen adducts increases down group 16[56].

Chapter Four: An Investigation into the use of Tris(Hydroxymethyl)Phosphine as a Coupling Agent for the Binding of Fluorescent Labels to Amine-Containing Solids

4.1 Introduction:

4.1.1 Fluorescence Microscopy and Fluorescent Compounds:

Fluorescence microscopy is a useful technique in biology. Many thousands of fluorescent labels have been devised for use in labelling nearly every type of biological system[73]. An example is the visualisation of cellular uptake, intracellular distribution, and localization of fluorescently labelled drugs[28]. Fluorescence can be described as the emission of light by an excited molecular entity, after the absorption of light that is typically of shorter wavelength, with retention of spin multiplicity[73-74]. Many organic compounds are fluorescent, the most useful are those that contain conjugated double bonds, often containing ring sructures[73]. Some metal complexes also have fluorescent properties[28].

Usually, the fluorescent label, also known as the fluorophore, is covalently bound to the species of interest. The hydrophilic, hydrophobic or amphiphilic character of the fluorophore is of importance when deciding which fluorophore is suitable for the biological system under study. Protein labelling is easily done due to labelling reagents having functional groups that form covalent bonds with amine groups[74].

Coumarin derivatives[75] and derivatives of *N*-alkyl-1,8-naphthalimides are well known fluorophores. The *N*-alkyl-1,8-naphthalimide derivatives have applications as fluorescent labels, as well as colorimetric sensors[76], metal ion sensors[77] and anion sensors[78]. They are also of interest because of their use in dyes and brighteners, as DNA cleaving agents and tumoricidals[79], and for their anti-viral properties[26]. Derivatives have also been used to design probes sensitive to variations in pH or metal ion concentration[26]. A derivative of *N*-alkyl-1,8-naphthalimide has been used to bind to DNA in cancer cells for visualisation using confocal fluorescence microscopy[78a].

4.1.2 Immobilisation of Ligands onto Insoluble Supports:

There has been much interest in immobilising ligands on insoluble supports. Silica is often chosen as the support solid, although there are many others. The ligands have applications in the extraction of metals or in chromatography, and immobilised metal complexes are used in catalysis[80]. Another type of solid support is re-precipitated bone powders and milled animal bone powders. Animal bone has important uses, for example, as a source of hydroxyapatite which is used as prosthesis material. It has been investigated into their use as support materials for enzyme immobilisation[27]. THP was used as a coupling reagent, via the N-H groups from residual collagen in the bone, for the immobilisation of trypsin[27].

4.1.3 Aims of This Project:

Tris(hydroxymethyl)phosphine (THP) can be used as a coupling reagent for the immobilisation of amine-containing compounds onto amine-functionalised solid materials, such as aminopropyl silica. The immobilisation of enzymes onto amine-functionalised surfaces has been discussed in section 1.3.1 on page 5. A potential

application of this coupling reaction is the binding of fluorescent labels onto a biological solid. There are no reports in the literature about using THP to couple fluorescent compounds onto solid supports. A suitable biological solid for investigation is bone material containing residual collagen, since discussions with an anthropologist have suggested that fluorescent labelling of residual collagen in bone is of interest.

The fluorescent label chosen for this project was *N*-(2-aminoethyl)-1,8-naphthalimide (**4**), the structure of which is shown below in Figure 4.1. THP can potentially bind to the NH_2 group and couple it to the solid material.

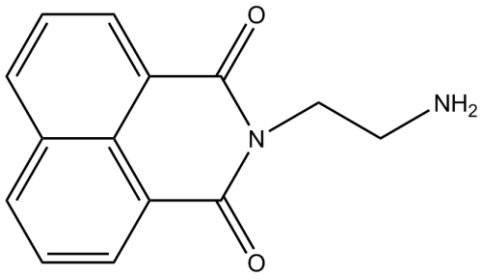

*Figure 4.1: The fluorescent label used, N-(2-aminoethyl)-1,8-naphthalimide, **4**.*

The coupling reaction was initially done using aminopropyl silica, shown in Figure 4.2, as it has a large amount of amine groups available for coupling. It has also been used in the past to immobilise enzymes using THP[17]. It is readily prepared[80] by treatment of silica with inexpensive 3-aminopropyltriethoxysilane, $(EtO)_3Si(CH_2)_3NH_2$.

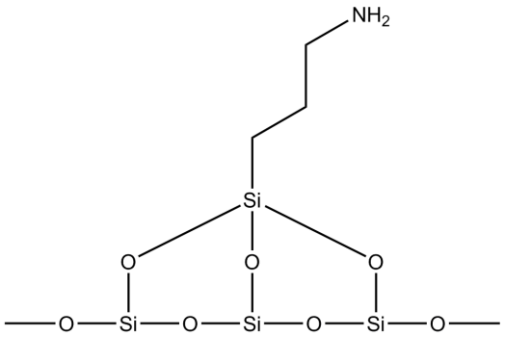

Figure 4.2: The structure of aminopropyl silica.

The reaction between **4** and a (hydroxymethyl)phosphonium salt, $Ph_2P(CH_2OH)_2Cl$, was also investigated. The structure of the predicted product, **5**, is shown in Figure 4.3.

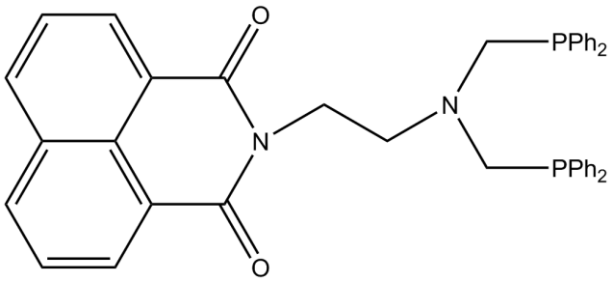

*Figure 4.3: The predicted product (**5**) of the reaction between **4** and $Ph_2P(CH_2OH)_2Cl$.*

4.2 Experimental:

4.2.1 General Procedures:

NMR spectroscopic data were obtained on a Bruker DRX400 NMR, with samples dissolved in $CDCl_3$. IR spectroscopic data were obtained on a Perkin-Elmer Spectrum 100FTIR with solid samples analysed as KBr discs and liquid samples between KBr windows. The UV lamp used was a UVitec-LF-204.LS producing wavelengths of 254 and 312 nm.

The chemicals used in this project were sourced as follows: the fluorescent label, *N*-(2-aminoethyl)-1,8-naphthalimide, was provided and prepared previously[26]; $Ph_2P(CH_2OH)_2Cl$ was also prepared previously[10]; triethylamine (Et_3N) was from Unilab; the methanol was drum grade; activated silica gel was from BDH Chemicals Ltd.; 3-Aminopropyltriethoxysilane was from Aldrich; aminopropyl SBA15 was prepared previously by Prof. Bill Henderson via the method used to prepare aminopropyl silica[80], from SBA15 obtained from Prof. M. Olea, Teesside University, UK; tetrakishydroxymethylphosphine chloride, THPC ($[P(CH_2OH)_4]^+Cl^-$) was from Albright & Wilson, UK Ltd. The water used was high grade MilliQ water which had been deionised using the Barnstead E-pure system (18.0MΩcm).

4.2.2 Preparation of Aminopropylsilica:

Aminopropylsilica was used was a trial amine-containing solid material. It was prepared via the method by Khatib and Parish[80]. The activated silica gel (10 g) was refluxed with 3-aminopropyltriethoxysilane ($[(EtO)_3Si(CH_2)_3NH_2]$, 3.1 g, 14

mmol) in dry toluene (65 mL) for 4 hours. The solid was filtered off, washed with toluene, then methanol, and dried at 100 °C overnight.

4.2.3 THP Coupling Reaction:

Aminopropyl silica (100 mg) was suspended in methanol (approximately 20 mL). An excess of THP solution (approximately 30 mL) was added (THP was prepared via the method mentioned previously in section 2.2.2 on page 23) and reacted for approximately 10 minutes with stirring. The solid was filtered off and washed with approximately 100 mL of distilled water to remove any unbound THP. The solid was then re-suspended in methanol straight away as the immobilized THP will slowly oxidise in air, making it unreactive towards coupling reactions with amines. To the re-suspended solid, an excess of *N*-(2-aminoethyl)-1,8-naphthalimide was added (50 mg) and reacted for approximately 10 minutes. After filtering the solid, it was washed thoroughly with methanol (approximately 50 mL) to remove any unbound naphthalimide label. The solid was dried in a desiccator overnight. Using a UV lamp and looking at the wavelengths 312 nm and 254 nm, the product was checked for fluorescence.

A control experiment was also carried out, by treating the aminopropyl silica with the naphthalimide label, omitting the THP coupling step.

4.2.4 Reaction of *N*-(2-aminoethyl)-1,8-naphthalimide with $Ph_2P(CH_2OH)_2Cl_2$:

The fluorescent compound, *N*-(2-aminoethyl)-1,8-naphthalimide (100 mg, 0.480 mmol), was dissolved in methanol (approximately 50 mL). To this, two mole equivalents of the phosphonium salt $Ph_2P(CH_2OH)_2Cl$ (271.5 mg, 0.9603 mmol) was added, as well as two drops of Et_3N. The solution was stirred for

approximately 20 minutes and evaporated in a fume hood overnight. Instead of a solid precipitate, an oil formed on the bottom of the flask. Precipitation was attempted by dissolving the oil in methanol and adding water. This however was not successful. Characterisation of the oil was attempted by IR and ^{31}P NMR spectroscopy, but the results were not clear.

4.3 Results and Discussion:

4.3.1 THP Coupling Reaction:

4.3.1.1 Synthesis:

The first attempt at coupling *N*-(2-aminoethyl)-1,8-naphthalimide to an amino containing solid using THP, used aminopropyl SBA-15 (an aminopropyl-modified mesoporous silica[81]) . This was a powder instead of a crystalline solid, therefore filtering was difficult. When the treatment of the solids with (or without) THP and then with *N*-(2-aminoethyl)-1,8-naphthalimide was completed, the THP-coupled product had a slight yellow tint (from the *N*-(2-aminoethyl)-1,8-naphthalimide) while the control remained white. However, when the product was examined under UV light, neither the product nor the control fluoresced. Because of this the reaction was repeated using aminopropyl silica. A small amount was prepared via the method above and the coupling reaction was repeated. Unlike when the reaction was performed using aminopropyl SBA-15, after drying the aminopropyl silica samples (the product and the control) both appear white.

4.3.1.2 Fluorescence under UV light:

The initial reaction with aminopropyl SBA-15 appeared to couple the fluorescent label to the silica, as the THP-coupled solid became yellow. However, under both wavelengths of the UV lamp, neither sample fluoresced like the starting material did (see Figure 4.4).

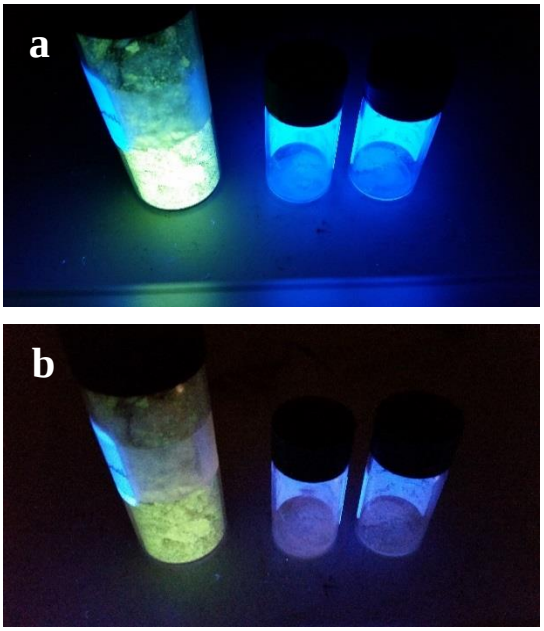

Figure 4.4: The aminopropyl SBA-15 samples under UV light. Left to right is N-*(2-aminoethyl)-1,8-naphthalimide, the silica product bound with THP and the control (no THP); (a) is under 312 nm and (b) under 254 nm.*

It was thought that the reaction was not successful because the amine containing solid was not aminopropyl silica. Therefore a fresh sample of aminopropyl silica was prepared and the reaction repeated.

Compared to the naphthalimide compound, both the THP-coupled product and the control do not appear to fluoresce. However, placing the two samples next to the starting material (aminopropyl silica) shows that they fluoresce slightly, see Figure 4.5. The samples fluoresce more strongly at 312 nm than at 254 nm.

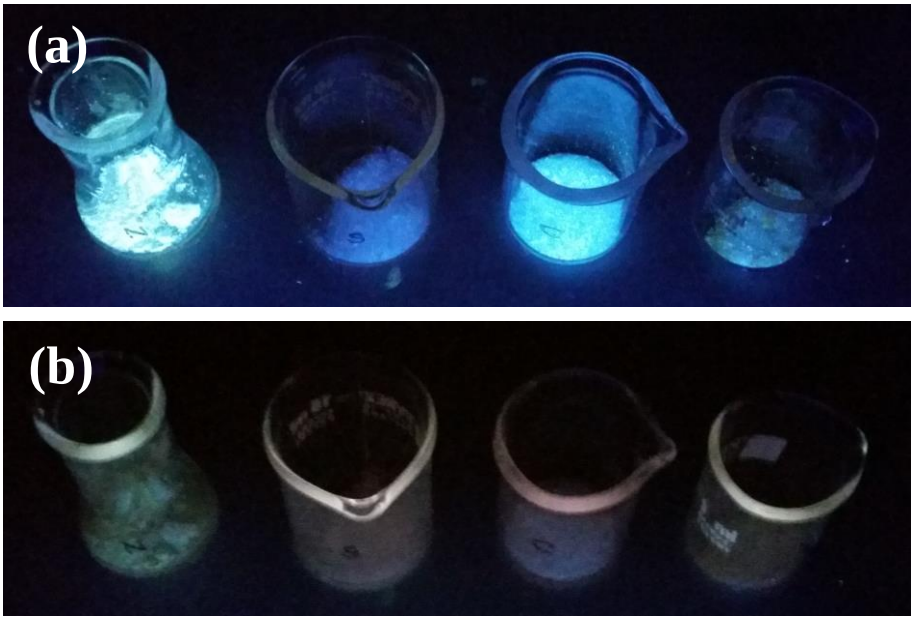

Figure 4.5: The THP coupling reaction repeated with aminopropyl silica. From left to right: N-*(2-aminoethyl)-1,8-naphthalimide, unreacted aminopropyl silica, the control and the THP-coupled product; (a) is 312 nm and (b) is 254 nm.*

The control (aminopropyl silica only treated with the naphthalimide compound) also appears to fluoresce more strongly than the THP-coupled product, especially at 312 nm. This was unexpected as the THP was supposed to bind the naphthalimide compound and the control was not supposed to retain any. In Figure 4.5 (a) especially the control appears to fluoresce nearly as brightly as the naphthalimide compound. It appears the fluorescent naphthalimide label adsorbs to the aminopropyl silica surface, and does not require coupling. The coupling reaction of the fluorescent label with THP may be quenching the fluorescence.

4.3.1.3 Spectroscopic analysis:

The interaction between the naphthalimide label and the silica was investigated using IR spectroscopy. The IR spectra of aminopropyl silica, the THP-bound product, the control (no THP step) and *N*-(2-aminoethyl)-1,8-naphthalimide were recorded. The naphthalimide compound is shown in Figure 4.6. Four peaks appear

in the υ(C=O) stretching region. The peak at 3347 cm^{-1} is the amine N-H stretch and the strong peak at 779 cm^{-1} is an N-H bend.

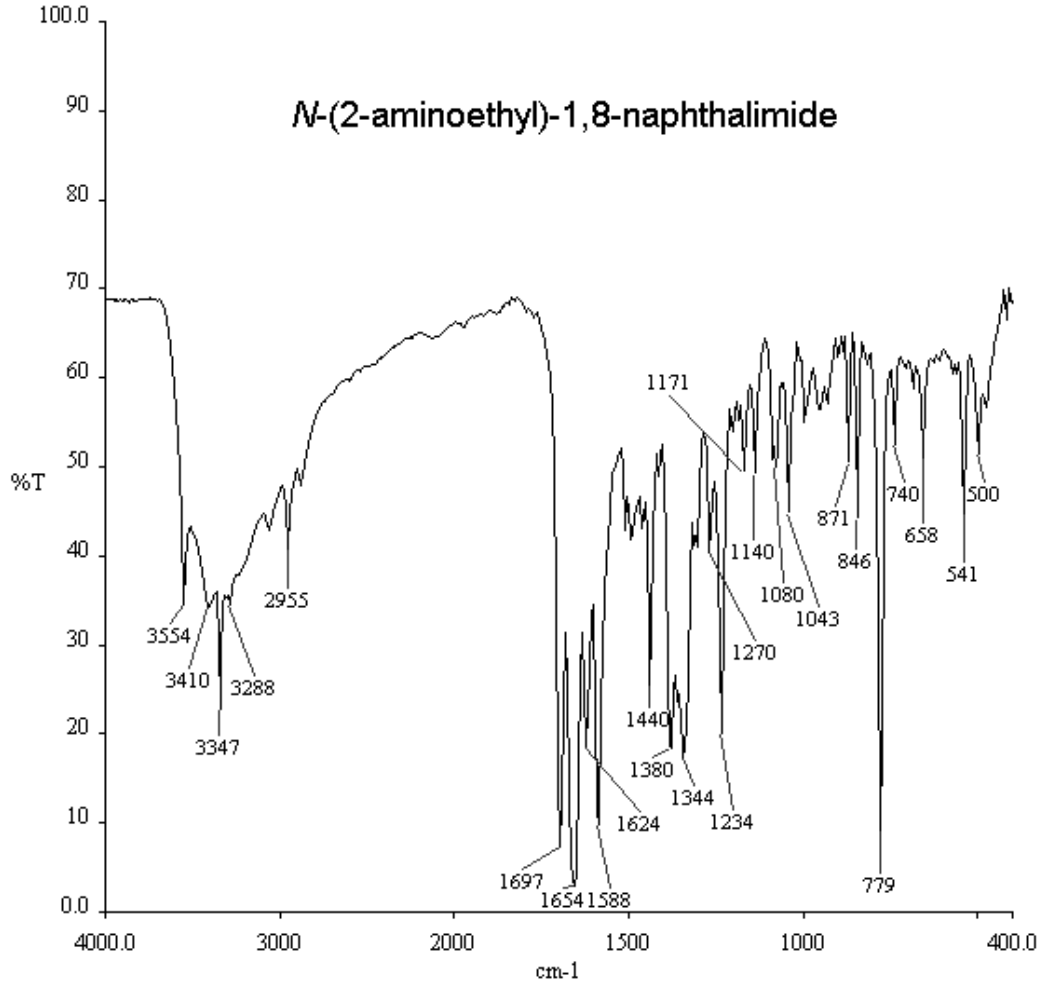

Figure 4.6: The IR spectrum of N-*(2-aminoethyl)-1,8-naphthalimide.*

All of the silica samples gave spectra with a very low baseline and only a few broad peaks. The spectra of all three samples appear the same, as shown in Figure 4.7. As expected, the spectra show a very strong and broad Si-O absorption.

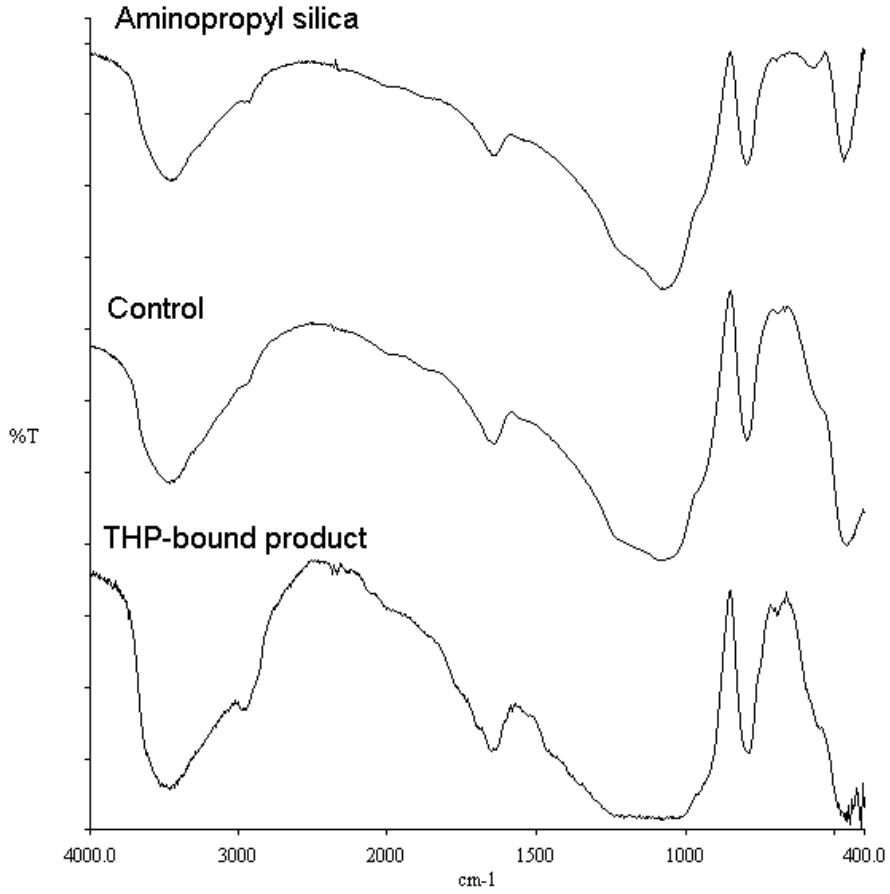

Figure 4.7: The IR spectra of aminopropyl silica, the control (no THP) and the THP-bound product.

There is very little difference between the spectra of THP-bound product (Figure 4.7, bottom spectrum) and the control (middle spectrum). The peak ~400 cm^{-1} in aminopropyl silica (top spectrum) increases in the control and product spectra. There is even less correlation between the spectra of the silica compounds and the spectrum of *N*-(2-aminoethyl)-1,8-naphthalimide (Figure 4.6). This compound does not have any strong peaks below 400 cm^{-1}, so it is unlikely the reason for the increase in the peak at ~400 cm^{-1}. The intensity of Si-O absorption makes identification of any weaker band very difficult.

4.3.2 Reaction of *N*-(2-aminoethyl)-1,8-naphthalimide with $Ph_2P(CH_2OH)_2Cl_2$:

4.3.2.1 Synthesis:

The reaction scheme for the attempted preparation of **5** from $Ph_2P(CH_2OH)_2Cl$ and **4** is shown in Figure 4.8.

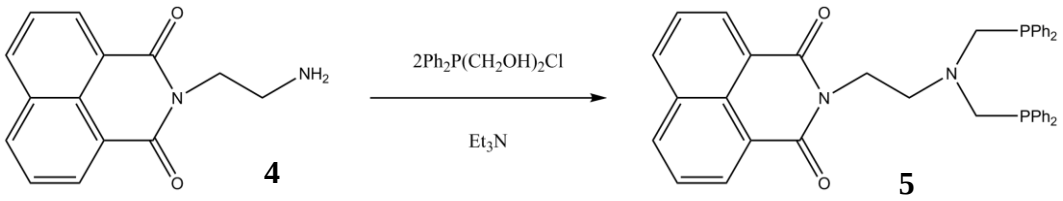

*Figure 4.8: The reaction between **4** and $Ph_2P(CH_2OH)_2Cl$ producing **5**.*

The product, **5,** may exist in the oil with dissolved salts. In order to get the product to form a solid, the oil was dissolved in methanol and water was added in an attempt to precipitate the product while any salts remained in solution. Initially there was no precipitate, but after approximately three hours the solution became cloudy. However, when this was filtered the filtrate appeared the same as the original solution (cloudy) and no solid was filtered off. After the solution had evaporated the product still formed an oil.

4.3.2.2 Fluorescence under UV light:

This reaction appears to also be unsuccessful as the product does not form a crystalline solid, rather it leaves an oil. This oil does not appear to fluoresce under UV light and this may be due to the phosphine quenching the fluorescence. The edges of the reaction beaker did however, as shown in Figure 4.9.

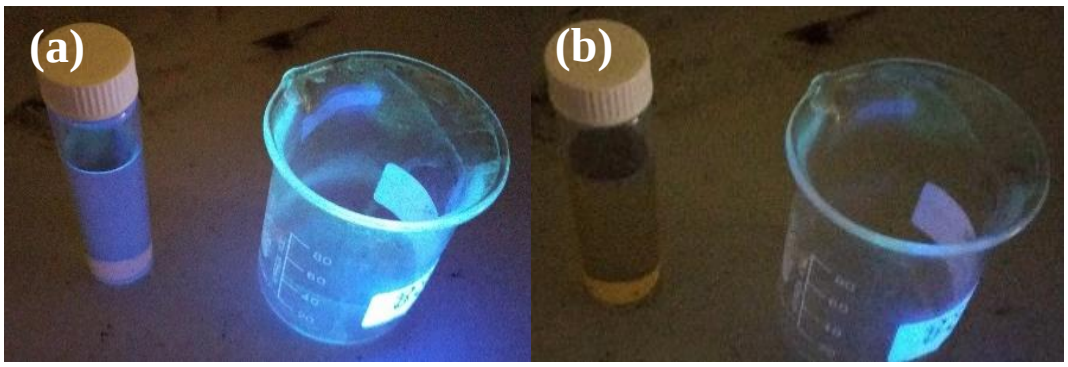

Figure 4.9: The reaction of $Ph_2P(CH_2OH)_2Cl$ and the naphthalimide fluorescent label. Left: the product dissolved in methanol, right: the reaction vessel; (a) is 312 nm and (b) is 254 nm.

The fluorescence on the reaction vessel could be from unreacted naphthalimide compound. To determine what the product of the reaction is, the oil was examined by NMR and IR spectroscopy.

4.3.2.3 Spectroscopic analysis:

The ^{31}P NMR spectrum of the oil is shown in Figure 4.10. The spectrum shows extra peaks, and the main peak at 29.37 ppm likely corresponds to an oxide product. This product may be due to the intended product oxidising when the solution was evaporating.

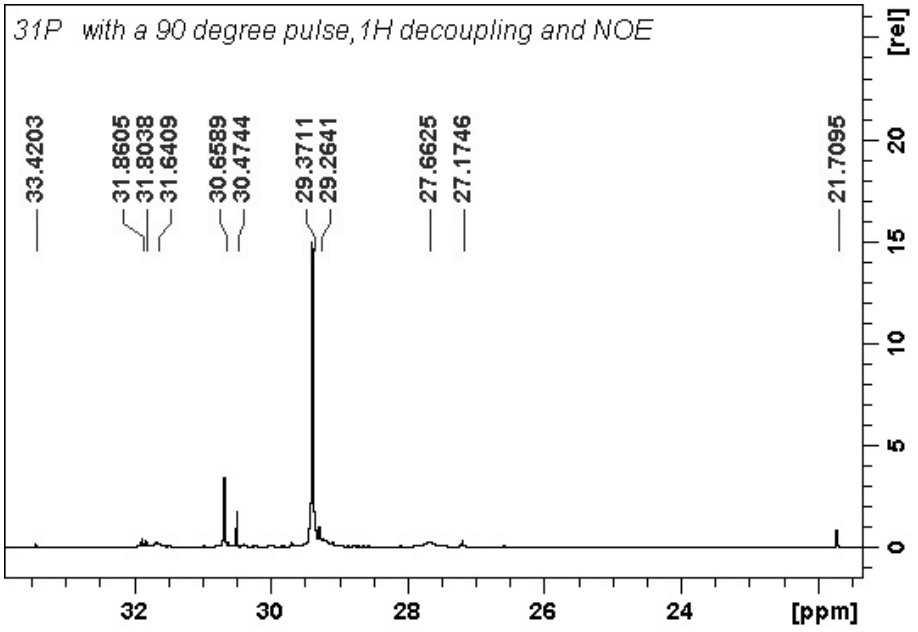

Figure 4.10: ^{31}P NMR spectrum of the reaction of $Ph_2P(CH_2OH)_2Cl$ and N-*(2-aminoethyl)-1,8-naphthalimide.*

In order to see whether this was the case, the experiment was repeated and the ^{31}P NMR spectrum recorded as soon as the reaction had finished. The spectrum, shown in Figure 4.11, also contained many peaks. What appears to be the two largest peaks appear are actually two closely-spaced singlets. The two at around 32 ppm appear in the phosphine oxide/phosphine sulfide region, and the two at around -29 ppm are in the phosphine region.

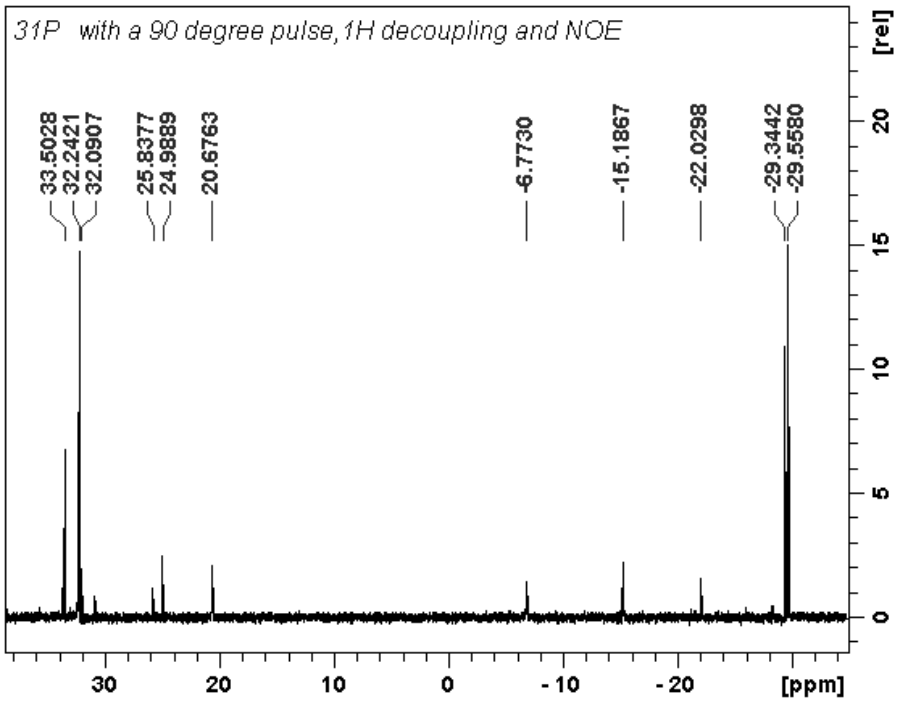

Figure 4.11: The ^{31}P NMR spectrum for the reaction oil formed between $Ph_2P(CH_2OH)_2Cl$ and N-*(2-aminoethyl)-1,8-naphthalimide.*

The oil product was also analysed by IR spectroscopy. Figure 4.12 shows the spectra of the product, as well as the starting materials, *N*-(2-aminoethyl)-1,8-naphthalimide and $Ph_2P(CH_2OH)_2Cl$.

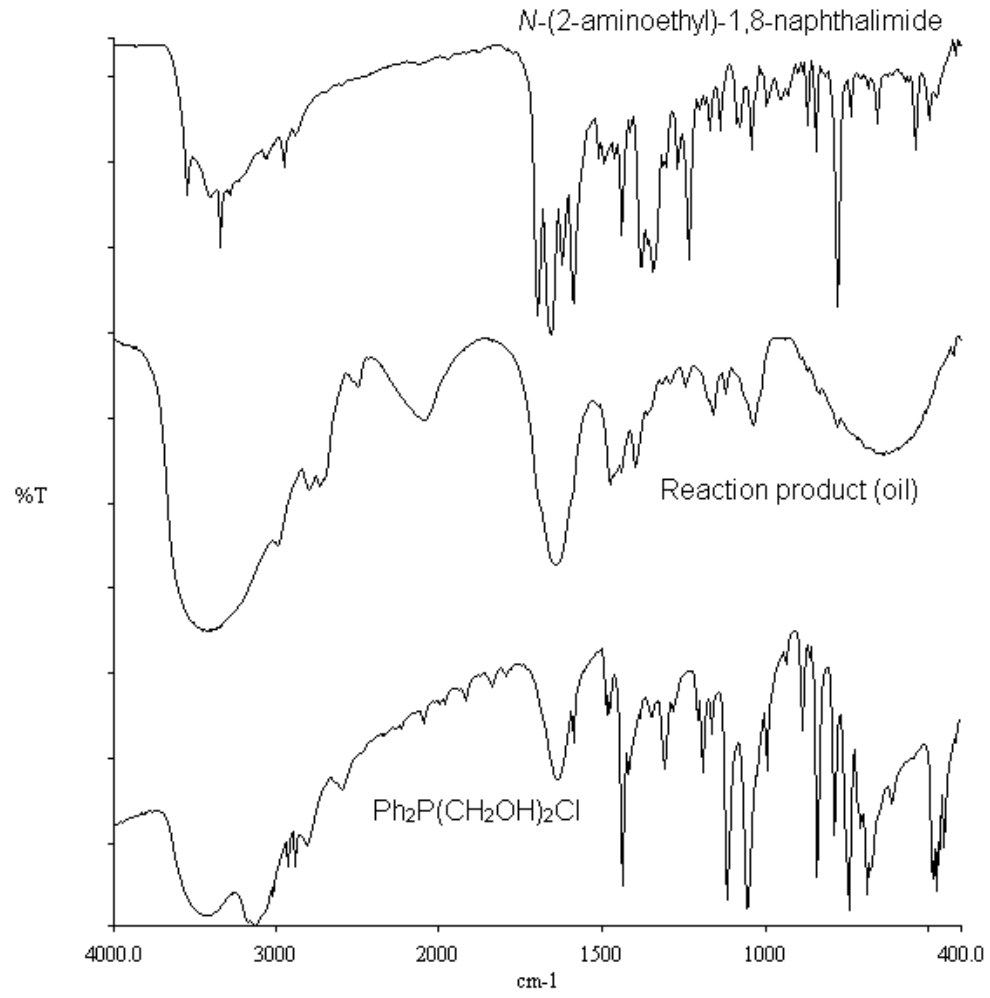

Figure 4.12: The IR spectra of N-*(2-aminoethyl)-1,8-naphthalimide (top), the reaction oil (middle) and* $Ph_2P(CH_2OH)_2Cl$ *(bottom).*

The peaks in the IR spectrum of the reaction oil appear broader, due to the compound being an oil. The υ(C=O) peak at ~1650 cm^{-1} in the naphthalimide compound spectrum (top) is present in the spectrum of the reaction oil (middle), even if it appears broader in the middle spectrum. Characterisation of any other peaks that appear between the reaction oil and the starting materials is difficult. Without obtaining a crystalline solid, the structure of the product is unable to be determined.

4.4 Conclusions and Future Work:

The coupling reaction between aminopropyl silica and **4** does not appear to have retained the fluorescence of the label. The control appears to fluoresce more strongly, and both the THP-coupled aminopropyl silica and the control fluoresce more strongly than the starting aminopropyl silica. It appears the fluorescent label **4**, may adsorb to the surface of the aminopropyl silica, and the THP quenches the fluorescence. IR spectroscopy was inconclusive at determining the presence of bound material. The reaction between $Ph_2P(CH_2OH)_2Cl$ and **4** was also not successful.

Future work could involve repeating both reactions using a different fluorescent label. The surface of the coupled silica samples could be examined using reflectance IR (this could not be done in this project due to equipment failure). ^{31}P solid state NMR may also be useful.

References:

1. James, B. R.; Lorenzini, F., Developments in the chemistry of tris(hydroxymethyl)phosphine. *Coord. Chem. Rev.* **2010,** *254*, 420-430.

2. Frank, A. W.; Daigle, D. J.; Vail, S. L., Chemistry of Hydroxymethyl Phosphorus Compounds. Part III. Phosphines, Phosphine Oxides, and Phosphonium Hydroxides. *Tex. Res. J.* **1982,** *52*, 738-750.

3. Moiseev, D. V.; James, B. R., Air-stability of aqueous solutions of $(HOCH_2)_3P$ and $(HOCH_2CH_2CH_2)_3P$. *Inorg. Chim. Acta* **2011,** *379*, 23-27.

4. Frank, A. W.; Daigle, D. J.; Vail, S. L., Chemistry of Hydroxymethyl Phosphorus Compounds: Part II. Phosphonium Salts. *Tex. Res. J.* **1982,** *52*, 678-693.

5. Carlson, R. H. Tetrakis(α-hydroxyorgano)phosphonium acid salts from elemental phosphorus. 1973.

6. Gonschorowsky, M.; Merz, K.; Driess, M., Cyclohexylbis(hydroxymethyl)phosphane: A Hydrophilic Phosphane Capable of Forming Novel Hydrogen-Bonding Networks. *Eur. J. Inorg. Chem.* **2006**, 455-463.

7. Ellis, J. W.; Harrison, K. N.; Hoye, P. A. T.; Orpen, G.; Pringle, P. G.; Smith, M. B., Water-Soluble Tris(hydroxymethyl)phosphine Complexes with Nickel, Palladium, and Platinum. Crystal Structure of $[Pd\{P(CH_2OH)_3)_4].CH_3OH$. *Inorg. Chem.* **1992,** *31*, 3026-3033.

8. Goodwin, N. J.; Henderson, W.; Nicholson, B. K., Hydrogen bonding in hydroxymethylphosphine chalcogenides. *Inorg. Chim. Acta* **2002,** *335*, 113-118.

9. Vail, S. L.; Daigle, D. J.; Frank, A. W., Chemistry of Hydroxymethyl Phosphorus Compounds: Part I: Introduction. *Tex. Res. J.* **1982,** *52* (671-677).

10. Henderson, W.; Olsen, G. M., Application of electrospray mass spectrometry to the characterization of hydroxymethylphosphonium salts, -phosphines, and their oxide, sulfide and selenide derivatives. *Polyhedron* **1996,** *15* (13), 2105-2115.

11. Chatt, J.; Leigh, J.; Slade, R. M., Rhodium(I), Rhodium(III), Palladium(II), and Platinum(II) Complexes containing Ligands of the Type PR_nQ_{3-n} (n = 0, 1, or 2; R = Me, Et, Bu^t, or Ph; Q = CH_2OCOMe or CH_2OH). *J. Chem. Soc., Dalton Trans.* **1973,** (19), 2021-2028.

12. Komiya, S.; Awata, H.; Ishimatsu, S.; Fukuoka, A., Synthesis of water-soluble (tri(hydroxymethyl)phosphine)gold(I) complexes containing a nucleoside ligand. *Inorg. Chim. Acta* **1994,** *217*, 201-202.

13. Harnack, O.; Ford, W. E.; Yasuda, A.; Wessels, J. M., Tris(hydroxymethyl)phosphine-Capped Gold Particles Templated by DNA as Nanowire Precursors. *Nano Lett.* **2002,** *2* (9), 919-923.

14. Alley, S. R.; Henderson, W., New ferrocene-derived hydroxymethylphosphines: $FcP(CH_2OH)_2$ [Fc = (η^5-C_5H_4)] and the dppf analogue 1,1'-Fc'[$P(CH_2OH)_2$]$_2$ [Fc' = (η^5-C_5H_4)$_2$]. *Inorg. Chem. Commun.* **2001,** *4*, 741-744.

15. Fukuoka, A.; Kosugi, W.; Morishita, F.; Hirano, M.; McCaffrey, L.; Henderson, W.; Komiya, S., Water-soluble iridium and rhodium complexes with tris(hydroxymethyl)phosphine and their catalysis in biphasic hydrogenation and hydroformylation. *Chem. Commun.* **1999**, 489-490.

16. Petach, H. H.; Henderson, W.; Olsen, G. M., $P(CH_2OH)_3$ - A New Coupling Reagent for the Covalent Immobilisation of Enzymes. *J. Chem. Soc., Chem. Commun.* **1994**, 2181-2182.

17. Oswald, P. R.; Evans, R. A.; Henderson, W.; Daniel, R. M.; Fee, C. J., Properties of a thermostable β-glucosidase immobilized using tris(hydroxymethyl)phosphine as a highly effective coupling agent. *Enzyme Microb. Technol.* **1998,** *23* (14-19).

18. Bonnington, L. S.; Henderson, W.; Petach, H. H., $P(CH_2OH)_3$-polyetheramine-derived polymeric films for enzyme immobilization. *Enzyme Microb. Technol.* **1995,** *17*, 746-750.

19. Zhang, J.; Vittal, J. J.; Henderson, W.; Wheaton, J. R.; Hall, I. H.; Hor, T. S. A.; Yan, Y. K., Tricarbonylrhenium(I) complexes of phosphine-derivatized amines, amino acids and a model peptide: structures, solution behavior and cytotoxicity. *J. Organomet. Chem.* **2002,** *650*, 123-132.

20. Ruzin, S. E., *Plant Microtechnique and Microscopy*. Oxford University Press: New York, 1999.

21. Fuquen, M.; Lechat, J. R., Structure of the 1:1 Complex Formed by Triphenylphosphine Oxide and 4-Nitrophenol. *Acta Crystallogr., Sect. C* **1992,** *48* (9), 1690-1692.

22. Etter, M. C.; Baures, P. W., Triphenylphosphine Oxide as a Crystallization Aid. *J. Am. Chem. Soc.* **1988,** *110* (2), 639-640.

23. Institute of Medicine (US), *Veterans and Agent Orange: Health Effects of Herbicides Used in Vietnam*. National Academies Press: Washington, D.C., 1994.

24. Zingaro, R. A.; Hedges, R. M., Phosphine oxide-halogen complexes: effect on P-O and P-S stretching frequencies. *J. Phys. Chem.* **1961,** *65*, 1132-1138.

25. Mueller, M., *Introduction to Confocal Fluorescence Microscopy*. 2nd ed.; SPIE: Bellingham, 2005; Vol. 69.

26. Licchelli, M.; Biroli, A. O.; Poggi, A.; Sacchi, D.; Sangermani, C.; Zema, M., Excimer emission induced by metal ion coordination in 1,8-naphthalimide-tethered iminopyridine ligands. *Dalton Trans.* **2003**, 4537-4545.

27. Johnson, G. S.; Mucalo, M. R.; Lorier, M. A.; Gieland, U.; Mucha, H., The processing and characterization of animal-derived bone to yield materials with biochemical applications. Part II: milled bone powders, reprecipitated hydroxyapatite and the potential uses of these materials. *J. Mater. Sci. - Mater. Med.* **2000,** *11*, 725-741.

28. Harrison, R. J. E., Confocal Microscopy: Exploring the Cellular Uptake and Intracellular Distribution of Fluorescent Metal-Based Drugs. *Aust. J. Chem.* **2009,** *62*, 90.

29. Campbell, N. A.; Reece, J. B.; Urry, L. A.; Cain, M. L.; Wasserman, S. A.; Minorsky, P. V.; Jackson, R. B., *Biology*. 8th ed.; Pearson Education Inc.: SanFrancisco, CA, USA, 2008.

30. Madigan, M. T.; Martinko, J. M.; Dunlap, P. V.; Clark, D. P., *Brock Biology of Microorganisms*. 12th ed.; Pearson Education Inc.: San Francisco, CA, 2009.

31. Hernando, I.; Perez-Manuera, I.; Lluch, M. A., Microstructural characterization of Burgos cheese using different microscopy techniques. *Food Sci. Tech. Int.* **2000,** *6* (2), 151-157.

32. Hino, H.; Ammitzboll, T.; Asboe-Hansen, G., Ultrastructure of skin and hair of an Egyptian mummy. Transmission and scanning electron microscopic observations. *J. Cutan. Pathol.* **1982,** *9* (1), 25-32.

33. Walt, I. M., *The Principles and Practice of Electron Microscopy*. 2nd ed.; Cambridge University Press: Cambridge, New York, 1997.

34. Delatollaa, R.; Tufenkjia, N.; Comeaub, Y.; Lamarrec, D.; Gadboisc, A.; Berka, D., In situ characterization of nitrifying biofilm: Minimizing biomass loss and preserving perspective. *Water Res.* **2009,** *43*, 1775-1787.

35. Pathan, A. K.; Bond, J.; Gaskin, R. E., Sample preparation for scanning electron microscopy of plant surfaces - Horses for courses. *Micron.* **2008,** *39*, 1049-1061.

36. Weston, A. E.; Armer, H. E. J.; Collinson, L. M., Towards native-state imaging in biological context in the electron microscope. *J. Chem. Biol.* **2010,** *3*, 101-112.

37. Karcz, J.; Bernas, T.; Nowak, A.; Talik, E.; Woznica, A., Application of Lyophilization to Prepare the Nitrifying Bacterial Biofilm for Imaging with Scanning Electron Microscopy. *Scanning* **2012,** *34*, 26-36.

38. Orhel, P., HMDS and Specimen Drying for SEM. *Microscopy Today* May 1997, 1997, pp 1-24.

39. Dohnalkova, A. C.; Marshall, M. J.; Arey, B. W.; Williams, K. H.; Buck, E. C.; Fredrickson, J. K., Imaging Hydrated Microbial Extracellular Polymers: Comparative Analysis by Electron Microscopy. *Appl. Environ. Microbiol.* **2011,** *77* (4), 1254-1262.

40. Kenyon, E. M.; Hughes, M. F., A concise review of the toxicity and carcinogenicity of dimethylarsinic acid. *Toxicology* **2001,** *160*, 227-236.

41. Institute of Medicine (US), *Veterans and Agent Orange: Update 2010*. National Academies Press: Washington, D.C, 2012.

42. Liu, B. Y.; Zhang, G. M.; Li, X. L.; Chen, H., Effect of Glutaraldehyde Fixation on Bacterial Cells Observed by Atomic Force Microscopy. *Scanning* **2012,** *34*, 6-11.

43. Horie, I.; Onda, S.; Nagao, K., Color reaction of glutaraldehyde with amino acids and its application to analyses related to gelatin. *Photogr. Gelatin 2, Proc. Symp., [3rd]* **1976**, 297-315.

44. Tsugio, T.; Kiyoshi, I. Fixation of proteins on protein fibers without discoloration. 1988.

45. Hopwood, D., Some aspects of fixation with glutaraldehyde. *J. Anat.* **1967,** *101* (1), 83-92.

46. Hopwood, D.; Allen, C. R.; McCabe, M., The reactions between glutaraldehyde and various proteins. An investigation of their kinetics. *Histochem. J.* **1970,** *2*, 137-150.

47. Cochrane, F. C.; Petach, H. H.; Henderson, W., Application of tris(hydroxymethyl)phosphine as a coupling agent for alcohol dehydrogenase immobilization. *Enzyme Microb. Technol.* **1996,** *18*, 373-378.

48. MacIntosh, B. R.; Gardiner, P. F.; McComas, A. J., *Skeletal Muscle: Form and Function*. 2nd ed.; Human Kinetics: Champaign, IL, 2006.

49. Martins, G. F.; Ramalho-Ortigão, J. M.; Pimenta, P. F. P., Morphological features of the heart of six mosquito species as revealed by scanning electron microscopy. *Int. J. Trop. Insect Sci.* **2011,** *31* (1-2), 98-102.

50. Harrison, J. J.; Ceri, H.; Yerly, J.; Stremick, C. A.; Hu, Y.; Martinuzzi, R.; Turner, R. J., The use of microscopy and three-dimensional visualization to evaluate the structure of microbial biofilms cultivated in the Calgary Biofilm Device. *Biol. Proced. Online* **2006,** *8* (1), 194-215.

51. Stokes, K. L.; Forbes, S. L.; Tibbet, M., Freezing skeletal muscle tissue does not affect its decomposition in soil: Evidence from temporal changes in tissue mass, microbial activity and soil chemistry based on excised samples. *Forensic Sci. Int.* **2009,** *183* (1-3), 6-13.

52. James, B. R., New chemistry, including pulp bleaching processes, of the golden-aged, water-soluble compound, tris(hydroxymethyl)phosphine. In *Catalysis of Organic Reactions Twenty-second Conference*, Prunier, M. L., Ed. Chemical Industries: Boca Raton, FL, United States, 2008; pp 1-14.

53. Pogorelov, A. G.; Selezneva, I. I., Evaluation of Collagen Gel Microstructure by Scanning Electron Microscopy. *Bull. Exp. Biol. Med.* **2010,** *3*, 153-156.

54. Franco-Acuña, D. O.; Pinheiro, J.; Oliveira-Menezes, A.; Brandolini, S. V. P. B.; DaMatta, R. A.; de Souza, W., Light and scanning electron microscopy of sporocysts of Eurytrema coelomaticum (Giard et Billet, 1892) Looss, 1907. *Vet. Parasitol.* **2011,** *177* (1–2), 72-78.

55. Reipert, S.; Steinbock, F.; Fischer, I.; Bittner, R. E.; Zeold, A.; Wiche, G., Association of Mitochondria with Plectin and Desmin Intermediate Filaments in Striated Muscle. *Exp. Cell Res.* **1999,** *252*, 479-491.

56. Devillanova, F. A., *Handbook of Chalcogen Chemistry: New Perspectives in Sulfur, Selenium and Tellurium*. The Royal Society of Chemistry: Cambridge, UK, 2007.

57. Tefteller, W.; Zingaro, R. A.; Isbell, A. F., Phosphines and Phosphine Sulfides Containing Highly Condensed Aromatic Groups. *J. Chem. Eng. Data* **1965,** *10* (3), 301-302.

58. Zingaro, R. A.; McGlothlin, R. E., Some Phosphines, Phosphine Sulfides, and Phosphine Selenides. *J. Chem. Eng. Data* **1963,** *8* (2), 226-229.

59. Tefteller, W.; Zingaro, R. A., Phosphine Sulfides: Donor Properties towards Halogens. *Inorg. Chem.* **1966,** *5* (12), 2151-2155.

60. Apperley, D. C.; Bricklebank, N.; Hursthouse, M. B.; Light, M. E.; Coles, S. J., Vibrational, ^{31}P NMR and crystallographic studies of diiodine adducts of some bidentate tertiary phosphine sulfides. *Polyhedron* **2001,** *20*, 1907-1913.

61. Apperley, D. C.; Bricklebank, N.; Burns, S. L.; Hibbs, D. E.; Hursthouse, M. B.; Malik, K. M. A., Crystal structure of triphenylphosphine sulfide diiodine; the first crystallographically characterised 1:1 molecular charge-transfer complex

of a tertiary phosphine sulfide with diiodine. *J. Chem. Soc., Dalton Trans.* **1998,** *8*, 1289-1292.

62. Schweikert, W. W.; Meyers, E. A., The Crystal Structure of the Triphenylphosphine Sulfide-Iodine Addition Complex. *J. Phys. Chem.* **1968,** *72* (5), 1561-1565.

63. Kaur, S.; Lobana, T. S., Spectroscopic determination and thermodynamic parameters of species formed on reactions of some mono- and di-tertiary-phosphine sulfides with molecular iodine in different solvents. *J. Inorg. Nucl. Chem.* **1981,** *43* (10), 2439-2441.

64. Arca, M.; Demartin, F.; Devillanova, F. A.; Garau, A.; Isaia, F.; Lippolis, V.; Verani, G., A new assembly of diiodine molecules at the triphenylphosphine sulfide template. *J. Chem. Soc., Dalton Trans.* **1999**, 3069-3073.

65. Zingaro, R. A.; McGlothlin, R. E.; Meyers, E. A., Phosphine oxide, sulfide, and selenide complexes with halogens: visible and ultraviolet studies. *J. Phys. Chem.* **1962,** *66*, 2579-2584.

66. Blake, A. J.; Cristiani, F.; Devillanova, F. A.; Garau, A.; Gilby, L. M.; Gould, R. O.; Isaia, F.; Lippolis, V.; Parsons, S.; Radek, C.; Schroder, M., Structural and solution studies of diiodine charge-transfer complexes of thioether crowns. *J. Chem. Soc., Dalton Trans.* **1997**, 1337-1346.

67. Godfrey, S. M.; Jackson, S. L.; McAuliffe, C. A.; Pritchard, R. G., Reaction of R_3PSe with I_2; crystal structures of Ph_3PSeI_2, $(Me_2N)_3PSeI_2$ and $(Et_2N)_3PSeI_2$, the first crystallographically characterised charge-transfer complexes of tertiary phosphine selenides with diiodine. *J. Chem. Soc., Dalton Trans.* **1997**, 4499-4502.

68. Davies, J. A.; Dutremez, S.; Pinkerton, A. A., Solid-State ^{31}P NMR and X-ray Crystallographic Studies of Tertiary Phosphines and Their Derviatives. *Inorg. Chem.* **1991,** *30* (10), 2380-2387.

69. Zingaro, R. A., Phosphine Sulfides and Selenides: The Phosphorus-Sulfur and Phosphorus-Selenium Stretching Frequencies. *Inorg. Chem.* **1963,** *2* (1), 192-196.

70. Kosolapoff, G. M.; Maier, L., *Organic Phosphorus Compounds*. Wiley-Interscience: New York, 1972; Vol. 4.

71. Cross, W. I.; Godfrey, S. M.; Jackson, S. L.; McAuliffe, C. A.; Pritchard, R. G., The reaction of the tertiary phosphine sulfides R_3PS (R = Ph, Me_2N or C_6H_{11}) with X_2 (X_2 = I_2, Br_2, IBr or ICl); structural characterisation of the CT complexes $(Me_2N)_3PSI_2$ and $Ph_3PS(I_{0.89}Br_{0.11})Br$ and the ionic compound $[\{(Me_2N)_3PS\}_2S]_2^+$ $2[Br_3]^-$. *J. Chem. Soc., Dalton Trans.* **1999**, 2225-2230.

72. The Royal Society of Chemistry Modern Chemical Techniques: Infrared Spectroscopy. http://www.rsc.org/learn-chemistry/resource/res00001299/infrared-spectroscopy (accessed 12/02/2015).

73. Lichtman, J. W.; Conchello, J., Fluorescence Microscopy. *Nat. Methods* **2005,** *2* (12), 910-919.

74. Valeur, B.; Berberan-Santos, M. N., *Molecular Fluorescence: Principles and Applications*. 2nd ed.; Wiley-VCH: Weinheim, 2013.

75. Tsukamoto, K.; Shinohara, Y.; Iwasaki, S.; Maeda, H., A coumarin-based fluorescent probe for Hg^{2+} and Ag^+ with an N'-acetylthioureido group as a fluorescence switch. *Chem. Commun.* **2011,** *47*, 5073-5075.

76. Nicholson, B. K.; Crosby, P. M.; Maunsell, K. R.; Wyllie, M. J., An orthomanganation route to 2-substituted derivatives of N-methyl-1,8-naphthalimide. *J. Organomet. Chem.* **2012,** *716*, 49-54.

77. Jeong, Y.; Yoon, J., Recent progress on fluorescent chemosensors for metal ions. *Inorg. Chim. Acta* **2012,** *381*, 2-14.

78. (a) Duke, R. M.; Veale, E. B.; Pfeffer, F. M.; Krugerc, P. E.; Gunnlaugsson, T., Colorimetric and fluorescent anion sensors: an overview of recent developments in the use of 1,8-naphthalimide-based chemosensors. *Chem. Soc. Rev.* **2010,** *39*, 3936-3953; (b) Gunnlaugsson, T.; Glynn, M.; Tocci, G. M.; Kruger, P. E.; Pfeffer, F. M., Anion recognition and sensing in organic and aqueous media using luminescent and colorimetric sensors. *Coord. Chem. Rev.* **2006,** *250*, 3094-3117; (c) Bao, X.; Wang, L.; Wu, L.; Li, Z., A Simple Colorimetric and Fluorescent Anion Sensor Based on 4-Amino-1,8-naphthalimide: Synthesis and its Recognition Properties. *Supramol. Chem.* **2008,** *20* (5), 467-472.

79. Kilpin, K. J.; Clavel, C. M.; Edafe, F.; Dyson, P. J., Naphthalimide-Tagged Ruthenium−Arene Anticancer Complexes: Combining Coordination with Intercalation. *Organometallics* **2012,** *31*, 7031-7039.

80. Khatib, I. S.; Parish, R. V., Insoluble ligands and their applications: I. A comparison of silica-immobilized ligands and functionalized polysiloxanes. *J. Organomet. Chem.* **1989,** *369*, 9-16.

81. Aiello, D.; Folliet, N.; Laurent, G.; Testa, F.; Gervais, C.; Babonneau, F.; Azaïs, T., Solid state NMR characterization of phenylphosphonic acid

encapsulated in SBA-15 and aminopropyl-modified SBA-15. *Microporous and Mesoporous Mater.* **2013,** *166,* 109-116.